

UCSF

UC San Francisco Electronic Theses and Dissertations

Title

Genetic and Environmental Contributions to Adult Social Attachment

Permalink

<https://escholarship.org/uc/item/9zq3c2z8>

Author

Larios, Rose Deanna

Publication Date

2021

Peer reviewed|Thesis/dissertation

Genetic and Environmental Contributions to Adult Social Attachment

by
Rose Deanna Larios

DISSERTATION
Submitted in partial satisfaction of the requirements for degree of
DOCTOR OF PHILOSOPHY

in
Neuroscience

in the
GRADUATE DIVISION
of the
UNIVERSITY OF CALIFORNIA, SAN FRANCISCO

Approved:

DocuSigned by:
Eric Huang Eric Huang
9A805C3F0428410... Chair

DocuSigned by:
DEVANAND MANOLI DEVANAND MANOLI

DocuSigned by:
Lisa Gunaydin Lisa Gunaydin

DocuSigned by:
Stephan Sanders Stephan Sanders
E1D618DE050845D...

Committee Members

Copyright 2021

by

Rose Deanna Larios

To my Larios and Pelliccia families who have proven their wit and grit around the world
and passed on determination for me to take the opportunities I have met.

To Mom and Dad, thank you for teaching me to be my authentic self,
I took care of my business.

ACKNOWLEDGEMENTS

Thank you to everyone who made completing this dissertation possible.

To my thesis advisor, Dev Manoli, thank you for taking a chance on me to build the lab from an empty suite and 10 breeding pairs to the engine it has become. It was been an honor to watch the lab grow and I am excited for all the future discoveries and trainees that will come out of it.

To all members of the Manoli lab, Mike for being the world's best vole whisperer, Ruchira for molecular biology expertise, Gina for running in situ experiments, Kara for teaching me to code over Zoom, Kristen, Nerissa, Shuyu, Kim, and DéJenaé, and Matt and Tatiana for all the encouragement and continued friendship.

To my committee members, Eric Huang, Stephan Sanders, Lisa Gunaydin, and Dena Dubal for thoughtful feedback and mentorship over these 7 years. To the Neuroscience program coordinators, Pat and Lucita, the foundation on which this program stands. To all I worked alongside in the Diversity Equity & Inclusion Committee, Kira Poskanzer, Anatol Kreitzer, Evan Feinberg, Meryl Horn, Frances Cho, and Anna Lipkin, for allowing me to bring my authentic self and visions of the inclusive future to my UCSF community. To Howard Hughes Medical Institute and the entire Gilliam family, this milestone would not have been possible without the community support I received through my Gilliam Fellowship. The annual meetings at HHMI Headquarters with their invaluable workshops and fireside chats, reunions at SACNAS conferences, and the lifelong friendships have helped me find my place in academia when I needed it most.

To my many housemates in San Francisco, to Kyle da Silva for unwavering support and incredible house dinners over 4 years of living together, to Esther Gao for

understanding a side of life we both need, and to Zazie for comic relief. To Catriona, Katie, Skyler, Becca, Joel, Jimmy, and everyone else who passed through 2nd to None. To my Bay Area friends, Irene Grossrubatscher for the most loving friendship I could ask for and too many adventures to count including a neuroscience course in Japan; to Mike Reitman for years of fight club, singing, and the best motivational talks; to the Ohmies Louis, Tobias, and Devon; to Katie Benthall; and to Jeff Knowles who left us too suddenly soon, for walking me through my first committee meeting while we lived together, I've taken your advice through the end of my dissertation.

To my hometown NYC best friends, to Rebecca Berger for understanding me across decades and for many therapeutic hours of phone calls, and to Lisa and Anna for lifelong friendships. To another East Coast best, Brigit High, for being able to talk about everything science to everything life and friendship continued from east to west coasts.

To my partner Colin, for motivating me in little bee steps to continue working during the pandemic and being far from home, for making all the days of the thesis hole writing together a little sweeter while pet sitting in Berkeley & South Bay, (shoutout to Cirrus, Sprite, and Schatze), and for teaching me what the voles already know is amazing.

To Mom and Dad for teaching me to be my authentic self and pursue my dreams to the fullest whatever they may be! Thank you for leading me into the opportunities I took and always allowing me the freedom to follow my heart. To my sister Angela, for love and support and kindness, I'm excited to see all you will do! To my grandparents Grandma Rhoda and Popi, Papa and Tita, my great grandma Bea and Salvatore, thank you for all the strength you showed to bring me here and give me this amazing life.

Most importantly, to the voles, thank you for your contribution to science and understanding of the living brain.

*There's a calm surrender, to the rush of day
When the heat of a rolling wind, can be turned away
An enchanted moment, and it sees me through
It's enough for this restless warrior, just to be with you*

Elton John

Genetic and Environmental Contributions to Adult Social Attachment

Rose Deanna Larios

Abstract

Social relationships are the basis of all civilization, and vital to an individual's role in society and well-being. In particular, the complex behaviors that comprise social attachment are necessary to maintain successful bonds with other individuals throughout life. Deficits in adult social attachment behaviors and disruptions in social relationships are observed across many psychiatric diseases, and are fundamental diagnostic criteria for Autism Spectrum Disorders (ASD). ASD is a clinically heterogeneous disorder with a complex and highly variable etiology, with studies indicating both genetic and environmental contributions to risk. The underlying neurobiology of ASD is not well understood, and thus there exists a lack of biologically based diagnosis and treatments for social attachment deficits. Further research into the neural mechanisms of social attachment deficits has been restricted by the lack of model organisms which display ethologically relevant social bonding behaviors analogous to humans.

In this dissertation I report on experiments describing genetic and environmental manipulations on social attachment behaviors in a socially monogamous rodent, the prairie vole (*Microtus ochrogaster*). Prairie voles form enduring and selective social attachments between mates, defined as a pair bond, which can be robustly and reliably measured in the laboratory.

Varied mutations in *Shank3* in humans have been identified as contributing high risk to ASD symptomology. I used CRISPR-mediated mutagenesis to generate two vole lines bearing unique mutations in *Shank3*, which alter specific isoforms of Shank3 protein. I identified a female- and mutation- specific behavioral phenotype of diminished social attachment to a bonded male partner in heterozygous *Shank3* mutants. These studies establish a clinically relevant prairie vole model for the social deficits observed in ASD, and provide novel results which begin to isolate which functional domains of Shank3 protein are implicated in social attachment deficits.

Secondly, I show an environmental contribution to social attachment behaviors by demonstrating that early life social isolation impairs adult social attachment, in female prairie voles. Early life stress has been attributed to increased adult vulnerability to psychiatric disease. Specifically, early life social isolation can cause an increase in disinhibited attachment, defined by lack of selectivity in social relationships, as well as autistic-like features, such as impaired social relationships. I report that 4 weeks of juvenile isolation is sufficient to extinguish social attachment behaviors typical in female prairie voles.

Taken together, these results (1) establish the prairie vole as a model of adult social attachment deficits in psychiatric disease, (2) describe the contribution of a specific and clinically relevant gene mutation to adult social attachment deficits, and (3) provide an example of an environmental basis of adult social attachment deficits.

Beyond social attachment, these investigations highlight the use of species specific innate behaviors to calibrate a research question, and establishes several molecular genetic, histological, and behavioral techniques for use in the prairie vole.

TABLE OF CONTENTS

<u>CHAPTER 1: INTRODUCTION.....</u>	<u>1</u>
SOCIAL ATTACHMENT DEFICITS IN PSYCHIATRIC DISEASE.....	1
THE PRAIRIE VOLE AS A MODEL SYSTEM FOR ADULT SOCIAL ATTACHMENT BEHAVIORS	3
NEUROBIOLOGY AND EVOLUTIONARY CONSERVATION OF ADULT SOCIAL ATTACHMENT	5
NEURAL CIRCUITRY OF ADULT SOCIAL ATTACHMENT	8
GENETIC ETIOLOGY OF AUTISM SPECTRUM DISORDERS	11
NEUROBIOLOGY OF <i>SHANK3</i> IN ASD	13
ANIMAL MODELS OF <i>SHANK3</i> MUTATIONS.....	16
ENVIRONMENTAL ETIOLOGY OF SOCIAL ATTACHMENT DEFICITS	24
SUMMARY	27
<u>CHAPTER 2: THE ROLE OF <i>SHANK3</i> IN ADULT SOCIAL ATTACHMENT BEHAVIORS.....</u>	<u>28</u>
INTRODUCTION	28
RESULTS	32
GENERATION OF <i>SHANK3</i> MUTANT PRAIRIE VOLES	32
<i>SHANK3</i> PROTEIN CHARACTERIZATION OF 2 DISTINCT <i>SHANK3</i> MUTANT PRAIRIE VOLE LINES	36
HETEROZYGOUS <i>SHANK3</i> MUTANT PRAIRIE VOLE LINES DO NOT SHOW DIFFERENCES IN EXPLORATORY BEHAVIORS AND LOCOMOTOR ACTIVITY COMPARED TO THEIR SAME-SEX WILD-TYPE SIBLINGS	39
HETEROZYGOUS <i>SHANK3</i> MUTANT PRAIRIE VOLES DO NOT SHOW DIFFERENCES IN SOCIABILITY AND SOCIAL NOVELTY AS COMPARED TO THEIR SAME-SEX WILD-TYPE SIBLINGS	40
BONDED FEMALE <i>SHANK3</i> ^{ΔE9/+} VOLES SHOW DIMINISHED PREFERENCE FOR THEIR PARTNER.....	43
BONDED FEMALE <i>SHANK3</i> ^{ΔE9/+} VOLES SHOW REDUCED ATTACHMENT BEHAVIORS TOWARDS THEIR PARTNER FOLLOWING ACUTE SEPARATION.....	45

BONDED FEMALE <i>SHANK3</i> ^{ΔE9/+} AND <i>SHANK3</i> ^{ΔE14/+} VOLES SHOW DECREASED SEXUAL RECEPTIVITY TO MALE PARTNERS	47
SEXUALLY NAÏVE <i>SHANK3</i> MUTANT VOLES SHOW AFFILIATIVE SOCIAL BEHAVIORS TOWARDS A NOVEL VOLE CONSISTENT WITH THEIR WILD-TYPE CONTROL SIBLINGS, AND <i>SHANK3</i> ^{ΔE9/+} FEMALES SHOW DIMINISHED DEFENSIVE REARING	49
PAIR BONDED <i>SHANK3</i> MUTANT VOLES SHOW AGGRESSIVE SOCIAL BEHAVIORS TOWARDS A NOVEL VOLE CONSISTENT WITH THEIR WILD-TYPE CONTROL SIBLINGS, AND <i>SHANK3</i> ^{ΔE9/+} FEMALES SHOW DIMINISHED INVESTIGATION	50
<i>SHANK3</i> ^{ΔE9/+} FEMALES SHOW COMPARABLE NUMBERS OF OT AND AVP POSITIVE CELLS ACROSS THE PVN	51
DISCUSSION	53
<i>SHANK3</i> ^{ΔE9/+} FEMALES SHOW A SEX- AND MUTATION- SPECIFIC DEFICIT IN ADULT SOCIAL ATTACHMENT BEHAVIORS EXPRESSED THROUGH THE PAIR BOND	54
<i>DIFFERENTIAL EXPRESSION OF SHANK3 ISOFORMS BETWEEN ΔE9 AND ΔE14 TARGETED MUTATIONS</i>	<i>56</i>
<i>SEX DIFFERENCES IN GENETIC CONTRIBUTION OF ASD RISK</i>	<i>60</i>
<i>THE PRAIRIE VOLE IN CLASSIC MOUSE SOCIABILITY AND SOCIAL NOVELTY ASSAYS</i>	<i>62</i>
<i>MECHANISMS OF OXYTOCINERGIC SIGNALING IN SHANK3</i> ^{ΔE9/+} <i>FEMALE PRAIRIE VOLES.....</i>	<i>63</i>
<i>THERAPEUTIC IMPLICATIONS</i>	<i>64</i>
FIGURES & TABLES	66
METHODS	89
 <u>CHAPTER 3: THE ROLE OF EARLY LIFE STRESS & SENSORY CUES IN PAIR BOND</u>	
<u>EXPRESSION</u>	<u>102</u>
 INTRODUCTION	102
RESULTS	105

FEMALE PRAIRIE VOLES SHOW A DEFICIT IN ADULT PREFERENCE FOR A PARTNER FOLLOWING EARLY LIFE SOCIAL ISOLATION	105
BONDED MALE PRAIRIE VOLES PREFER THEIR BONDED FEMALE PARTNER'S BEDDING-ASSOCIATED CHEMOSENSORY CUES OVER CUES FROM A SEXUALLY NAÏVE STRANGER FEMALE	106
NEITHER MALES NOR FEMALES DISCRIMINATE BETWEEN BEDDING COLLECTED FROM THEIR PARTNER VERSUS ANOTHER OPPOSITE BONDED VOLE	107
DISCUSSION	108
FIGURES	112
METHODS	115
<u>REFERENCES</u>	<u>117</u>

LIST OF FIGURES

Figure 2.1 Timed mating paradigm.....	66
Figure 2.2 Map of 6 sgRNAs targeted to prairie vole <i>Shank3</i>	67
Figure 2.3 Four CRISPR-mediated mutation events in <i>Shank3</i>	70
Figure 2.4 <i>Shank3</i> $\Delta E9$ mutation detection.....	71
Figure 2.5 <i>Shank3</i> $\Delta E14$ mutation detection.....	72
Figure 2.6 Schematic of Shank3 isoforms in prairie vole	73
Figure 2.7 Western blot of Shank3 isoforms in wild type and <i>Shank3</i> mutant prairie voles.....	74
Figure 2.8 Control behavior paradigm.....	75
Figure 2.9 Open Field Test.....	76
Figure 2.10 Sociability & Social Novelty.....	77
Figure 2.11 Behavior paradigm for social attachment behaviors across pair bonding.....	78
Figure 2.12 <i>Shank3</i> ^{$\Delta E9/+$} females show diminished preference for their partner.....	79
Figure 2.13 Bonded <i>Shank3</i> ^{$\Delta E9/+$} females show reduced attachment behaviors towards partners in reunification.....	81
Figure 2.14 Bonded <i>Shank3</i> ^{$\Delta E9/+$} and <i>Shank3</i> ^{$\Delta E14/+$} females show reduced mating behaviors with male partners.....	82
Figure 2.15 Sexually naïve <i>Shank3</i> mutant and wild-type voles show prosocial behaviors to a novel opposite sex vole.....	84

Figure 2.16 Bonded wild-type, *Shank3*^{ΔE9/+}, and *Shank3*^{ΔE14/+} voles show aggressive behaviors towards a novel stranger vole **85**

Figure 2.17 *Shank3*^{ΔE9/+} and wild-type females show comparable densities of OT and AVP positive cells across the PVN..... **86**

Figure 2.18 Predicted Shank3 isoforms in female mutants..... **88**

Figure 3.1 Female prairie voles do not display partner preference following early life social isolation..... **112**

Figure 3.2 Bedding preference assay between bonded partner and naïve stranger..... **113**

Figure 3.3 Bedding preference assay between bonded partner and bonded stranger..... **114**

LIST OF TABLES

Table 2.1 Founder voles, G0s, of *Shank3* CRISPR-mediated mutagenesis.....**68**

Table 2.2 First filial generation, F1, of *Shank3* CRISPR-mediated mutagenesis.....**69**

Chapter 1: Introduction

Social attachment deficits in psychiatric disease

Social attachment behaviors form the basis for all human relationships, from friendship, kinship, and romantic partnerships, to social organization and function (Insel, 2010; Ebstein et al., 2010). Adult attachment between mates, for example human romantic love, is such a powerful and complex psychological phenomenon that it impacts multiple domains of behavior (Fisher et al., 2016). Close social attachments can have a profound effect on an individual's mental and physical health, as those with intimate relationships show increased lifespan, immune function, and cardiovascular health, and less depressive symptoms (Kiecolt-Glaser & Newton, 2001; Potretzke & Ryabinin, 2019). In humans, daily adult-to-adult attachment behaviors are often critical to maintaining employment, housing, and a support network which ameliorate physical and emotions distresses, and even influence formation of a cognitive map of our personal identities, to understand our life trajectories in our social world (Kirmayer & Gold, 2011).

Deficits in adult social attachment behavior are a core and common component of many psychiatric diseases and are fundamental diagnostic criteria for Autism Spectrum Disorders (ASD). Presently, little is definitively known about how these symptoms manifest, or how to treat these symptoms to improve patients' lives (Lim et al., 2005). The etiology of social attachment deficits is complex and highly variable, with studies indicating both experience and genetic based origins.

ASD is a behaviorally diagnosed neurodevelopmental disorder characterized by qualitative deficits in social communication and social interaction, as well as stereotyped,

repetitive behaviors (Baird et al., 2003). According to the DSM-5, these social impairments can include deficits in social-emotional reciprocity, deficits in nonverbal communication used for social interactions, and deficits in developing, maintaining and understanding relationships (American Psychiatric Association, 2013). All three of these symptom criteria, particularly the third, highlight impairments in social attachment behaviors. ASD is a relatively common psychiatric disorder, with a global prevalence estimated to be 2.64% (Kim et al., 2011). Reliable diagnosis can be made between age 2 to 3 years of age, and symptoms such as social attachment deficits persist through adulthood.

There currently exist no pharmacological treatments for ASD, and no validated biomarkers that allow for early diagnosis predating symptoms, although early intervention has been shown to result in improved social skills into adult life (Elder et al., 2017). Progress towards the development of biologically based diagnosis and treatment options for ASD patients are impeded by a lack of understanding of the neurobiology that underlies adult, or peer, attachment behaviors. The fields of behavioral and molecular neuroscience have not been able to address the brain's mechanisms for forming and maintaining adult attachments because the classic mammalian model organisms of neuroscience, namely the mouse and rat, do not display inherent attachment between adults. In our studies, we therefore seek to investigate the underlying neurogenetics and neurobiology of adult social attachment behaviors by employing a socially monogamous rodent model system renowned for its robust adult attachment behaviors.

The prairie vole as a model system for adult social attachment behaviors

The prairie vole (*Microtus ochrogaster*), native to grasslands of the Midwest United States, is one of less than 3-5% of mammalian species that exhibit monogamous social organization. This organization is defined by biparental care of offspring, highly affiliative behaviors towards conspecifics, and enduring and selective life-long pair bonds between mates (Carter et al., 1995; McGraw & Young, 2010; Carter & Getz, 1993). A pair bond is a long-term preferential association formed between two adults that have reached sexually maturity, although there is variability across the literature. The criteria of a pair bond generally includes consistent and selective preference for contact, affiliation, and mating with a partner conspecific over a stranger, and the selective rejection of novel potential mates (Young et al., 2011).

Field studies in the 1970's first reported that male and female prairie vole pairs were often captured together in wild trappings, suggesting that the species display pair bonds (Getz et al., 1981). Pioneering work by Sue Carter and her lab in the 1980's revealed that these male and female pairs were captured together multiple times over several months, even in non-breeding seasons, establishing a case for social monogamy. Parallel field studies found that when one vole in a pair bond dies, fewer than 20% of either male or female survivors ever establish a new partner (Carter et al., 1995). Consistent with the biparental care in monogamous social structures, field studies also report several observations of male prairie voles' high paternal behaviors, including nest guarding and nest building (Wilson, 1982). High affiliation between conspecifics, also common in monogamous social systems of other species, was observed in the form of alloparenting in prairie voles in the field. In the field, only 30% of juvenile voles leave the

parental pair's nest while the remaining progeny remain in the natal nest and display alloparenting towards their siblings, helping to care for the young (Getz et al., 1994; Kenkel et al., 2017).

In the lab, a pair bond can be quantified by preference for a partner, selective social contact with a partner, and selective aggression towards a conspecific stranger. The Partner Preference Test (PPT), first developed by Sue Carter's laboratory in the early 1990's, persists as the standard assay to measure a vole's preference for its partner, and thus is a means of quantifying social attachments between mates (Williams et al., 1992; McGraw & Young, 2010). The PPT is a three chamber assay in which the subject vole is allowed to freely explore for three hours between chambers containing either its mating partner or a sexually naïve opposite-sex stranger, and a central empty chamber. The stimulus voles are traditionally "tethered" within their chambers by a leash, allowing them uninhibited range of motion and physical contact with the subject vole. Both males and females display significant preference for their partner in this assay, as measured by time spent in social contact with either stimulus animal. Females display partner preference by 6 hours of cohabitation, if there has been at least one mating event, and by 24 hours of cohabitation, even in the absence of mating (Williams et al., 1992). Males require at least 24 hours of cohabitation with mating to exhibit preference for their female partner in the PPT. In the Manoli lab, I and others have adapted the PPT to robustly and reliably quantify partner preference in the prairie vole in order to measure attachment between prairie vole mates under experimental conditions.

Another standard behavior assay for quantifying pair bond formation in prairie voles is the Selective Aggression (or Resident Intruder) Assay, which measures selective

rejection of potential mates once a vole is bonded (Young et al., 2011). When an adult sexually naïve vole is first introduced to a conspecific, it tends to display prosocial behaviors and low levels of aggression, and thus nearly 100% of male-female pairs assigned to cohabitation begin to form a pair bond. Once a vole is bonded, if it is introduced to a sexually naïve opposite-sex conspecific it will engage in robust rejection of this novel animal, displaying significantly more aggressive behaviors than observed towards an opposite-sex animal prior to bonding. Male prairie voles will even reject a sexually receptive naïve female stranger, reflective of highly unusual mate selectivity among mammals (Winslow et al., 1993).

Prairie voles have been validated, in both the field and the laboratory, to demonstrate significant and persistent selective attachments between mates, as assessed through pair bond formation and maintenance. Our work utilizes the prairie vole's innate potential for enduring bonds between mates to investigate the neurobiology of adult social attachment, through both genetic and environmental perturbations causing distinct social attachment phenotypes. Below we lay the foundation of what is understood about social attachment in the brain.

Neurobiology and evolutionary conservation of adult social attachment

Oxytocin (OT) and arginine vasopressin (AVP) are two closely related neuropeptides, both nine-amino-acid peptides (nonapeptides), that have been implicated in modulating social behaviors including mating, parental, and attachment behaviors across all mammalian species (Carter et al., 2008). The social role of closely related nonapeptides is evolutionarily conserved across all vertebrates, and ancestral peptides

have even been shown to have evolutionarily conserved reproductive function in invertebrates (Insel et al., 1998).

Consistent with their social regulation across species, OT and AVP have been discovered to play an essential role in prairie vole pair bond formation (Young et al., 2011; Potretzke & Ryabinin, 2019). Comparative studies between prairie voles and the closely related, but non-monogamous montane (*Microtus montanus*) and meadow (*Microtus pennsylvanicus*) voles, show that prairie voles have significantly higher densities of oxytocin receptor (OXTR) in the nucleus accumbens (NAcc), caudate putamen (CP), medial prefrontal cortex (mPFC), and bed nucleus of the stria terminalis (BNST). Furthermore, prairie voles have higher densities of the vasopressin 1a receptor (V1aR) in the ventral pallidum (VP), medial amygdala (MeA), and mediodorsal thalamus (Smeltzer et al., 2006; Insel & Shapiro, 1992; Insel et al., 1994; Albers, 2015). Exogenous central or intracerebroventricular (ICV) administration of OT and AVP has been shown to facilitate pair bond formation, even in the absence of mating or cohabitation periods typically required to promote bonding (Cho et al., 1999; Williams, et al., 1994). Conversely, ICV infusion of an OXTR or V1aR antagonist blocks mating-induced displays of partner preference in both males and females (Insel & Hulihan, 1995; Winslow et al., 1993). Overexpression of OXTR and V1aR by viral vector-mediated gene transfer, specifically in brain regions which demonstrate significantly increased receptor densities in monogamous vs non-monogamous vole species, can promote pair bond display. Overexpression of V1aR in the VP of male prairie voles is sufficient to facilitate partner preference in the absence of mating (Pitkow et al., 2001). Similarly, overexpression of OXTR in the NAcc of sexually naïve prairie voles is sufficient to accelerate formation of

partner preference to 12 hours of cohabitation, in the absence of mating (Ross et al., 2009). Taken together, these studies indicate that OT and AVP signaling is necessary and sufficient to influence pair bond formation in both male and female prairie voles.

Recent studies have demonstrated that genetic variation in OXTR and V1aR correlates to phenotypic diversity in prairie vole adult attachment behaviors. A natural polymorphism in the OXTR intron, localized near a putative cis-regulatory element, was identified by next-generation sequencing and was shown to increase OXTR expression in the NAcc and CP. Male prairie voles homozygous for this allele presented enhanced social attachment in the PPT (King et al., 2016). Polymorphisms in repeat numbers and sequence content of microsatellites upstream of the V1aR transcription start site play a role in cell-type specific V1aR expression (Hammock & Young, 2004; Ophir et al., 2008b). Voles with longer microsatellites showed increased V1aR expression in the VP and MeA (Ophir et al., 2008a). Interestingly, although not yet replicated by subsequent studies, males bred to have longer V1aR alleles displayed increased preference for their partner in the PPT, while males bred to have shorter V1aR alleles did not show a preference in the PPT (Hammock & Young, 2005).

The molecular mechanisms and neural circuits mediating oxytocin and vasopressin actions are deeply evolutionarily conserved amongst all eutherian species. Therefore, OT and AVP are expected to have translational significance based on studies implicating them in adult human social attachment-like behaviors as well (Meyer-Lindenberg et al., 2011). Woolley et al. demonstrated that intranasal OT administration in patients with schizophrenia improved their ability to understand others' expressed emotions and thoughts (Woolley et al., 2014). Auyeung et al. reported that intranasal OT

administration increased eye contact in males both with and without ASD diagnosis. ASD participants with the lowest baseline eye contact, and the most severe deficits in social communication, showed the greatest benefit from OT treatment (Auyeung et al., 2015). Brain imaging studies have implicated regions with high densities of OXTR expression, including the globus pallidus, substantia nigra, and thalamus, in early romantic love, and Schneiderman et al. reported that OT levels in blood plasma in the initial stages of a romantic relationship could predict relationship success (Acevedo et al., 2012; Schneiderman et al., 2012). Similarly, Brunnie et al. showed that intranasal AVP administration increased willingness to cooperate during a game task involving risk, thus implicating AVP in human social approach and social communication behaviors (Brunnie et al., 2016). Intriguingly, Tabak et al. showed intranasal AVP, but not OT, enhanced empathy in a subset of participants who reported experience of high paternal warmth (Tabak et al., 2014). Empathy is a core component of human's motivation for social communication and prosocial interaction, thus Tabak's work further supports the role of AVP in human adult social attachment (Batson et al., 1998).

The evolutionarily conserved roles for OT and AVP in adult social attachment behaviors between prairie voles and humans strongly suggests that investigations into attachment behaviors in the vole brain will translate to humans and could lead to clinical benefit for those with psychiatric diseases including ASD.

Neural circuitry of adult social attachment

Through mapping of immediate early gene expression, such as *fos*, the prairie vole MeA, BNST, and medial preoptic area (MePOA) all show increases in markers of

neuronal activation after cohabitating and mating with a partner. Axon-sparing lesion studies in male prairie voles revealed that the corticomedial amygdala, but not the basolateral nucleus of the amygdala, is necessary for typical affiliative behaviors towards a partner female (Kirkpatrick et al., 1994a).

Integrating observed patterns of neuronal activation and the above described roles of OT and AVP in the prairie vole brain through bonding, Young and Wang (2004) propose that the neural circuitry of pair bond expression is an effect arising from a coupling of the reinforcing and rewarding properties of mating circuitry, with olfactory sensory integration of the mate, yielding a conditioned partner preference (Young & Wang, 2004). In prairie voles as well as mice, mating in both sexes is shown to activate the ventral tegmental area (VTA), a region appropriately known for reward signaling (Pfaus & Heeb, 1997). The VTA has dopaminergic projections to the NAcc and PFC, which have been implicated in pair bonding through dopamine (DA) and OT signaling, respectively (Lammel et al., 2014). Olfactory sensory cues of the partner are processed primarily by the main and accessory olfactory bulbs, and secondarily by the MeA and lateral septum (LS). AVP projections are prominent from the MeA and BNST to the VP and LS, while OT projections to the amygdala and NAcc originate from the hypothalamus (DeVries & Buijs, 1983).

Amadei et al. utilized electrophysiology and optogenetic techniques to elucidate how projections from mPFC to NAcc dynamically modulated female prairie voles' initial attachment to their partner and display of partner preference, confirming a key component of the above model (Amadei et al., 2017). This study reported that individual variation in the strength of mPFC to NAcc connectivity can predict how quickly voles display affiliative side by side contact, or huddling, with their partner during cohabitation, and subsequently

demonstrated that optogenetic activation of this circuit is sufficient to induce partner preference in the absence of mating. More recent studies have investigated the larger connectivity networks which underlie pair bond formation, using resting state functional magnetic resonance imaging (rsfMRI), a non-invasive neuroimaging technique which measures activity across the whole brain by localized changes in oxygen concentration in the blood. By this method, López-Gutiérrez et al. also demonstrated that mPFC and NAcc were critical regions of interest when comparing voles before and after pairs were bonded. This study mapped a total of 16 regions of interest suggesting dynamic interactions between regions (López-Gutiérrez et al., 2021). Bales et al. confirmed the role of the NAcc and VP in pair bonding is conserved in primates, as a PET investigation in monogamous titi monkeys (*Callicebus cupreus*) showed more activity in these brain regions following pairing with a partner (Bales et al., 2007).

Finally, within the hypothalamus, OT and AVP are synthesized by magnocellular neurons in the paraventricular (PVN) and supraoptic (SON) nuclei and secreted into the blood by axon terminals in the posterior pituitary, from which they can modulate circuits throughout the brain (Brownstein et al., 1980). The PVN has also been shown to have direct oxytocinergic projections to the NAcc, VTA, amygdala, mPFC, and hippocampus, all areas involved in social salience (Walum & Young, 2018). Mating has also been shown to directly activate OT neurons in the PVN as well as locally secrete OT into the blood (Tabbaa et al., 2016). Several prairie vole studies have implicated the PVN as a region that demonstrates changes in OT and AVP expression levels in direct response to changes in parental status, social isolation, separation from a partner, and anxiolytic effects of mating and partner interaction (Tabbaa et al., 2016).

While the foundation of the neurobiology and neural circuitry of adult social attachment has been established, it remains to be investigated how genetic and environmental factors contribute to the neural development, neural activity, and circuit function necessary for adult social attachment. Additionally, how disruptions in these factors may lead to disorders characterized by attachment deficit, such as ASD, is unknown.

Genetic etiology of Autism Spectrum Disorders

ASD is a clinically heterogeneous disorder with a significant and multifactorial genetic contribution; genetic studies have estimated up to 1000 genes potentially associated with symptom presentation (Ramaswami & Geschwind, 2018). Heritable genetic components account for a large portion of variability, with an overall estimated heritability of 0.5-0.8 (Sandin et al., 2014; Hallmayer et al., 2011). This calculation comes from traditional studies which directly compare relatedness of patients' with ASD diagnosis, to their affected or unaffected family members, and report concordance rates of 30-99% among monozygotic twins, 0-65% among dizygotic twins, and 3-30% among siblings (Ramaswami & Geschwind, 2018). Furthermore, accelerated by new advances in genome sequencing technologies and large patient databases over the last decade, more recent efforts suggest that genetic, but nonheritable, de novo mutations contribute significantly to ASD risk. Such nonheritable de novo mutations are estimated to account for 15% to 25% of ASD risk, and include large-scale copy number variants (CNVs), point mutations or single-nucleotide variants (SNVs), and small insertions and deletions (indels) (Ronemus et al., 2014).

A wide array of techniques comparing chromosomes and higher resolution genomic sequences have made it possible to identify specific loci which contribute to ASD risk (Rylaarsdam & Guemez-Gamboa, 2019; Grove et al., 2019). Linkage analyses, a method of linking known heritable alleles to their chromosomal location, have identified rare inherited variants that contribute to ASD risk. These include the synaptic scaffolding protein SH3 and multiple ankyrin repeat domains 3 (*SHANK3*), and the family of neuroligins, neuronal adhesion proteins involved in synapse development and function, specifically *NRXN1* and *NRXN3* (Moessner et al., 2007; Vaags et al., 2012). Cytogenetic techniques, a method of visualizing the number and morphology of chromosomes, first discovered the contribution of large CNVs to ASD risk (Levy et al., 2011). With the development of comparative genomic hybridization with optimized oligonucleotide microarrays, several studies over past decade have identified submicroscopic CNVs that were not detectable by traditional cytogenetics (Sanders et al., 2011). Applying such high resolution comparative genomic techniques to large patients cohorts such as the Simons Simplex Collection (SSC), a collection of about 2,600 families with one high-functioning child with ASD symptoms and unaffected siblings, has revealed that most de novo CNVs with high ASD risk arise in genes involved in neuronal signaling, synaptic function, and chromatin remodeling (Sanders et al., 2015).

The development and optimization of high-throughput exome sequencing, the sequencing of all exons or functional coding domains of the genome, has also been a critical technique for identifying both heritable and nonheritable genetic contributions to ASD risk. Applying this technique to cohorts such as the SSC identified that several genes, such as *POGZ* and *SCN2A*, contain SNVs which either cause loss of function or

disrupted function in the respective protein, and significantly contribute to ASD risk. Risk genes identified by exome sequencing also converge around genes that play a role in synaptic formation and function, chromatin remodeling, and transcriptional regulation (Sanders et al., 2015; Geschwind & State, 2015).

Most recently, whole-genome sequencing (WGS), which sequences non-coding regulatory domains in addition to coding exons, has been employed to broaden the approach to identifying genes and their specific regulatory elements which contribute to ASD risk. Convincingly, Turner et al. performed WGS on families that did not demonstrate any expected mutations between affected and unaffected siblings through microarray nor exome sequencing. Using this methodology, they identified multiple small CNVs in putative regulatory elements of the same genes that predict neurodevelopmental risk when disrupted in coding regions (Turner et al., 2016).

The decades of investigation into the genetic etiology of ASD discussed above reveals that there is a strong genetic component of ASD pathology that centers around disruptions in synaptic development and function, chromatin remodeling, and transcriptional regulation (Sanders et al., 2015). However, the link between disruption in a particular risk gene, and a resulting specific clinical endophenotype of ASD, has yet to be established. This fine-grained understanding of ASD etiology is a crucial step towards personalized care for patients with ASD both in diagnosis and treatment possibilities.

Neurobiology of *Shank3* in ASD

The human *Shank3* gene has been most comprehensively defined as one of the genes located within the chromosomal deletion that causes Phelan-McDermid Syndrome

(PMS), or 22q13.3 deletion syndrome. This syndrome is a rare neurodevelopmental disorder characterized by global developmental delay, moderate to severe intellectual impairment, absent or severely delayed speech, neonatal hypotonia, and dysmorphic features (Phelan & McDermid, 2011). More than half of patients with PMS also meet criteria for ASD diagnosis. Deletion mapping of specific case studies have indicated that disruption of *Shank3* function, particularly in 4 de novo variants, is associated with the cognitive and behavioral symptoms of PMS which overlap with ASD diagnostic criteria (De Rubeis et al., 2018). Curiously, increasing resolution of genetic analysis in ASD patients, as detailed above, has implicated a variety of *Shank3* mutations as risk for ASD, in the absence of PMS. Since ASD is largely characterized by deficits in social behaviors, including social attachment, we therefore hypothesized that *Shank3* function plays a role in social attachment behaviors.

Linkage analysis initially identified the locus containing *Shank3* as a heritable genetic component of ASD presentation, and ample genome sequencing techniques have more recently identified a wide and varied collection of specific *Shank3* mutations that contribute to ASD risk. In 2007, Durand et al. used FISH analysis of *Shank3*, as well as direct sequencing, to identify 3 distinct *Shank3* mutations associated with ASD presentation in a familial pedigree. All mutations yielded a deletion of all or most of the *Shank3* locus despite arising from different events: 1) a de novo mutation in intron 8 that caused premature truncation, 2) an inherited SNV of a heterozygous single G nucleotide insertion in exon 21 causing a frameshift and truncated protein, and 3) an inherited paternal translocation causing terminal and partial deletion of the locus, scalable to the symptom severity of two siblings (Durand et al., 2007). In the same year, Moessner et al.

employed sequencing and microarray-based comparative intensity analysis to screen 400 ASD patients and relatives for mutations in *Shank3*, and described 4 additional mutations, including a de novo SNV of A→G substitution in exon 8 (Moessner et al., 2007). Gauthier et al. confirmed the association as they contributed two additional diverse *Shank3* mutations to this collection, distinctly disrupting 5'- and 3' sites of *Shank3* (Gauthier et al., 2009).

In the last decade, large ASD patient cohorts from Japan, the United States, Italy, and China have made it possible to identify 14 additional distinct mutations in *Shank3* that account for ASD risk as compared to unaffected siblings, further confirming the association between *Shank3* and ASD. These mutations consistently include both inherited and de novo mutations and cause disruption in each of almost all functional domains of Shank3 protein (Waga et al., 2011; Gong et al., 2012; Boccuto et al., 2013). Large-effect mutations in *Shank3* are predicted to explain 1-2% of ASD risk, and the catalogue of already described mutations stresses the impact of *Shank3* in ASD pathology, while highlighting the complexity of the *Shank3* function, as associated mutations are found in nearly every part of the gene with diverse effects on protein structure (Leblond et al., 2014).

Shank3 encodes a scaffolding protein localized to the postsynaptic density of glutamatergic synapses. Shank3 consists of 5 main protein interaction domains: N-terminal ankyrin repeats (ANK), an Src homology 3 domain (SH3), a PDZ domain, a proline-rich region, and a C-terminal Sterile Alpha Motif domain (SAM). Each of these regions interact with specific postsynaptic density proteins, and are generally involved in glutamate receptor signaling and plasticity, and actin cytoskeleton development,

structure, and function (Ebert & Greenberg, 2013). The ANK domain contains binding sites for alpha-fodrin, which regulates the actin cytoskeleton, and sharpin, which mediates homomultimerization of the Shank protein complex (Costales & Kolevzon, 2015). The SH3 domain interacts with GRIP, an adapter protein that directly interacts with the C-termini of AMPA receptors (AMPA). The PDZ domain binds guanylate kinase-associated protein (GKAP), a scaffolding molecule involved in synaptic signaling of NMDA receptors (NMDAR) through a complex of PSD-95/SAP90 proteins (Kim & Sheng, 2004). The proline rich domain contains recognition sites for docking proteins including Homer, which directly interacts with metabotropic glutamate (mGluR) receptors, and cortactin, which also regulates actin cytoskeleton dynamics (Costales & Kolevzon, 2015). It should be noted that the SH3, PDZ, and proline-rich domains each play a role in a distinct pathway of glutamatergic signaling, by protein-protein interactions with AMPAR, NMDAR, and mGluR, respectively. Finally, the SAM domain is conserved in all Shank family proteins and contains conserved protein interaction domains that mediate homooligomerization. Genomic and protein analysis of mouse *Shank3* has identified that *Shank3* contains a complex and wide array of intragenic promoters and alternative splice sites, and demonstrated that translation of the protein results in several isoform variants, each containing a unique combination of the above functional domains (Wang et al., 2014).

Animal models of *Shank3* mutations

Several mouse models of distinct *Shank3* mutations, each functionally disrupting the protein in a unique way, have been behaviorally characterized to understand the

mechanisms by which *Shank3* mutations affect mouse behaviors analogous to ASD, such as sociability and repetitive behaviors.

Peça et al. generated a mutation in the PDZ domain, deleting exons 13-16, that caused a total knockdown of the full length Shank3 protein (Shank3A) as well as the 5'-derived isoform containing the ANK, SH3, and PDZ domains (Shank3B), and significantly reduced expression of the 3'-derived isoform containing the proline-rich and SAM domains (Shank3C) (Peça et al., 2011). Adult male mice homozygous for this mutation (called *Shank3B*^{-/-}) demonstrate significant social interaction deficits. In a three-chamber arena, these mice show significant preference for an empty chamber over a chamber containing another mouse, whether it is a familiar or novel conspecific. *Shank3B*^{-/-} males also spent significantly less time interacting with a wild-type animal, as compared to pairs of wild-type animals, in an open arena dyadic interaction assay, as measured by time spent in reciprocal interaction, and lower frequency of nose-to-nose interactions and anogenital sniffing. Interestingly, another homozygous mutant (called *Shank3A*^{-/-}) in the same study which targeted the ANK domain and therefore only deleted the Shank3A full isoform but retained expression of Shank3B and Shank3C, displayed preference for a chamber containing a social stimulus over an empty chamber in the same assays, similar to wild-type mice. However, *Shank3A*^{-/-} mutants showed a deficit in social novelty as they did not show a significant preference for a novel over a familiar stranger as observed in wild-type mouse behavior. Both male and female *Shank3B*^{-/-} mice also showed marked repetitive behaviors in the form of self-grooming to the point of self-injurious lesions. Although *Shank3B*^{-/-} mice evidently demonstrated phenotypes analogous to symptom manifestation in ASD, particularly diminished social interaction and surges in repetitive

behaviors, it is important to note that the *Shank3B*^{-/-} mice were also reported to exhibit seizures upon handling as well as increased anxiety-like behaviors, as demonstrated by decreased exploration in both the elevated zero maze and light-dark emergence test. In contrast, *Shank3A*^{-/-} mice did not exhibit lesions, seizures, nor heightened anxiety-like behaviors. Although the *Shank3B*^{-/-} mouse model at first appears promising for translational ASD research, it is important to note that this mutation causes loss of nearly all *Shank3* protein function, which does not parallel heterozygous loss of function mutations causing truncated *Shank3* proteins typically identified by genetic analysis in ASD patient cohorts (Ramaswami & Geschwind, 2018). While *Shank3* mutations associated with ASD risk in humans suggest a haploinsufficiency model of *Shank3* function, the *Shank3B*^{-/-} mutant described by Peça et al. represents a more severe phenotype with homozygous loss of *Shank3* function, as implied by the reported seizures and increased anxiety in addition to ASD related symptoms.

Wang et al. utilized homologous recombination in mice to delete *Shank3* exons 4-9, which code for the ANK domain, similar to Peça et al.'s *Shank3A*^{-/-} mice, in an attempt to model the de novo SNV missense mutations that have been reported in exons 5-9 in ASD patient populations (Wang et al., 2011). This mutation caused a frame shift with a stop codon in exon 11, and Western Blot analysis with a C-terminal antibody revealed that the full length *Shank3* protein was absent (*Shank3A*), while smaller size isoforms, presumably *Shank3C* and *Shank3D* were present. Sequencing of RT-PCR products further described homozygous *Shank3*^{Δ4-9} mice as lacking both *Shank3A* and *Shank3B* transcripts, while confirming *Shank3C*, *D*, and *E* are conserved, as expected from known intragenic promoters downstream of the mutation. Behaviorally, both male and female

homozygous *Shank3*^{e4-9} mice showed significant deficits in social behavior in the form of decreased preference for a social stimulus over an inanimate stimulus, as compared to wild-type animals, with *Shank3*^{e4-9} females showing more interaction with the social stimulus than *Shank3*^{e4-9} males. However, no deficit was observed for either sex in the preference for social novelty, as both male and female homozygous *Shank3*^{e4-9} mice showed wild-type-like preference for a novel social stimulus over a familiar social stimulus. Homozygous *Shank3*^{e4-9} mice also demonstrated deficits in social behavior in the dyadic interaction test, in which both male and female mutants spent significantly less time socially investigating, as compared to wild-type mice, in bidirectional interactions with a wild-type mouse, and notably never initiated the first interaction with the wild-type mouse. Homozygous *Shank3*^{e4-9} mice also demonstrated increased repetitive behaviors, and deficits in learning and memory, and males but not females demonstrated mild motor learning impairments. These data represent a clinically relevant *Shank3* mutation and possible loss-of-function social deficits related to specifically 5'-derived isoform loss, particularly function of the ANK, SH3, and PDZ domains. However, again these behavioral phenotypes were only observed in homozygous mutants, which does not mimic the heterozygous mutations described in ASD patients.

To specifically investigate the effect of haploinsufficiency of *Shank3* on mouse social behaviors, in a model more analogous to ASD-associated mutations, Bozdagi et al. developed a *Shank3* mutant mouse line similar to Wang et al. (2011), in which the ANK domain is directly disrupted by conditional deletion of exons 4 through 9 by Cre recombinase (Bozdagi et al., 2010). Mice heterozygous for this mutation showed a 50% reduction in full-length *Shank3* mRNA, by qPCR, as well as reduced expression of the

full-length protein, by Western Blot, consistent with a haploinsufficiency model of Shank3 function. Interestingly, male mice heterozygous for this mutation showed significantly less time socially sniffing and emitted fewer ultrasonic vocalizations than their wild-type siblings in a 5 minute freely moving social interaction test with wild-type females. While this mouse model most closely genetically represents ASD-associated mutations, the limited repertoire of social behaviors displayed by mice, as well as the absence of adult social attachment behaviors in this species, precludes phenotypic modeling of the specific social deficits in ASD.

Two subsequent studies generated distinct mouse models of *Shank3* mutations in exon 21, in an effort to more precisely mimic the inherited SNV of a G insertion in exon 21 and disruption of Homer binding domain identified by Durand et al. (2007) in two brothers with ASD (Kouser et al., 2013; Zhou et al., 2016). Both studies report that homozygous mutants demonstrate deficits in social interaction behaviors, again consistent with the gene's association with ASD-related symptoms. Kouser et al. deleted all of exon 21 in mice using Cre-mediated excision. Mice homozygous for this deletion (*Shank3^{ΔC/ΔC}*) showed a loss of the largest 3 isoforms of Shank3, as identified by C-terminal, SH3 domain, and N-terminal antibodies in Western Blot, although the N-terminal antibody did identify isoforms of smaller sizes. This suggests that *Shank3^{ΔC/ΔC}* mice have total loss of the Shank3C isoform but may retain partial or truncated versions of the Shank3B isoform. In the three chamber arena sociability tests, *Shank3^{ΔC/ΔC}* mice demonstrated preference for a social stimulus over an inanimate stimulus similar to wild-type mice; however *Shank3^{ΔC/ΔC}* mice did not discriminate between preference for a novel mouse over a familiar mouse, as compared to the significant preference for social novelty

displayed by wild types. The authors report this finding as minimal social interaction deficits in the *Shank3*^{ΔC/ΔC} mice, and additionally characterize these homozygous mutants as displaying reduced spatial learning, memory, and motor coordination, hypersensitivity to heat, and novelty avoidance. Meanwhile, heterozygous mutants did not show any of these phenotypes, suggesting again a more severe developmental phenotype associated with homozygosity for this allele rather than as a consequence of the heterozygous mutation analogous to those associated with ASD. Interestingly, deficits in motor coordination and novelty avoidance have also been described in ASD patients, suggesting that perhaps the 3'-derived isoforms of *Shank3*, including the Homer to mGluR binding domain play a role in these functions, while the 5'-derived isoforms, including Shank3B and corresponding domains are more involved in the social behaviors disrupted by ASD-associated mutations.

Zhou et al. used homologous recombination to generate *Shank3* mutant mice with the precise SNV G insertion in exon 21 (InsG3680) reported by Durand et al. (2007), which causes a frame shift and consecutive stop codon, disrupting the Homer to mGluR binding domain (Zhou et al., 2016). By Western Blot analysis, they report that InsG3680 homozygotes show a full loss of isoforms identified by a C-terminal antibody. Although they predicted N-terminal antibodies may detect Shank3A and Shank3B isoforms truncated at the point of mutation, these were also not detected. Contrary to Kouser et al., Zhou et al. describe more significant social deficits in adult social behavior of InsG3680 homozygotes. These mutants do not show preference between a social stimulus and an inanimate stimulus, nor a preference between a novel and a familiar stimulus in contrast to the significant sociability and social novelty preferences of wild-

type mice. Although not seen in Kouser et al.'s *Shank3*^{ΔC/ΔC} mutants, the InsG3680 homozygotes showed a significant deficit in juvenile social play behavior at postnatal day 23, as measured by significantly decreased anogenital sniffing as well as following behavior. Consistent with studies of other mutants, InsG3680 homozygotes also showed self-injurious skin lesions as a result of repetitive grooming. As seen in previous mouse models, the mice heterozygous for this mutation demonstrate no phenotype of social deficit as either adults or juveniles, nor heightened repetitive behaviors. InsG3680 homozygotes also showed deficits in motor learning and coordination, consistent with Kouser et al.'s findings of the functional impact of disrupting exon 21 of *Shank3*.

Extensive investigations of various, discrete *Shank3* mutations in the mouse have linked *Shank3* functionality and behavior deficits analogous to behaviors described in ASD. As stated above, one major critique of the *Shank3* mouse models is that they generally identify behavioral phenotypes in homozygous mutants, while the loss of function mutations identified in ASD patient cohorts are usually heterozygous in nature, with one wild-type *Shank3* allele conserved in symptomatic probands. Therefore, evaluation of homozygous mutant mouse models may be describing much more severe developmental or systemic phenotypes than those present in patients with ASD. As mentioned, a second major caveat of *Shank3* mouse models is that the limited array of social behaviors available for characterization, such as preference for a social versus nonsocial stimulus, and novel social stimulus versus familiar social stimulus, may be too simple to be considered as analogous to the social attachment deficits in ASD. Adult mice do not form social attachments with other adult mice, including mating partners. Thus, the basic neural circuitry underling social approach in mice may not even include the

components of social attachment behavior that are altered in ASD. Therefore, to truly investigate the role of ASD-associated *Shank3* mutations in social behaviors disrupted in ASD, we have utilized the socially monogamous prairie vole, and characterized multiple facets of their specific adult social attachment behaviors affected by heterozygous loss of function mutations in genes associated with ASD.

Recently, Zhou et al. generated a primate model of ASD-associated *Shank3* mutants to further investigate the role of disrupted *Shank3* functionality in a system more similar to the human brain (Zhou et al., 2019). They used CRISPR-mediated mutagenesis to target exon 21 in the macaque (*Macaca fascicularis*), with the rationale of modeling the inherited SNV identified by Durand et al. (2007) and modeled in the mouse by Kouser et al. (2013) and Zhou et al. (2016). Because of many costs associated with breeding macaques in the laboratory, the authors focused on 5 mutagenized generation zero (G0) subjects which harbored a combination of homozygous, compound-homozygous, and heterozygous mutations, some with genetic mosaicism for multiple alleles. These mutants demonstrated impaired social interaction, as measured by a significant decrease in aggregate prosocial behaviors in a juvenile social interaction assay, as compared to wild-type macaques. Additionally, the mutants showed severe sleep disturbances, motor deficits, and increased repetitive behaviors. A major benefit of modeling the *Shank3* mutation in a primate is the potential to quantify changes in social behavior more related to patterns of behavior in humans, and thus to uncover phenotypes relevant to improving diagnosis in patients. For example, the authors noted that the *Shank3* mutant macaques demonstrated alterations in pupillary reflex and gaze fixation also noted in young children who will present ASD symptoms. However, as detailed in this study, the major caveat to

the primate model is lack of abundance of a standardized and controlled *Shank3* mutant line, which is necessary to control the relevant isoforms expressed and map disrupted *Shank3* functional domains to their relevant behavioral deficits. Therefore, while the Zhou et al. (2019) study is a powerful example of how *Shank3* mutations may manifest clinically relevant social affiliation, or attachment, deficits, the prairie vole is a unique model to study the effects of *Shank3* mutations on social attachment behaviors in a tractable and scalable rodent system.

Environmental etiology of social attachment deficits

In addition to the genetic component of ASD described above, environmental factors have also been proven to impact presentation of ASD symptoms, and specifically impact deficits in adult social attachment behaviors. Aligning with the early life symptom manifestation of ASD, the environmental etiology of social attachment deficits centers around experiences of early life, particularly early life stresses including prenatal and perinatal factors, socioeconomic status, and drugs and toxic exposure (Fuld, 2018; Chaste & Leboyer, 2012). Early life stress has been attributed to increased adult vulnerability across many psychiatric diseases, with 80% of adults who report early life neglect or abuse being diagnosed with a psychiatric disorder (Lukkes et al., 2009b).

Last year, Castlebaum et al. described a theory of ASD symptom etiology in which the genetic component explains more susceptibility to ASD than previously reported, while the severity and presentation of ASD symptoms is modified by environmental experience more than genetic components (Castlebaum et al., 2020). This study quantified sub-clinical autistic traits between discordant monozygotic twins, genetically

identical twins in which one has been diagnosed with ASD and the other has not. The trait measurements focused on observations of patients in naturalistic social settings using The Social Responsiveness Scale, and measures of social affect score to evaluate social deficit severity, using the Autism Diagnostic Observation Schedule (Constantino & Gruber, 2012; Lord et al., 2000). Even in twins that were labeled discordant by diagnosis, the unaffected twin showed sub-clinical social deficits on both scales. This suggests that the genetic risk to ASD may be concordant between all monozygotic twins, and presents a susceptibility to manifesting ASD traits that is then affected by environmental experience to result in symptomatic pathology and perhaps scales to severity. These data indicate that environmental factors may play a direct role in manifestation of social attachment deficits, though this may depend on the genetic susceptibility of an individual.

Studies using various approaches have described how early life stress contributes to ASD risk. For example, Magnusson et al. investigated how parental migration status impacted child ASD risk, and found that children of migrant parents to Sweden had an increased risk of low-functioning ASD, including intellectual disability (Magnusson et al., 2012). This risk was increased if the parents migrated from a country with a low human development index, indicating a more stressful experience, and peaked when migration occurred during pregnancy. A similar risk for high-functioning ASD was not observed, and the authors conclude that high- and low- functioning ASD may arise from different mechanisms, a hypothesis further supported by whole exome sequencing of large ASD patient cohorts (Iossifov et al., 2014).

Rutter et al.'s longitudinal studies of 324 children adopted within the UK provide some of the most direct evidence supporting the contribution of stressful early life

environments to social deficits consistent with ASD (Rutter et al., 2007a&b). They compared behavior of 11-year-old children raised in socially deprived institutions in Romania with children who were not raised in deprived institutions and adopted before the age of 6 months. Disinhibited attachment, defined by lack of selectivity in social relationships particularly between a parent and a stranger, was measured by an investigator-based semi-structured interview and strongly correlated with institutional rearing. This correlation agrees with previous diagnosis of an attachment disorder by clinical professionals among 10 children, all of the Romanian institution. They also measured patterns of ASD-like behaviors at ages 6 and 11 through standardized interviews and report that 1 in 10 children raised in the Romanian institution present with ASD-like symptoms, including impaired social relationships. The consequences of such impairments included overall disinhibited attachment, which persisted until age 11, sometimes 7 years after adoption into well-functioning families. They distinguish these symptoms from clinically defined ASD because although some children met ASD criteria at age 6, some of their symptoms were diminished by age 11, which is not typical of ASD. However, in children that presented with ASD-like symptoms at age 6, over half continued to present disinhibited attachment and poor peer relationships by age 11, indicating that early life environmental and social stress can increase risk specifically for disruptions in social attachment behaviors. The persistence of these symptoms through resocialization may indicate that the human brain experiences a critical period of development for social and attachment behaviors before 6 years of age, and that stresses during this developmental period may affect underlying attachment mechanisms of the adult brain.

In this dissertation, we therefore sought to investigate how genetic factors as well as environmental factors, in the form of early life social deprivation, may impact the prairie vole's profound displays of adult social attachment.

Summary

In the present series of studies, we utilize molecular and genetic techniques amenable to the prairie vole to explore how distinct mutations in *Shank3* and early life stress impact the reliable and robust adult social attachment behaviors of pair bonded voles. The main questions we ask are:

- 1) How do distinct heterozygous mutations in *Shank3* similarly and differentially disrupt adult attachment behaviors and corresponding neuroanatomy in male and female prairie voles?
- 2) Does early life social isolation in prairie voles disrupt adult pair bond expression even after resocialization?
- 3) Do male and female voles use different sensory cues to determine expression of partner preference?

Chapter 2: The Role of *Shank3* in Adult Social Attachment Behaviors

INTRODUCTION

The ability to form and express social relationships is vital to one's role in society and well-being. Specifically, the complex behavior of social attachment is necessary to maintain successful bonds with other individuals throughout life. Deficits in adult social attachment behaviors and ensuing disruptions in social relationships are observed across many psychiatric diseases, and are fundamental diagnostic criteria for Autism Spectrum Disorders (ASD) (Baird et al., 2003). Genomic sequencing of large patient databases reveals a strong genetic component of ASD, and has identified many high risk genes that contribute to ASD pathogenesis (Rylaarsdam et al., 2019; Grove et al., 2019). However, ASD is a clinically heterogenous disorder, and the contribution of any specific mutation in one of these risk genes to an explicit behavior consistent with ASD is not well understood. The main hindrance to investigating the role of specific mutations in the pathogenesis of ASD-related social deficits is that the common mammalian model organism of neuroscience, namely the house mouse *Mus musculus*, does not innately express social attachment between mature adults.

In the present study, we utilize the socially monogamous prairie vole, *Microtus ochrogaster*, as a model to explore the role of discrete mutations in a high risk ASD gene in complex adult social attachment behaviors between mating partners. Adult prairie voles form lifelong enduring attachments between mates, defined as a pair bond (Carter and Getz, 1993; McGraw and Young, 2010). Conveniently, prairie voles display formation and maintenance of this pair bond under laboratory conditions, and the strength of the pair bond can be reliably and robustly quantified through behavioral assays. Our lab has

recently developed the use of CRISPR-Cas9 mutagenesis in prairie voles to generate targeted mutations along the vole genome.

Shank3 (SH3 and multiple ankyrin repeat domains 3) has been identified by several genome sequencing studies as a high risk gene for both heritable and de novo mutations associated with ASD (Durand et al., 2007; Moessner et al., 2007; Gauthier et al., 2009; Sanders et al., 2015). *Shank3* encodes a large scaffolding protein containing a number of distinct protein-protein interaction domains, and is localized to the postsynaptic density of glutamatergic synapses (Naisbitt et al., 1999). Extensive work has demonstrated that Shank3 regulates glutamatergic signaling and plasticity, and actin cytoskeleton development, structure, and dynamics (Sheng et al., 2011). Previous work has detailed the many intragenic promoters and alternative splicing events of mouse *Shank3*, revealing that Shank3 protein is expressed as several different isoforms, each containing a unique combination of its 5 functional protein-protein interaction domains (Wang et al., 2014). Genome sequencing studies in large ASD patient cohorts have identified unique mutations in many varied domains of *Shank3* that do not converge on disruption of a single isoform or combination of isoform expression (Waga et al., 2011; Gong et al., 2012; Boccuto et al., 2013). The correlation between specific mutations in *Shank3* and related symptom manifestations of ASD remains to be characterized.

Several mouse studies have investigated the behavioral phenotypes associated with targeted mutations in *Shank3* (Peça et al., 2011; Wang et al., 2011; Bozdagi et al., 2010; Kouser et al., 2013; Zhou et al., 2016). Notably, mice with mutations in exon 21, corresponding to a familial ASD mutation identified by Durand et al., 2007 and which disrupts the 3'-derived isoforms involved in metabotropic glutamate receptor (mGluR)

signaling, demonstrate reduced sociability, diminished preference for social novelty, and deficits in juvenile play behavior, as well as increased repetitive behavior such as self-grooming (Kouser et al., 2013; Zhou et al., 2016). Mouse models with mutations in exons 4-9 and 13-16, also based on unique mutations identified through human genomic sequencing, which disrupt 5'-derived isoforms involved in NMDAR and AMPAR signaling, and actin cytoskeleton dynamics, also show decreased sociability and increased repetitive behaviors (Peça et al., 2011; Wang et al., 2011; Bozdagi et al., 2010). However, mice do not demonstrate complex social bonds between adults and without this finer resolution of social behaviors, determining the specific mutations in *Shank3* that contribute to specific social deficits in ASD through a mouse model is not possible. Although ASD is an inherently human disorder, here we identify behavioral deficits that more closely resemble symptoms experienced by patients by describing discrete changes in social behavior as measured by pair bond formation and maintenance in prairie voles.

The neurobiology of prairie vole attachment has been recognized as translationally applicable to human attachment, as the neuropeptides oxytocin (OT) and vasopressin (AVP) have been implicated in modulating social attachment, mating, parental behaviors, social reward, social learning, and memory behaviors across both species (Carter et al., 2008; Insel and Shapiro, 1992; Meyer-Lindenberg et al., 2011). Recent studies in mice have demonstrated that socially rewarding stimuli increases activity of OT neurons in the paraventricular nucleus of the hypothalamus (PVN), and that activation of these neurons is necessary for sociability (Resendez et al., 2020). Interestingly, Resendez et al. further demonstrated that *Shank3b*^{-/-} mice (a mutation in the 5' derived isoforms) express decreased levels of OT positive cells in the medial PVN, and that intraperitoneal

administration of an OT agonist rescues the social deficits of *Shank3b^{-/-}* mice. Together these data suggest that dysfunction of oxytocinergic signaling may be responsible for the social deficits observed in ASD and their analogous mouse models.

In this work we characterize the contribution of two distinct *Shank3* mutations in the prairie vole on adult social attachment behaviors throughout pair bond formation and maintenance. We used CRISPR-Cas9 mutagenesis to generate 2 *Shank3* mutant vole lines. In the first line, we targeted *Shank3* exon 9 and caused a premature stop codon in the ankyrin repeat domain of *Shank3*, which we predict disrupts the binding sites for alpha-fodrin, which regulates the actin cytoskeleton; and sharpin, which mediates homomultimerization of the Shank protein complex; as well as the downstream Src homology 3 domain (SH3), which interacts with the C-termini of AMPA receptors through an adapter protein GRIP. (Ebert and Greenberg, 2013; Costales and Kolevzon, 2015; Lim et al., 2001). In the second line, we targeted *Shank3* exon 14 and caused a premature stop codon in *Shank3*'s highly conserved PDZ-domains which, also based on homology to mouse, we predict code for binding sites for guanylate kinase-associated protein (GKAP), a scaffolding molecule involved in synaptic signaling of NMDA receptors via PSD-95/SAP90 proteins. (Shin et al., 2012).

We evaluated both female and male *Shank3* mutant voles in equivalent behavioral assays, as sexually dimorphic effects of genetic contribution to ASD risk have been reported in humans (Rylaarsdam and Guemez-Gamboa, 2019; Zhang et al., 2020). As prairie voles have more robust and nuanced displays of adult social attachment than mice, we sensitized our model from previous homozygous mutant mouse models by using only heterozygous mutant voles in behavior, to recapitulate the haploinsufficiency of

Shank3 function observed in patients with ASD. Finally, we investigated if social attachment deficits in our mutant vole cohort are associated with changes in OT or AVP expression in the PVN.

Our study provides novel evidence for a mutation- and sex- specific effect of *Shank3* on adult social attachment behavior in the prairie vole model. We find that female, but not male, voles heterozygous for a 10 base pair deletion in exon 9 show diminished attachment when bonded with a male mating partner. However, a 4 base pair disruption in exon 14 does not significantly alter expression of attachment behaviors associated with the pair bond in either sex. We explore frameworks and future experiments to elucidate which functional domains of *Shank3* are differentially expressed between these two mutants, and thus contribute to adult social attachment deficits.

RESULTS

Generation of *Shank3* mutant prairie voles

In order to generate *Shank3* mutant prairie vole lines, we utilized a protocol to harvest large quantities of single cell embryos from female prairie voles. Female prairie voles do not ovulate cyclically, as in mice and most mammals, but must be induced into ovulation by mating and sensory cues from male prairie voles (Carter et al., 1987). Therefore, we developed a timed mating protocol in which we synchronize mating time between pairs in order to harvest 12 hour old, single cell embryos (Figure 2.1).

The prairie vole *Shank3* gene has 92.8% alignment coverage when compared to the mouse *Shank3* gene, and functional domains are highly conserved (Figure 2.2). We

designed 18 small guide RNAs (sgRNAs) to sites along the prairie vole *Shank3* gene, and through the cloning process and a screen for potential off-target effects, we selected 6 sgRNAs for mutagenesis. Of these 6, 2 each specifically target *Shank3* exon 9, exon 14, and exon 22, regions which each code for unique protein interaction domains (Figure 2.2). Exon 9 includes ankyrin repeats, which mediate protein-protein interactions. Based on homology to the mouse genome, we expect exon 9 in the prairie vole *Shank3* sequence to code for binding sites for alpha-fodrin, which regulates the actin cytoskeleton, and sharnin, which mediates homomultimerization of the Shank protein complex (Ebert and Greenberg, 2013; Costales and Kolevzon, 2015; Lim et al., 2001). Exon 14 encodes highly conserved PDZ-domains which, also based on homology to mouse, we predict codes for binding sites for guanylate kinase-associated protein (GKAP), a scaffolding molecule involved in synaptic signaling of NMDA receptors via PSD-95/SAP90 proteins (Shin et al., 2012). By nonsense mediated decay, missense mutation, or a premature stop codon, a successful mutagenesis event in either exon 9 or 14 could also disrupt the Src homology 3 (SH3) domains of exons 11 and 12, which code for interaction with GRIP, an adapter protein that directly interacts with the C-termini of AMPA receptors. Exon 22 contains proline rich domains of conserved recognition sites for docking proteins including Homer, which directly interacts with metabotropic glutamate (mGluR) receptors, and cortactin, which also regulates actin cytoskeleton dynamics.

We performed 4 rounds of electroporation on ~30 embryos each, using either 2 or 4 sgRNAs per round. Each round of electroporation yielded 10-22 viable blastocysts that were transferred into a pseudopregnant female prairie vole, who was previously induced into estrous by mating and cohabitation with a vasectomized male. Each recipient female

successfully birthed a litter of pups, generating a total of 15 G0 pups from all 4 electroporation events. Of the G0 pups, 14 were male and 1 was female (Table 2.1).

We genotyped and screened samples of tail DNA from all G0 pups and found the one G0 female had a heterozygous 10bp deletion in exon 9 (*Shank3*^{ΔE9/+}), targeted by sgRNA-K (GTAATCAAGACCCACAAAGACT) (Figure 2.3). This deletion causes a frame shift in the *Shank3* gene and predicting the protein structure indicates a premature stop codon.

We next bred 14 G0 voles to wild-type outcrossed prairie voles. We collected between 1 to 7 litters from each pair and screened every F1 pup for possible CRISPR-mediated mutagenesis in *Shank3*. Fortunately, we found that the *Shank3*^{ΔE9/+} mutation identified in the female G0 had successfully penetrated the germline, and all F1 pups of this pair expressed the mutation with Mendelian inheritance.

Among the F1 generation from the remaining G0 breeding pairs, we identified 3 more heterozygous unique mutations in *Shank3*, consistent with sites targeted by our sgRNAs (Table 2.2). Our sgRNA-N (ATGACAGCCTCACTTCACAC) successfully generated 2 unique mutation events found in 2 different lines. One mutation, *Shank3*^{ΔE14/+}, is a 4bp deletion in exon 14, responsible for a full frame shift and also predictive of a premature stop codon in Shank3 protein. The second mutation by sgRNA-N is a 3bp deletion and a 1bp substitution in exon 14, not indicative of a frame shift nor any significant changes to amino acids. Our third identified mutation was also targeted by sgRNA-K in exon 9, and is a single 3bp substitution. This mutation did not predict any changes into a stop codon or frame shift, so it is unlikely to significantly alter Shank3 protein function (Figure 2.3).

Therefore, we continued to breed and outcross heterozygous *Shank3*^{ΔE9/+} and *Shank3*^{ΔE14/+} voles with wild-type voles in our behavior colony. We outcrossed each line, alternating males and females as the mutant carrying parent, until we generated an F7 generation for both mutations, to separate *Shank3* mutations from unlinked possible off target effects of CRISPR-mediated mutagenesis. For each mutation, we maintained 4 heterozygote to wild-type breeding pairs, as well as 2 heterozygote to heterozygote breeding pairs, in order to generate homozygotes, heterozygotes, and control wild-type siblings for both exon 9 (ΔE9) and exon 14 (ΔE14) mutations.

We developed 2 unique genotyping schemes to identify wild-type and mutant alleles of each mutation. To identify the 10bp deletion in exon 9, of *Shank3*^{ΔE9/+} voles, we designed one universal oligonucleotide reverse primer (REV2_ex9sh3) that would anneal to either allele. We also designed two oligonucleotide forward primers that have specificity to either only the wild-type allele (wtB_ex9sh3), by including and ending in the ten base pairs deleted in the mutant, or have specificity to only the mutant allele (delB_ex9sh3), by spanning the 10bp deletion with 21bp before the deletion and a critical 2bp after the mutation (Figure 2.4 A,B). Following many genotyping strategies, we found the highest specificity between wild-type and mutant alleles when the final 2bp of the forward primer were in a unique sequence, for example within the deletion or precisely 3' of the deletion. This strategy yielded a unique 513bp wild-type allele product with wtB and REV2 primers, and a unique 521bp mutant allele product with delB and REV2 primers (Figure 2.4 A,B). Therefore, this scheme was able to distinguish between wild-type, heterozygote, homozygote genotypes of the 10bp deletion ΔE9 mutation. We also developed primers (g,Sh3,6) to amplify a 958bp sequence spanning all of exon 9 and intronic region on either

side, which could be sent with a unique sequencing primer (s,Sh3,6a) 359bp 5' of the mutation to confirm genotype of any DNA sample by Sanger sequencing (Figure 2.4 C,D).

Alternatively, to identify the 4bp deletion in exon 14, of *Shank3*^{ΔE14/+} voles, we designed a PCR amplification reaction to isolate a 120bp band including all of exon 14, and then performed a restriction enzyme digest on this product to visualize a unique footprint of bands for either wild-type, heterozygote, or homozygote genotypes of ΔE14 alleles (Figure 2.5 A). The restriction enzyme CviKI-1 has a recognition site found in the wild-type allele, but not the mutant allele. Therefore, a wild-type animal is identified by a full digestion to 2 bands (77bp and 43bp), a heterozygote is identified by a mixture of digested and non-digested product in 3 bands (120bp, 77bp, and 43bp), and a homozygote is identified by a lack of digestion and intact 120bp product (Figure 2.5 B). The FWD primer to amplify the 120bp product can also be used as a sequencing primer to genotype the ΔE14 allele by Sanger sequencing (Figure 2.5 C).

Shank3 protein characterization of 2 distinct *Shank3* mutant prairie vole lines

We next characterized differences in expression of Shank3 protein isoforms between wild type and ΔE9 and ΔE14 mutants. We performed Western Blot analysis on brain tissue collected from wild-type voles, and voles homozygous for each mutation, for both males and females. Investigations into the protein structure of mouse Shank3 has uncovered many intragenic promoters and alternative splicing sites that yield translation of an extensive array of unique isoforms of Shank3 protein (Wang et al., 2014). We used the UCSC Genome Browser annotation on the mouse *Shank3* gene (mG8/mm10) to identify intragenic promoter regions and aligned them to the vole genome (Figure 2.6).

The respective sequences in the vole aligned with 92-95% conservation to the mouse. These promoter regions were in agreement with respective isoforms described in mouse and we mapped the 5 most prevalent isoforms to the prairie vole *Shank3* gene based on homology to annotation in the mouse (Figure 2.6).

We collected brains of 8-10 week old animals, sliced them into 4 sagittal sections, flash froze them on dried ice and stored at -80C. We used the Santa Cruz *Shank3* antibody (sc-30193), which has an epitope with 98% alignment to prairie vole, located at the end of exon 22. We found that both male and female prairie voles homozygous for either mutation no longer express the full *Shank3* protein of 190kDa band (Figure 2.7; Female: 2way ANOVA interaction $p < 0.0001$; Dunnett's multiple comparisons test: Wild Type vs *Shank3* ^{$\Delta E9/\Delta E9$} $p < 0.0001$, Wild Type vs *Shank3* ^{$\Delta E14/\Delta E14$} $p < 0.0001$; Male: 2way ANOVA interaction 0.0107, Wild Type vs *Shank3* ^{$\Delta E9/\Delta E9$} $p = 0.0058$, Wild Type vs *Shank3* ^{$\Delta E14/\Delta E14$} $p = 0.0061$).

Both *Shank3* ^{$\Delta E14/\Delta E14$} males and females also showed a loss of the second largest protein band ~160kDa bound by this *Shank3* antibody, which has been identified as the *Shank3c* and *Shank3d* isoform according to the mouse genome (Figure 2.7; Dunnett's multiple comparisons test: Female: Wild Type vs *Shank3* ^{$\Delta E14/\Delta E14$} $p < 0.0001$; Male: Wild Type vs *Shank3* ^{$\Delta E14/\Delta E14$} $p < 0.0001$). The complete loss of the ~160kDa band was not seen in the *Shank3* ^{$\Delta E9/\Delta E9$} voles, which was expected because the promoter for *Shank3c* and *Shank3d* isoforms occurs just 5' of exons 12 and 13, respectively, which is downstream of the $\Delta E9$ mutation and shortly upstream of the $\Delta E14$ mutation. This leads us to hypothesize that the $\Delta E14$ mutation disrupts both *Shank3c* and *Shank3d* isoforms by generating a severely shortened version of the respective mRNA that is subject to

nonsense mediated decay, while expression of the full protein is not hindered by the $\Delta 9$ mutation upstream of the promoters for these isoforms. Similarly, both *Shank3* ^{$\Delta E14/\Delta E14$} females and males showed a decrease in expression of the ~150kDa band. This band may indicate a splice variant of isoform Shank3d whose protein structure is not affected by the $\Delta E14$ mutation, but still manifests decreased expression levels as a consequence of $\Delta E14$, but not $\Delta 9$, mutations (Figure 2.7; Dunnett's multiple comparisons test: Female: Wild Type vs *Shank3* ^{$\Delta E14/\Delta E14$} $p < 0.0001$; Male: Wild Type vs *Shank3* ^{$\Delta E14/\Delta E14$} $p = 0.0321$).

Interestingly, *Shank3* ^{$\Delta E9/\Delta E9$} females, but not males, show a decrease in protein expression of the ~160kDa band Shank3c/d isoform (Figure 2.7; Dunnett's multiple comparisons test: $p = 0.0084$), indicating that although this isoform may be intact, the $\Delta 9$ mutation alters expression level, possibly in a sex-specific manner. Consistently, we also found a distinct sex difference in the expression level of two of the largest protein bands of Shank3 identified with this antibody, bands ~140kDa and ~100kDa, which likely correspond to Shank3e and Shank3f isoforms, respectively, based on annotation of the mouse genome. *Shank3* ^{$\Delta E9/\Delta E9$} and *Shank3* ^{$\Delta E14/\Delta E14$} females, but not males, show a decrease in expression level for both of these bands as compared to wild-type females (Figure 2.7; Dunnett's multiple comparisons test: 140kDa: Wild Type vs *Shank3* ^{$\Delta E9/\Delta E9$} $p = 0.0067$, Wild Type vs *Shank3* ^{$\Delta E14/\Delta E14$} $p < 0.0001$; 100kDa: Wild Type vs *Shank3* ^{$\Delta E9/\Delta E9$} $p < 0.0001$, Wild Type vs *Shank3* ^{$\Delta E14/\Delta E14$} $p < 0.0001$). The mechanisms of how mutations not localized within an isoform can affect expression levels of said isoform requires further investigation. Alternately, decreases in expression level of certain bands may be explained by redundancy of band size with not yet described isoforms and splice variants of prairie vole Shank3 protein that include mutation sites.

Heterozygous *Shank3* mutant prairie vole lines do not show differences in exploratory behaviors and locomotor activity compared to their same-sex wild-type siblings

To investigate exploratory and anxiety-like behaviors, sociability, social novelty, and general locomotor activity in our *Shank3* mutant prairie vole lines, we devised a 3 day paradigm of control behavior assays (Figure 2.8). The Open Field Test (OFT) is a standard assay in animal behavior to measure exploratory and anxiety-like behaviors. We constructed an OFT arena of 22" x 22" with 15" high walls, built proportionally for the size of the prairie vole, as based on relative standard sizes for the mouse and rat. We utilized automated scoring based on contour tracing, developed in the Manoli Lab, to track the position of the prairie vole and assign it to either the "center zone," the 11"x11" central square of the arena, or the "edge zone," the outer perimeter of the arena (Figure 2.9 A,B). More time in the center zone is correlated with more exploratory behavior and less anxiety-like behaviors (Walsh & Cummins, 1976).

As expected, both sexes spent significantly more time in the Edge zone than Center zone, regardless of genotype (Figure 2.9 C; Two-way repeated-measures ANOVA shows Zone accounts for 97.39% of variation, $p < 0.0001$; with Bonferroni's multiple comparisons $p < 0.0001$ for all 8 genotype x sex conditions). Females and males of both *Shank3* ^{$\Delta E9/+$} and *Shank3* ^{$\Delta E14/+$} genotypes showed no significant difference in time spent in center and edge zones when compared directly to their same-sex wild-type siblings (Figure 2.9 D,E; Mann-Whitney Test: Female Wild Type $\Delta E9$ Sibling vs Female *Shank3* ^{$\Delta E9/+$} $p = 0.8148$; Female Wild Type $\Delta E14$ Sibling vs Female *Shank3* ^{$\Delta E14/+$}

p=0.5787; Male Wild Type $\Delta E9$ Sibling vs Male *Shank3* ^{$\Delta E9/+$} p=0.4234; Male Wild Type $\Delta E14$ Sibling vs Male *Shank3* ^{$\Delta E14/+$} p=0.2345). *Shank3* ^{$\Delta E9/+$} and *Shank3* ^{$\Delta E14/+$} females and males also showed no difference in locomotor activity, as measured by total distance traveled, when compared directly to their same-sex wild-type siblings (Figure 2.9 F; Mann-Whitney Test: Female Wild Type $\Delta E9$ Sibling vs Female *Shank3* ^{$\Delta E9/+$} p=0.8884; Female Wild Type $\Delta E14$ Sibling vs Female *Shank3* ^{$\Delta E14/+$} p=0.1051; Male Wild Type $\Delta E9$ Sibling vs Male *Shank3* ^{$\Delta E9/+$} p=0.2359; Male Wild Type $\Delta E14$ Sibling vs Male *Shank3* ^{$\Delta E14/+$} p=0.6454). These data indicate that *Shank3* ^{$\Delta E9/+$} and *Shank3* ^{$\Delta E14/+$} voles have similar locomotor activity, and exploratory and anxiety-like behaviors as compared to their same-sex wild-type siblings. Additionally, we have established an open field paradigm using a 22in² arena which induces thigmotaxis and/or centrophobicity in the prairie vole, as seen in all sex and genotype groups (n=70).

Heterozygous *Shank3* mutant prairie voles do not show differences in sociability and social novelty as compared to their same-sex wild-type siblings

We investigated if male and female *Shank3* ^{$\Delta E9/+$} and *Shank3* ^{$\Delta E14/+$} voles demonstrate differences in sociability as compared to their same-sex wild-type siblings. Sociability was assessed in the three chamber sociability test, in which we measured time spent between either a chamber containing a metal cup holding a naïve same-sex juvenile stranger vole (Stranger I) or a novel object (a wooden block), as well as time spent interacting with each stimulus. All assays were scored by contour tracing code developed in the Manoli lab, in which the duration of the vole in the chamber was

determined by summations of the centroid position of the contour, and interaction time was defined by touching of the vole contour to either the defined left or right cup contour.

Females and males of both *Shank3*^{ΔE9/+} and *Shank3*^{ΔE14/+} genotypes showed no significant difference in preference for the social stimulus as compared to their same-sex wild-type siblings, over measures of both time spent in chamber and interaction time (Figure 2.10 A,B; Two-way repeated-measures ANOVA, for each condition p-value is listed using Genotype as the source of variation: Female Wild Type ΔE9 Sibling vs Female *Shank3*^{ΔE9/+} Chamber: p=0.3638 Interaction: p=0.5094; Female Wild Type ΔE14 Sibling vs Female *Shank3*^{ΔE14/+} Chamber: p=0.1737 Interaction: p=0.1099; Male Wild Type ΔE9 Sibling vs Male *Shank3*^{ΔE9/+} Chamber: p=0.3532 Interaction: p=0.6852 Male Wild Type ΔE14 Sibling vs Male *Shank3*^{ΔE14/+} Chamber: p=0.1448 Interaction: p=0.1743). The sociability interaction index, in which a value >0 indicates a preference for the social stimuli, also indicates no significant difference between heterozygous animals and their wild-type siblings, when separating by sex (Figure 2.10 C; Mann-Whitney Test: Female Wild Type ΔE9 Sibling vs Female *Shank3*^{ΔE9/+} p=0.0721; Female Wild Type ΔE14 Sibling vs Female *Shank3*^{ΔE14/+} p=0.9626; Male Wild Type ΔE9 Sibling vs Male *Shank3*^{ΔE9/+} p=0.3176; Male Wild Type ΔE14 Sibling vs Male *Shank3*^{ΔE14/+} p=0.2786) (Rein et al., 2020). Males from both ΔE9 and ΔE14 families, as well as females from Δ9 families showed a significant preference for the social stimuli over novel object both by chamber time and interaction time, as previously reported in voles (Figure 2.10 A,B; Two-way repeated-measures ANOVA for each condition is listed p-value for Genotype as source of variation: Female Wild Type ΔE9 Sibling vs Female *Shank3*^{ΔE9/+} Chamber: p=0.0263 Interaction: p=0.0036; Male Wild Type ΔE9 Sibling vs Male *Shank3*^{ΔE9/+} Chamber:

p=0.0009 Interaction: p=0.0009; Male Wild Type $\Delta E14$ Sibling vs Male *Shank3* ^{$\Delta E14/+$} Chamber: p=0.0151 Interaction: p=0.0007) (Sailer et al., 2019; Horie et al., 2019). However, preference did not reach significance in females from $\Delta E14$ families (Figure 2.10 A,B; Two-way repeated-measures ANOVA, p-value for Genotype as source of variation: Female Wild Type $\Delta E14$ Sibling vs Female *Shank3* ^{$\Delta E14/+$} Chamber: p=0.2885 Interaction: p=0.1287).

Preference for social novelty was sequentially assessed by replacing the novel object of the sociability assay with a novel naïve same-sex juvenile vole (Stranger II) and allowing the subject vole 10 mins of investigation between Stranger I and Stranger II. Females and males of both *Shank3* ^{$\Delta E9/+$} and *Shank3* ^{$\Delta E14/+$} genotypes show no significant difference in preference for the novel Stranger II as compared to their same-sex wild-type siblings, over measures of both time spent in chamber and interaction time (Figure 2.10 D,E; Two-way repeated-measures ANOVA, for each condition is listed p-value for Genotype as source of variation: Female Wild Type $\Delta E9$ Sibling vs Female *Shank3* ^{$\Delta E9/+$} Chamber: p=0.6455 Interaction: p=0.5492; Female Wild Type $\Delta E14$ Sibling vs Female *Shank3* ^{$\Delta E14/+$} Chamber: p=0.2301 Interaction: p=0.3925; Male Wild Type $\Delta E9$ Sibling vs Male *Shank3* ^{$\Delta E9/+$} Chamber: p=0.1496 Interaction: p=0.6599; Male Wild Type $\Delta E14$ Sibling vs Male *Shank3* ^{$\Delta E14/+$} Chamber: p=0.6292 Interaction: p=0.6167). The novelty interaction index, in which a value >0 indicates a preference for novel stranger, also indicates no significant difference between heterozygous animals and their wild-type siblings, when separating by sex (Figure 2.10 F; Mann-Whitney Test: Female Wild Type $\Delta E9$ Sibling vs Female *Shank3* ^{$\Delta E9/+$} p=0.3943; Female Wild Type $\Delta E14$ Sibling vs Female *Shank3* ^{$\Delta E14/+$} p=0.2073; Male Wild Type $\Delta E9$ Sibling vs Male *Shank3* ^{$\Delta E9/+$} p=0.7789; Male

Wild Type $\Delta E14$ Sibling vs Male *Shank3* ^{$\Delta E14/+$} $p=0.8785$). Males of both $\Delta E9$ and $\Delta E14$ families, and females of $\Delta E14$ families, showed preference for social novelty, by spending significantly more time interacting with Stranger II (Figure 2.10 D,E; Two-way repeated-measures ANOVA, for each condition is listed p-value for Chamber as source of variation: Male Wild Type $\Delta E9$ Sibling vs Male *Shank3* ^{$\Delta E9/+$} Chamber: $p=0.0263$ Interaction: $p=0.0001$; Male Wild Type $\Delta E14$ Sibling vs Male *Shank3* ^{$\Delta E14/+$} Chamber: $p=0.0020$ Interaction: $p=0.0042$; Female Wild Type $\Delta E14$ Sibling vs Female *Shank3* ^{$\Delta E14/+$} Chamber: $p=0.0542$ Interaction: $p=0.0305$). Notably, both wild-type and heterozygous females from $\Delta E9$ families did not show a significant preference towards either stranger (Figure 2.10 D,E; Two-way repeated-measures ANOVA, for each condition is listed p-value for Chamber as source of variation: Female Wild Type $\Delta E9$ Sibling vs Female *Shank3* ^{$\Delta E9/+$} Chamber: $p=0.1102$ Interaction: $p=0.7403$). Unexpectedly, wild-type females of $\Delta E9$ families showed a trend towards preference for the familiar stranger, Stranger I (Figure 2.10 D-F;; Mann-Whitney Test: Female Wild Type $\Delta E9$ Sibling Median= -0.08807 , $n=7$; Female *Shank3* ^{$\Delta E9/+$} Median= 0.1917 , $n=8$).

Bonded female *Shank3* ^{$\Delta E9/+$} voles show diminished preference for their partner

We investigated adult attachment behaviors of both male and female prairie voles through pair bonding, and compared both *Shank3* ^{$\Delta E9/+$} and *Shank3* ^{$\Delta E14/+$} mutant behavior to that of their wild-type control siblings. We developed a 10 day paradigm which incorporated a series of 5 social behaviors tests to assess pair bond formation and maintenance: Introduction to Partner, Timed Mating, Partner Preference Test (PPT), Separation and Reunification, and Resident Intruder (Figure 2.11).

The PPT is a standard test in the prairie vole field used to measure expression of a pair bond. Typical bonded voles show significant preference for a partner as measured by time spent in the partner's chamber and time spent huddling (engaged in side-by-side contact), with the partner (Figure 2.12 A). Our female voles of all genotypes showed preference for their partner, as compared to stranger, by time spent in the partner chamber (Figure 2.12B; Two Way Repeated Measured ANOVA Chamber Effect $p < 0.0001$; Sidak's multiple comparisons test Partner-Stranger: Wild Type $p < 0.0001$, *Shank3* ^{$\Delta E9/+$} $p = 0.0116$, *Shank3* ^{$\Delta E14/+$} $p < 0.0001$) and time spent huddling with their partner (Figure 2.12C; Two Way Repeated Measured ANOVA Stimulus Vole Effect $p < 0.0001$; Sidak's multiple comparisons test Partner-Stranger: Wild Type $p < 0.0001$, *Shank3* ^{$\Delta E9/+$} $p = 0.0216$, *Shank3* ^{$\Delta E14/+$} $p < 0.0001$). Notably, bonded *Shank3* ^{$\Delta E9/+$} females, but not bonded *Shank3* ^{$\Delta E14/+$} females, demonstrate significantly diminished preference for their partners as compared to wild-type females, when comparing time spent in the partner and stranger chambers (Figure 2.12D; Chamber Time: Two Way Repeated Measured ANOVA Genotype x Chamber Interaction $p = 0.0075$; Sidak's multiple comparisons test Partner: Wild Type vs *Shank3* ^{$\Delta E9/+$} $p = 0.0026$, Wild Type vs *Shank3* ^{$\Delta E14/+$} $p = 0.8914$; Stranger: Wild Type vs *Shank3* ^{$\Delta E9/+$} $p = 0.0230$, Wild Type vs *Shank3* ^{$\Delta E14/+$} $p = 0.9748$). Bonded *Shank3* ^{$\Delta E9/+$} females, but not bonded *Shank3* ^{$\Delta E14/+$} females, further demonstrate significantly diminished preference for huddling with their partners as compared to wild-type females (Figure 2.12E; Huddle Time: Two Way Repeated Measured ANOVA Genotype x Stimulus Vole Interaction $p = 0.0046$; Sidak's multiple comparisons test Partner: Wild Type vs *Shank3* ^{$\Delta E9/+$} $p = 0.0003$, Wild Type vs *Shank3* ^{$\Delta E14/+$} $p = 0.7812$; Stranger: Wild Type vs *Shank3* ^{$\Delta E9/+$} $p = 0.3384$, Wild Type vs *Shank3* ^{$\Delta E14/+$} $p = 0.9929$).

In contrast, bonded male voles heterozygous for either mutant allele do not demonstrate any difference in preference for their partners as compared to their bonded wild-type control siblings. Bonded male voles of all 3 genotypes show a preference for their partner by time spent in the partner chamber (Figure 2.12F; Two Way Repeated Measured ANOVA Chamber Effect $p < 0.0001$; Sidak's multiple comparisons test Partner-Stranger: Wild Type $p = 0.2662$, *Shank3* ^{$\Delta E9/+$} $p = 0.0054$, *Shank3* ^{$\Delta E14/+$} $p = 0.0427$) and a significant preference to huddle with their partner over a stranger (Figure 2.12G; Two Way Repeated Measured ANOVA Stimulus Vole Effect $p < 0.0001$; Sidak's multiple comparisons test Partner-Stranger: Wild Type $p = 0.0244$, *Shank3* ^{$\Delta E9/+$} $p = 0.0004$, *Shank3* ^{$\Delta E14/+$} $p = 0.0043$). Neither bonded male mutant showed a difference in preference as compared to wild type by either chamber time (Figure 2.12H; Chamber Time: Two Way Repeated Measured ANOVA Genotype x Chamber Interaction $p = 0.3967$; Sidak's multiple comparisons test Partner: Wild Type vs *Shank3* ^{$\Delta E9/+$} $p = 0.2406$, Wild Type vs *Shank3* ^{$\Delta E14/+$} $p = 0.9555$; Stranger: Wild Type vs *Shank3* ^{$\Delta E9/+$} $p = 0.4567$, Wild Type vs *Shank3* ^{$\Delta E14/+$} $p = 0.7856$), or huddle duration (Figure 2.12I; Huddle Time: Two Way Repeated Measured ANOVA Genotype x Stimulus Vole Interaction $p = 0.3907$; Sidak's multiple comparisons test Partner: Wild Type vs *Shank3* ^{$\Delta E9/+$} $p = 0.4201$, Wild Type vs *Shank3* ^{$\Delta E14/+$} $p = 0.9304$; Stranger: Wild Type vs *Shank3* ^{$\Delta E9/+$} $p = 0.4900$, Wild Type vs *Shank3* ^{$\Delta E14/+$} $p = 0.7180$).

Bonded female *Shank3* ^{$\Delta E9/+$} voles show reduced attachment behaviors towards their partner following acute separation

Following the above finding of a sex- and mutation- specific reduction in partner preference displayed by female *Shank3* ^{$\Delta E9/+$} voles, we next quantified adult attachment

behaviors in male and female prairie voles of both *Shank3* mutations, as compared to their wild-type siblings, in the Separation and Reunification assay. In this assay, bonded vole pairs are separated for one hour on day 7 (female subject) and day 8 (male subject) of cohabitation (day 4 and 5 respectively following mating), and we quantify the prosocial, aggressive, and huddling behaviors of the subject vole upon reunification in the home cage. Typical bonded prairie voles spend the majority of the 30 minute reunification huddling with their partner following separation.

Males and females of all genotypes spent at least half of the reunification assay huddling with their partners, however bonded *Shank3*^{ΔE9/+} females showed significantly less time huddling with their partners as compared to their wild-type female siblings (Figure 2.13 A; Mann-Whitney Test: Female Wild Type vs *Shank3*^{ΔE9/+} p=0.0135, Female Wild Type vs *Shank3*^{ΔE14/+} p=0.8201, Male Wild Type vs *Shank3*^{ΔE9/+} p=0.7348, Male Wild Type vs *Shank3*^{ΔE14/+} p=0.8747). Similarly, bonded *Shank3*^{ΔE9/+} females showed significantly reduced total time engaged in prosocial behaviors with their partners, including nose-to-nose investigations, anogenital sniffing, and huddling, as compared to their wild-type siblings, while *Shank3*^{ΔE14/+} females and both male mutants showed time in prosocial behavior indistinguishable from their respective wild-type siblings (Figure 2.13 B; Mann-Whitney Test: Female Wild Type vs *Shank3*^{ΔE9/+} p=0.0066, Female Wild Type vs *Shank3*^{ΔE14/+} p=0.7762, Male Wild Type vs *Shank3*^{ΔE9/+} p=0.7670, Male Wild Type vs *Shank3*^{ΔE14/+} p=0.9103).

Bonded female *Shank3*^{ΔE9/+} and *Shank3*^{ΔE14/+} voles show decreased sexual receptivity to male partners

As pair bonding is closely tied to mating behaviors, we also investigated how our distinct *Shank3* mutations affect mating behaviors in both males and females. We utilized a timed mating paradigm described in Figure 2.1 to induce the female of the pair into estrous by dividing the pair in the same cage overnight, and then quantified 30 minutes of mating behaviors when the female was in estrus and thus receptive to mating upon removal of the divider. We observed no overall differences between either *Shank3* mutant and wild-type control siblings in what percent of pairs demonstrate mating behaviors during the assay (Figure 2.14 A-D; Fisher's exact test: Female Wild Type vs *Shank3*^{ΔE9/+} p=0.3304 for mounting, p>0.9999 for intromission; Female Wild Type vs *Shank3*^{ΔE14/+} p=0.6609 for mounting, p=0.4283 for intromission; Male Wild Type vs *Shank3*^{ΔE9/+} p>0.9999 for mounting, p>0.9999 for intromission; Male Wild Type vs *Shank3*^{ΔE14/+} p=0.7241 for mounting, p>0.9999 for intromission). Of the pairs that demonstrated mating behaviors, both *Shank3*^{ΔE9/+} and *Shank3*^{ΔE14/+} females expressed decreased sexual receptivity as compared to their wild-type control siblings. When females of either *Shank3* mutant genotype were paired with wild-type males, we observed less time that the pair displayed mating behaviors, as measured by the sum of seconds mounting and intromitting. (Figure 2.14 E; Mann-Whitney Test: Female Wild Type vs *Shank3*^{ΔE9/+} p=0.0127; Female Wild Type vs Female *Shank3*^{ΔE14/+} p=0.0435). This reduction in time spent mating is also illustrated by a decrease in number of mounting events by males in pairs with either *Shank3*^{ΔE9/+} and *Shank3*^{ΔE14/+} females (Figure 2.14 F; Mann-Whitney Test: Female Wild Type vs *Shank3*^{ΔE9/+} p=0.0075; Female Wild Type vs Female

Shank3^{ΔE14/+} p=0.0404). Wild-type males paired with *Shank3*^{ΔE9/+} females demonstrated a decrease in number of intromission events as well, consistent with decreased receptivity of mutant females, while pairs with *Shank3*^{ΔE14/+} females did not show decreased intromission (Figure 2.14 G; Mann-Whitney Test: Female Wild Type vs *Shank3*^{ΔE9/+} p=0.0222; Female Wild Type vs Female *Shank3*^{ΔE14/+} p=0.2828). Of pairs that mated during the assay, the female's genotype did not affect latency to mount (Figure 2.14 H) nor ratio of number of intromissions over mounting events (Figure 2.14 I), both additional measures of female mating receptivity. Both of these measures were similar to those observed in pairs in which the female was a wild type (Mann-Whitney Test: Latency to Mount: Female Wild Type vs *Shank3*^{ΔE9/+} p=0.0513; Female Wild Type vs Female *Shank3*^{ΔE14/+} p=0.2775; # Intromissions / # Mounts Ratio: Female Wild Type vs *Shank3*^{ΔE9/+} p=0.0939; Female Wild Type vs Female *Shank3*^{ΔE14/+} p=0.2828).

In contrast, in pairs with wild-type females paired with wild type or heterozygous *Shank3* mutants of either allele, the male's genotype in the mating pair had no effect on any of the above mating behaviors (Figure 2.14 J-N). Of the pairs that demonstrated mating during the assay, pairs including either *Shank3*^{ΔE9/+} or *Shank3*^{ΔE14/+} males performed indistinguishably from their wild-type control siblings across total duration spent in mating behaviors, number of mounts, number of intromissions, latency to mount, and the ratio of number of intromission events over mounting events (Mann-Whitney Test, all Males: Duration Mating: Wild Type vs *Shank3*^{ΔE9/+} p>0.9999; Wild Type vs *Shank3*^{ΔE14/+} p=0.3575; # Mounts: Wild Type vs *Shank3*^{ΔE9/+} p=0.9377; Wild Type vs *Shank3*^{ΔE14/+} p=0.3302; # Intromits: Wild Type vs *Shank3*^{ΔE9/+} p=0.5859; Wild Type vs *Shank3*^{ΔE14/+} p=0.2788; Latency to Mount: Wild Type vs *Shank3*^{ΔE9/+} p=0.1827; Wild Type

vs *Shank3*^{ΔE14/+} p=0.1264; # Intromissions / # Mounts Ratio: Wild Type vs *Shank3*^{ΔE9/+} p>0.9999; Wild Type vs *Shank3*^{ΔE14/+} p=0.1893).

Sexually naïve *Shank3* mutant voles show affiliative social behaviors towards a novel vole consistent with their wild-type control siblings, and *Shank3*^{ΔE9/+} females show diminished defensive rearing

We wished to investigate if voles bearing distinct *Shank3* mutations showed differences in social behavior upon introduction to their partner, before formation of the pair bond. We found that both female and male *Shank3*^{ΔE9/+} or *Shank3*^{ΔE14/+} voles showed prosocial behaviors towards the novel opposite sex vole similar to behaviors of their wild-type control siblings (Figure 2.15 A-C). There were no differences between genotypes in time spent huddling, nose-to-nose social investigation, nor anogenital investigation (Mann-Whitney Test : Female Wild Type vs *Shank3*^{ΔE9/+} p=0.4271 for huddling, p=0.9809 for nose-to-nose, p=0.6833 for anogenital; Female Wild Type vs *Shank3*^{ΔE14/+} p=0.8785 for huddling, p=0.8785 for nose-to-nose, p=0.4130 for anogenital; Male Wild Type vs *Shank3*^{ΔE9/+} p=0.3721 for huddling, p=0.5816 for nose-to-nose, p=0.5247 for anogenital; Male Wild Type vs *Shank3*^{ΔE14/+} p=0.4715 for huddling, p=0.4505 for nose-to-nose, p=0.0767 for anogenital).

There were also no differences in the initiation of aggressive behavior as an effect of *Shank3* genotype, including total number of aggressive events and latency to first aggressive event (Figure 2.15 D,E; Mann-Whitney Test : Female Wild Type vs *Shank3*^{ΔE9/+} p=0.3716 for bouts, p=0.1086 for latency; Female Wild Type vs *Shank3*^{ΔE14/+} p=0.1370 for bouts, p=0.1208 for latency; Male Wild Type vs *Shank3*^{ΔE9/+} p=0.6633 for

bouts, $p=0.6599$ for latency; Male Wild Type vs *Shank3* ^{$\Delta E14/+$} $p=0.1804$ for bouts, $p=0.8861$ for latency).

Interestingly, the sexually naïve *Shank3* ^{$\Delta E9/+$} female voles showed a significant reduction in time spent in defensive rears (Figure 2.15 F) and number of defensive rears (Figure 2.15 G) during the assay, as compared to their wild-type siblings (Mann-Whitney Test: Female Wild Type vs *Shank3* ^{$\Delta E9/+$} $p=0.0365$ for rear duration, $p=0.0032$ for rear #). This reduction was not observed among sexually naïve *Shank3* ^{$\Delta E14/+$} females (Mann-Whitney Test: Female Wild Type vs *Shank3* ^{$\Delta E14/+$} $p=0.7211$ for rear duration, $p=0.8284$ for rear #).

Pair bonded *Shank3* mutant voles show aggressive social behaviors towards a novel vole consistent with their wild-type control siblings, and *Shank3* ^{$\Delta E9/+$} females show diminished investigation

In the final assay of our behavioral paradigm, we used the Resident Intruder assay to evaluate if bonded *Shank3* mutant prairie voles show selective rejection of opposite sex novel strangers comparable to bonded wild-type voles. We found that both male and female bonded *Shank3* mutant prairie voles demonstrate aggressive behaviors towards a novel stranger consistent with behaviors seen by their wild-type control siblings. Both *Shank3* ^{$\Delta E9/+$} and *Shank3* ^{$\Delta E14/+$} voles show no difference in number of total aggressive bouts nor latency to first aggressive bout, as compared to their wild-type siblings (Figure 2.16 A,B; Mann-Whitney Test : Female Wild Type vs *Shank3* ^{$\Delta E9/+$} $p=0.8533$ for bouts, $p=0.7477$ for latency; Female Wild Type vs *Shank3* ^{$\Delta E14/+$} $p=0.4728$ for bouts, $p=0.1451$

for latency; Male Wild Type vs *Shank3*^{ΔE9/+} p=0.7386 for bouts, p=0.5604 for latency; Male Wild Type vs *Shank3*^{ΔE14/+} p=0.5438 for bouts, p=0.3561 for latency).

Consistent with their social deficits observed across previous assays, bonded *Shank3*^{ΔE9/+} females demonstrate reduced time engaged in prosocial interaction, including huddling, nose-to-nose investigation, and anogenital investigation, with the novel stranger, as compared to their wild-type siblings (Figure 2.16 C; Mann-Whitney Test: Female Wild Type vs *Shank3*^{ΔE9/+} p=0.0352). This reduction in prosocial interaction was not observed in *Shank3*^{ΔE14/+} females, nor male mutants of either *Shank3* genotype, as compared to their respective wild-type siblings. (Figure 2.16 C; Female Wild Type vs *Shank3*^{ΔE14/+} p=0.9385; Male Wild Type vs *Shank3*^{ΔE9/+} p=0.4735; Male Wild Type vs *Shank3*^{ΔE14/+} p=0.7375).

***Shank3*^{ΔE9/+} females show comparable numbers of OT and AVP positive cells across the PVN**

Previous work has determined that homozygous *Shank3b*^{-/-} mice exhibit reduced OT immunostaining in the PVN, specifically the medial PVN, and hypothesized that social deficits in *Shank3b*^{-/-} mice are partially due to OT system dysfunction (Resendez et al., 2020). Therefore, we wished to investigate if our heterozygous *Shank3*^{ΔE9/+} females showed a similar reduction in OT positive cells across the PVN compared to their wild-type siblings. We additionally investigated if *Shank3*^{ΔE9/+} females showed any differences in AVP positive cells across the PVN as compared to their wild-type siblings, as AVP has been implicated in social attachment behaviors in prairie voles as ubiquitously as OT.

We collected brains of same-sex group-housed *Shank3*^{ΔE9/+} females and their wild-type female siblings, at 7 to 9 at weeks of age. We perfused and performed immunohistochemistry on coronal sections to stain for OT, AVP, and used DAPI (4',6-diamidino-2-phenylindole) as a nuclear stain. By confocal microscopy, we imaged 28 stained serial sections of PVN, encompassing the full region from anterior to posterior, and quantified OT and AVP positive cells in each section.

We found no differences in total number of OT (Figure 2.17 A) or AVP (Figure 2.17 D) positive cells in the PVN of *Shank3*^{ΔE9/+} females as compared to their wild-type siblings (Mann-Whitney Test: Female Wild Type vs *Shank3*^{ΔE9/+} $p=0.6635$ for OT, $p=0.5887$ for AVP). We next aligned the 28 serial sections by anterior to posterior position and observed no difference in either number of OT or AVP positive cells in a particular region across the PVN (Figure 2.17 B,E). Finally, as performed by Resendez et al., 2020, we binned each PVN section into either rostral (sections 1-9), medial (sections 10-19), and caudal (sections 20-28) and compared OT and AVP positive cell counts between *Shank3*^{ΔE9/+} and wild-type animals, by PVN region (Figure 2.17 C,F,G). Again, we observed no difference in number of OT and AVP positive cells in either the rostral, medial, or caudal PVNs between *Shank3*^{ΔE9/+} and wild-type female voles (Mixed-effects model (REML): OT: PVN Region Factor $p<0.0001$, Genotype x PVN Region Factor $p=0.7828$, Sidak's multiple comparisons test Wild Type - *Shank3*^{ΔE9/+}: Rostral $p=0.6052$, Medial 0.9883, Caudal $p=0.9971$; AVP: PVN Region Factor $p<0.0001$, Genotype x PVN Region Factor $p=0.4831$, Sidak's multiple comparisons test Wild Type - *Shank3*^{ΔE9/+}: Rostral $p=0.7699$, Medial 0.9947, Caudal $p=0.1662$).

DISCUSSION

Varied mutations in *Shank3* have been associated with increased risk for ASD symptom presentation, including deficits in adult social attachment behaviors and disrupted social relationships (Baird et al., 2003; Durand et al., 2007; Moessner et al., 2007; Gauthier et al., 2009; Sanders et al., 2015). The contributions of specific *Shank3* mutations to ASD-related phenotypes has been evaluated in multiple mouse models; however mouse behavior studies are limited with regards to identifying complex social behaviors analogous to those disrupted in the context of ASD symptomology because mice do not display adult social bonds between mating partners. By targeted mutagenesis of two distinct exons in prairie vole *Shank3*, we generated two *Shank3* mutant vole lines with unique disruptions yielding differences in expression of certain Shank3 isoforms and their associated functional domains. Here we report that a 10 base pair deletion in exon 9, yielding a premature stop codon in the ankyrin repeat domain (ANK) of *Shank3* and likely resulting in truncated isoforms lacking ANK and SH3 domains, yields a female specific and heterozygous phenotype of disrupted adult social attachment behaviors evaluated through pair bond formation and maintenance. Interestingly, a 4 base pair deletion in exon 14, bearing a truncation in the more 3' PDZ-domain, does not cause any adult attachment phenotype in female nor male voles, although female voles heterozygous for this mutation show reduced sexual receptivity in the timed mating assay also observed in *Shank3*^{ΔE9/+} females. We do not see any differences in OT or AVP positive cell numbers in the PVN which correlate with social attachment deficits in *Shank3*^{ΔE9/+} females, suggesting that the mechanisms underlying social behavior deficits in this clinically relevant haploinsufficiency model may arise from other brain regions or

more complex circuit dynamics than in *Shank3b* homozygous knockout mice. Together these findings implicate distinct isoforms of Shank3 that may contribute to deficits in adult social attachment behaviors when disrupted. Additionally, our study establishes the *Shank3*^{ΔE9/+} female vole and our battery of behavioral assays as a novel model for probing the neurobiology and neural circuitry of adult social attachment behaviors. Elucidating the underlying mechanisms of how the brains builds social bonds can open the door for future advancements in diagnostic and treatment methods for individuals with ASD, or with any neurodevelopmental or psychiatric disorder for which social attachment deficits are a core component.

Shank3^{ΔE9/+} females show a sex- and mutation- specific deficit in adult social attachment behaviors expressed through the pair bond

Our consolidated findings demonstrate that *Shank3*^{ΔE9/+} female prairie voles show a deficit in adult social attachment behaviors as compared to their wild-type control siblings. This deficit is represented by distinct behavioral changes across all 5 assays in our paradigm designed to probe pair bond formation and maintenance. Most notably, *Shank3*^{ΔE9/+} females show diminished preference for their partner in the PPT, suggestive of either a failure to form, maintain, or recall a pair bond. Similarly, *Shank3*^{ΔE9/+} females huddle less with their partners when reunited following acute separation, another phenotype reflecting an attachment deficit as significantly increased huddle times are characteristic of wild-type voles following formation of the pair bond.

In the remaining three behavioral assays, *Shank3*^{ΔE9/+} females demonstrate social deficits that are attachment-related, and consolidating these differences allows us to build the endophenotype which arises from the ΔE9 mutations.

In the Timed Mating assay, *Shank3*^{ΔE9/+} females spend less time engaged in sexual activity with their male partner. This result could be reflective of a phenotypic decrease in sexual receptivity in *Shank3*^{ΔE9/+} females. We do not observe increased bouts of rears or strikes in *Shank3*^{ΔE9/+} females, which would be consistent with decreased sexual receptivity as the males attempt mating, however we did not quantify more passive indicators of decreased receptivity such as sitting.

In the Resident Intruder assay, bonded *Shank3*^{ΔE9/+} females show less time investigating the novel stranger, when pooling time in nose-to-nose and anogenital investigation. This result may reflect a decreased social interest in the stranger. As a pair bond is partially defined by a bonded vole displaying active rejection of an opposite sex stranger, this decrease in stranger investigation could be further evidence that *Shank3*^{ΔE9/+} females demonstrate an attachment deficit, as they are not as motivated by the presence of a stranger. Alternatively, decreased investigation of the stranger may arise from unrelated mechanisms, and consequentially yield fewer opportunities to reject the stranger.

The Introduction to Partner assay allows us to examine social behaviors rather independent of attachment in *Shank3*^{ΔE9/+} females prior to possible pair bond formation. In this assay, sexually naïve *Shank3*^{ΔE9/+} females defensively rear less than their wild-type siblings, when interacting with a novel male vole. Defensive rearing is a behavior exhibited by female voles to prevent anogenital or copulatory contact by the male. These

results suggest that sexually naïve *Shank3*^{ΔE9/+} females may be more receptive or discriminate less in receptivity than their wild-type control siblings. Because we observe no mating events among *Shank3*^{ΔE9/+} females in the Introduction assay, consistent with wild-type behavior, it is possible that the decrease in defensive rearing arises from a disinhibited attachment phenotype, observed in this mutant across the above assays.

Differential expression of Shank3 isoforms between ΔE9 and ΔE14 targeted mutations

By CRISPR-mediated mutagenesis we generated a 10 base pair deletion in *Shank3* exon 9 in our *Shank3*^{ΔE9/+} vole line, and a 4 base pair deletion in *Shank3* exon 14 in our *Shank3*^{ΔE14/+} vole line. Both deletions caused an immediate frame shift at the site of mutation, and a subsequent premature stop codon shortly after, in exon 10 for *Shank3*^{ΔE9/+} voles and in exon 16, still part of the PDZ-domain, for *Shank3*^{ΔE14/+} voles. Our Western Blot comparing homozygous brains of both mutants to wild type revealed that both ΔE9 and ΔE14 mutations caused complete loss of the full length Shank3 protein, isoform Shank3a. This reveals that in the presence of either mutation, Shank3 protein is only expressed as some unique combination of smaller Shank3 isoforms (see Figure 2.18 for schematic of Shank3 isoforms in prairie vole and predicted isoform expression of each mutation).

Our Western Blot also revealed that the ΔE14 mutation, but not the ΔE9 mutation, caused a full loss of the second largest isoform, which based on studies in mice likely corresponds to Shank3c isoforms (Wang et al., 2014). Interestingly, the ΔE9 mutation showed a female-specific reduction of expression of Shank3c isoforms as compared to wild type, though still demonstrated only a modest decrease in expression compared to

the total loss seen in $\Delta E14$. Shank3c is the largest of the Shank3 isoforms with a promoter downstream of the most N-terminus functional domain, the ankyrin repeat domain (ANK). Shank3c includes the PDZ-domain, which contains binding sites for guanylate kinase-associated protein (GKAP), a scaffolding molecule involved in synaptic signaling of NMDA receptors via PSD-95/SAP90 proteins; the proline-rich domain which includes recognition sites for docking proteins such as Homer, which directly interacts with metabotropic glutamate (mGluR) receptors, and cortactin, which regulates actin cytoskeleton dynamics; and the SAM domain (Sterile Alpha Motif) which mediates homooligomerization of Shank3. (Shin et al., 2012; Costales and Kolevzon, 2015). Shank3d is the second largest isoform with a promoter downstream of ANK, and contains all of the same above functional domains as Shank3c, only differing in that its promoter is slightly closer to the PDZ-domain. The $\Delta E14$ mutation yielded a reduction in Shank3d isoform expression in both sexes, while no difference of expression was seen between $\Delta E9$ and wild type.

The $\Delta E14$ mutation causes a more substantial decreased expression of isoforms with a promoter downstream of ANK and containing functional domains closer to the C-terminus, than the $\Delta E9$ mutation, particularly by quantification of Shank3c and Shank3d. Revealingly, *Shank3* ^{$\Delta E14/+$} females show adult social attachment behaviors characteristic of wild type, in assays in which *Shank3* ^{$\Delta E9/+$} females show a significant deficit. Based on these findings and the positioning of the mutations in each *Shank3* allele, we postulate that the functional domain of Shank3 which is necessary for typical adult social attachment behaviors in pair bonded female voles, is not localized to any of the above described isoforms with promoters downstream of ANK.

Based on the above findings we expect that the observed deficits in pair bonding in *Shank3*^{ΔE9/+} females arise from functional disruption of the most N-terminus *Shank3* isoform, *Shank3b*. According to characterization in the mouse, *Shank3b* contains the ankyrin-repeat domain (ANK), which includes binding sites for alpha-fodrin, which regulates the actin cytoskeleton, and shapin, which mediates homomultimerization of the Shank protein complex; the Src homology 3 domain (SH3), which binds with GRIP, an adapter protein that directly interacts with the C-termini of AMPA receptors; and continues through the PDZ-domain described above. (Ebert and Greenberg, 2013; Costales and Kolevzon, 2015; Lim et al., 2001). Human genomic sequencing studies have identified multiple clinically relevant mutations associated with ASD that would cause a discrete disruption of *Shank3b*, including a de novo premature truncation in intron 8 and a de novo single nucleotide variant (SNV) in exon 8 (Durand et al., 2007; Moessner et al., 2007). Similarly, of the various *Shank3* mutant mouse models that report social deficits, about half of those reported with phenotypes directly disrupt the *Shank3b* isoform (Peça et al., 2011; Wang et al., 2011; Bozdagi et al., 2010).

The epitope of the antibody used in our Western Blot experiment (Santa Cruz sc-30193) is located 3' of the termination of the *Shank3b* isoform and therefore was unable to detect any specific expression of *Shank3b*, and working antibodies against the N-terminus domains of prairie vole *Shank3* are not available. Nevertheless, disruption of *Shank3b* is the most likely candidate for contribution to our observed social bonding deficits, because the ΔE9 mutation lies early in the *Shank3b* isoform, within the most N-terminus functional domain ANK. Thus, the ΔE9 mutation is responsible for a frame shift for part of the ANK domain, and the entirety of the SH3 domain. Alternatively, it is likely

that the $\Delta E9$ mutation's premature stop codon results in nonsense mediated decay and the Shank3b isoform does not express at all. Notably, the $\Delta E14$ mutation occurs downstream of both the ANK and SH3 domains and is unlikely to disrupt these regions. Therefore, the behavior differences between our mutants can be explained by the Shank3b isoform, and specifically the ANK and/or SH3 domains, as the site of functional disruption which discretely contributes to deficits in social bonding.

Further work is necessary to confirm if the $\Delta E9$ mutation disrupts Shank3b in a manner different to that by the $\Delta E14$ mutation, and eventually localize which functional properties of Shank3b or other isoforms are necessary for typical pair bonding in female voles. While continuing to identify an antibody with an epitope specific to Shank3b, future work may include reverse transcription quantitative PCR (RT-qPCR) on complementary DNA (cDNA) synthesized from female *Shank3* ^{$\Delta E9/\Delta E9$} voles, *Shank3* ^{$\Delta E14/\Delta E14$} voles, and their wild-type siblings. In addition, future work should be done to design primers specific to various sites along the Shank3 isoforms, and by RT-qPCR, comprehensively quantify expression of the Shank3b isoform between both mutants and wild type (Camacho Londoño and Philipp, 2016). We predict that female *Shank3* ^{$\Delta E9/\Delta E9$} voles will show a significant decrease, or loss, of Shank3b expression, as compared to both *Shank3* ^{$\Delta E14/\Delta E14$} voles and wild type. Utilizing the same RT-qPCR protocol on heterozygote mutants, it will also be possible to characterize differences between mutants and wild type, and to understand the clinically derived haploinsufficiency model of Shank3 dysfunction in social behavior deficits.

Sex Differences in Genetic Contribution of ASD Risk

In all five of our social attachment assays, male prairie voles showed no difference in bonding associated behaviors when bearing either mutation in *Shank3*. Therefore, the $\Delta E9$ mutation appears to have a sex-specific effect in female voles only.

Interestingly, across time and populations a male biased sex difference in ASD prevalence has been reported, with estimated 4 affected males : 1 affected female (Werling and Geschwind, 2013; Idring et al., 2015; Halladay et al., 2015). This observation has motivated extensive research into the sex difference in ASD risk and studies have identified sex differences in phenotypic presentation, genetic contribution to ASD risk, and relative sex hormone levels all as potential mechanisms by which this sex difference arises (Werling and Geschwind, 2013). An overarching biological theory of sex differences in genetic contribution for ASD is that presentation is based on a multiple-threshold multifactorial liability model of cumulative effects of mutations in high risk genes (Reich et al., 1975; Ozonoff et al., 2011). Some human genome sequencing studies predict that females biologically have a higher threshold for ASD presentation, and therefore can carry a higher genetic mutation load without symptoms, as compared to males (Hallmayer et al., 2011). However, this model does not fit with our observation of the $\Delta E9$ mutation having a female-specific effect, in an otherwise wild-type background.

Additionally, human genome sequencing studies have identified case studies of individual loci that contribute to sex biased risk, including a microdeletion that only contributes to the risk for ASD in males in the *Shank1* locus, a member of the same gene family as *Shank3* (Autism Genome Project Consortium, 2007; Cantor et al., 2005; Stone et al., 2004; Sato et al., 2012). One hypothesis to explain our data is that the discrete

Shank3 ΔE9 mutation we have generated specifically contributes to the risk for ASD in females. Further studies are needed to investigate the mechanism by which this occurs in voles, or if analogous mutations in humans specifically cluster around female risk.

One potential mechanism that may underly our sex-specific findings, is that the genetic contribution of the *Shank3* ΔE9 mutation is regulated by sex hormones, and females are, by yet to be determined mechanisms, more vulnerable to this specific mutation than males. Recent studies have demonstrated that both sex hormones dihydrotestosterone (DHT) and 17 β-estradiol play a critical role in *Shank3* expression throughout early brain development, in a human neuroblastoma cell model (Berkel et al., 2018). An investigation of *Shank3* expression in androgen receptor knock-out mice showed the presence of sex hormones to be necessary. Quantification of protein levels in wild-type mice revealed that males show significantly higher *Shank3* expression levels as compared to females in early development, at embryonic day 17.5 and postnatal day 7.5 (Berkel et al., 2018). Future investigations must determine if this sex differential expression of *Shank3* also occurs in prairie voles. If it is, further studies could perform experimental hormone manipulations, such as castration and ovariectomy, to see if the sex difference in *Shank3*^{ΔE9/+} voles is dependent on differential sex hormone signaling.

A final hypothesis is that the phenotypic sex difference of *Shank3*^{ΔE9/+} voles arises from differences in display of attachment behaviors between the sexes. Males show a greater variation of display of partner preference, while females show less variable and stronger preference for bonded mates. It is possible that female patterns of social attachment behaviors provide a more sensitive phenotype in which to identify disruption by the resulting deficits of a heterozygous *Shank3* ΔE9 mutation, while the male vole's

range of partner preference represents a floor effect. Therefore, it is possible that the $\Delta E9$ mutation does not have different phenotypic effects on the sexes, by a role of sex hormones or genetic contributions, but rather, the *Shank3* ^{$\Delta E9/+$} prairie vole model we have established is female specific in its ability to quantify variability in attachment behaviors.

The Prairie Vole in Classic Mouse Sociability and Social Novelty Assays

Our Sociability and Social Novelty assays, adapted from standard mouse assays, reveal that the majority of our female wild-type cohorts do not demonstrate preference for a novel social stimulus over an inanimate stimulus, nor a preference for a novel social stimulus over a familiar social stimulus. Previous studies suggest a more robust preference for the novel social stimulus across all conditions (Sailer et al., 2019; Horie et al., 2019). Two explanations of our observations, which further testing must confirm, include first, that this assay needs to be sensitized to reveal a social preference over general exploration. Previous work demonstrating preference for a social stimulus over a novel object in prairie voles often use apparatuses with higher barriers of entry from chamber to chamber. For example, Sailer et al. demonstrate preference for a social stimulus over a novel object in both sexes, yet utilize a three cage apparatus, instead of three chamber, in which the animal must walk through small tubes to travel from one cage to the next. Similarly, Horie et al. demonstrate social preference in male prairie voles in a similar apparatus to ours, with the addition of “small entrances” directly under light to travel from one chamber to the next. Both of these studies therefore require extra effort, in Sailer et al., or augment social contact with an aversive stimulus, in Horie et al., thus generating a more sensitive assay to ours. Alternatively, it is possible that a caveat of our

automated scoring explains our reported lack of significant preference for social stimuli. Since the contour tracking method calculates position of the vole from the centroid of the contour, and does not delineate head from tail, it counts tail and side touches of the stimuli cup as moments of interaction. These data indicate that this scoring method may require fine tuning in defining an interaction successfully to more precisely determine social preference in our current apparatus.

We also encourage future work to characterize prairie vole preference for social novelty by this three chamber “cup” apparatus commonly used in mice, and evaluate if there is a sex difference in preference for social novelty in this assay. Consistent with our findings, Beery et al. report that cohorts of prairie voles that included males and females did not display a significant preference for the novel stranger in a similar apparatus and assay to ours (Beery et al., 2018). It would be interesting to separate these data by sex and observe if females are driving this lack of preference, as our data indicate, or if preference for social novelty with restriction to full physical contact by the metal cups is not a behavior typical of female prairie voles.

Mechanisms of Oxytocinergic Signaling in Shank3^{ΔE9/+} Female Prairie Voles

Contrary to what we hypothesized based on findings by Resendez et al., 2020, our *Shank3^{ΔE9/+}* females showed no difference in the numbers of cells expressing OT, or AVP, in the PVN. However, it is possible that differences in oxytocinergic signaling in the heterozygous mutant voles, as opposed to total *Shank3* knockouts in the mouse, are found in circuit dynamics rather than blanket cell counts, or in other populations of cells. To further investigate the role of OT in *Shank3^{ΔE9/+}* females' attachment deficits, we

propose two future experiments. First, we suggest a rescue experiment with oxytocin, in which OT is administered by intracerebral infusion into *Shank3*^{ΔE9/+} female voles who are then subjected to the same behavioral paradigm across pair bonding as detailed in the current study. If OT is able to restore *Shank3*^{ΔE9/+} social attachment deficits to wild-type level, we expect that dysfunction of OT signaling underlies the social attachment deficits of *Shank3*^{ΔE9/+} females.

Our lab has recently developed *in vivo* fiber photometry in prairie voles to record neural activity of free moving animals. A second exciting future experiment is to record neural activity in the PVN from *Shank3*^{ΔE9/+} females and their wild-type siblings during the PPT. By this technique, we can compare activity patterns between time in the partner vs stranger chambers, as well as during huddling bouts with the partner vs the stranger.

Therapeutic Implications

In our study, we establish a novel and clinically relevant model of the contribution of a specific *Shank3* mutation to social attachment deficits, analogous to ASD symptomology, in female prairie voles. Future studies with this model can establish the neurobiological mechanisms which underlie adult social attachment deficits and open the door to promising developments in diagnostic and treatment options for individuals with ASD.

We hope that by illuminating the neural mechanisms of social attachment, future research can identify molecular or neural signaling biomarkers that can allow for earlier diagnosis of ASD than current symptom-based diagnosis. Earlier diagnosis could allow for noninvasive, therapeutic interventions from infancy that may reduce symptoms later

in development. Developing empirical biomarkers would also help reduce bias in ASD diagnosis. Children of ethnic and racial minority groups, including African Americans and Latinos, are less likely to be documented with ASD and more likely to have ASD symptoms attributed to intellectual disability, conduct disorder, or attention deficit/hyperactivity disorder (Mandell et al., 2009). The development of measurable approaches to ASD diagnosis will allow for earlier clinical intervention, as well as more equitable and accurate diagnosis and therapeutic care, and reduced social stigma.

FIGURES & TABLES

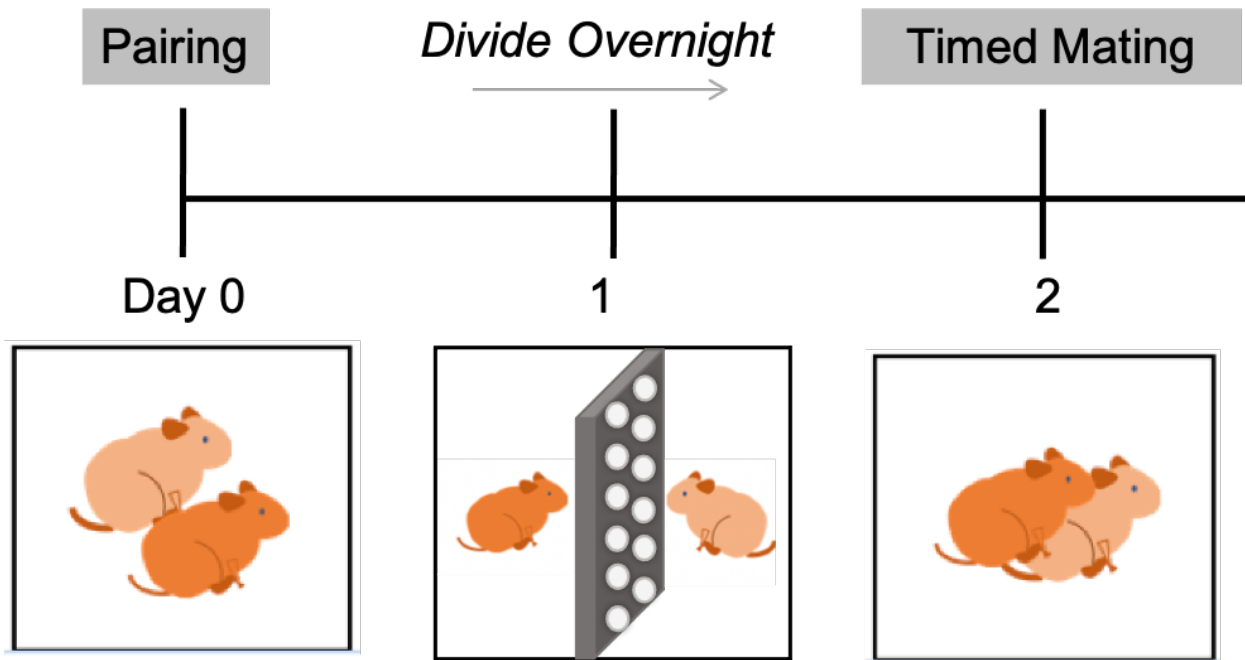


Figure 2.1 Timed mating paradigm. Sexually naïve females were paired with stud males on Day 0. On Day 1 a divider was placed in the cage to separate voles and remained for 12 hours overnight. On Day 2, the divider was removed, and voles engage in mating behaviors. Females were collected and sacrificed for embryo collection 12 hours post mating.

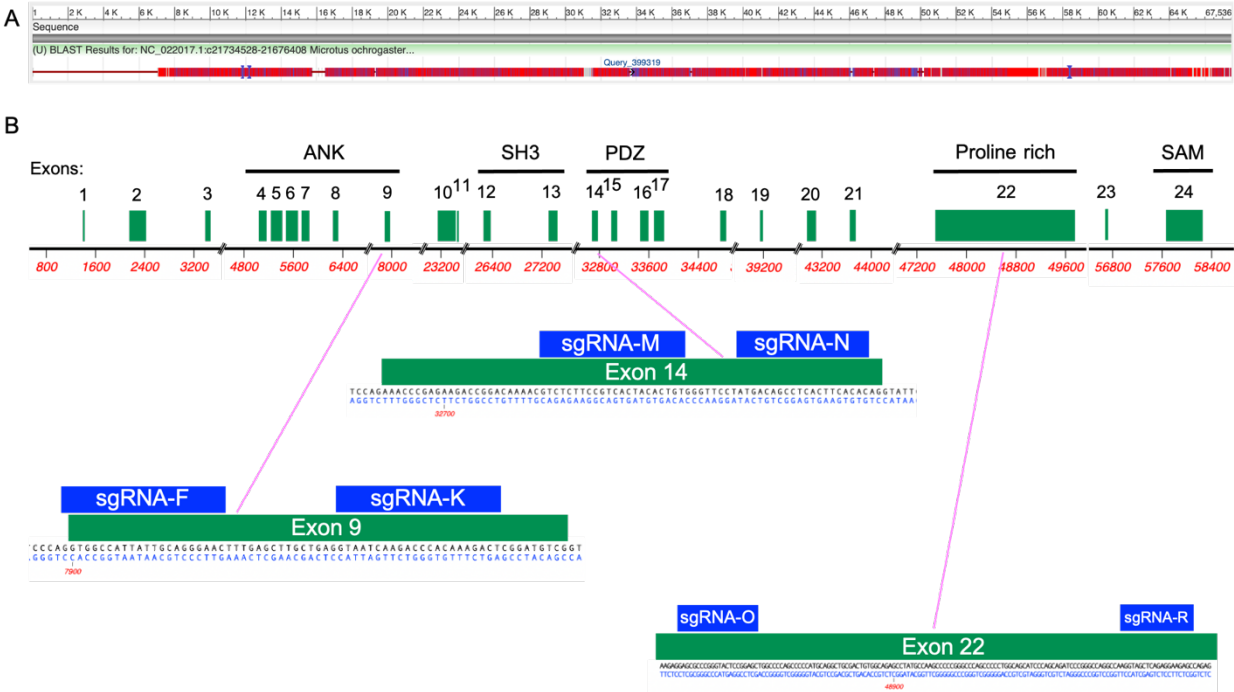


Figure 2.2 Map of 6 sgRNAs targeted to prairie vole *Shank3*. Alignment of prairie vole (*Microtus ochrogaster*) to mouse (*Mus musculus*) *Shank3* yields 92.8% coverage (A). ANK = conserved Ankyrin repeat (ANK) domains, which mediate diverse protein-protein interactions. SH3 = Src homology 3 domain superfamily, which are protein interaction domains that bind proline-rich ligands with moderate affinity and selectivity. PDZ = specific protein-protein interactions with most commonly C-terminal polypeptides. Proline rich domains are conserved recognition sites for docking proteins, in *Shank3* exon 22 these include binding sites for Homer and cortactin. SAM = Sterile Alpha Motif domain of Shank1,2,3 family proteins, which are conserved protein interaction domains prone to homooligomerization.

Table 2.1 Founder voles, G0s, of *Shank3* CRISPR-mediated mutagenesis. A screen for mutation events in the G0 generation of 15 voles with direct CRISPR-mediated electroporation events of the embryo yields 1 prairie vole with a unique mutation in *Shank3* exon 9.

G0 Vole	SgRNAs Electroporated	Sex	Screen for Mutation Event	Bred
T4C	F, K, M, N	Male	None	No
T4F	F, K, M, N	Male	None	Yes
T4A	F, K, M, N	Male	None	Yes
T4D	F, K, M, N	Male	None	Yes
T4B	F, K, M, N	Male	None	Yes
T4E	F, K, M, N	Male	None	Yes
T6A	F,K,O,R	Male	None	Yes
T6B	F,K,O,R	Male	None	Yes
T7A	F,K	Male	None	Yes
T7E	F,K	Male	None	Yes
T7F	F,K	Male	None	Yes
T5A	F,K,O,R	Male	None	Yes
T7B	F,K	Male	None	Yes
T7C	F,K	Male	None	Yes
T7D	F,K	Female	YES: 10bp deletion exon 9	Yes

Table 2.2 First Filial Generation, F1, of *Shank3* CRISPR-mediated mutagenesis. A screen for mutation events in the F1 generation of 14 G0 voles yields 4 prairie vole lines with unique, germline mutations in *Shank3*.

G0 Vole	SgRNAs Electroporated	Sex	# Litters Screened	F1 Screen for Mutation Event
T4F	F, K, M, N	Male	4	YES: 3bp deletion + 1bp substitution in exon 14
T4A	F, K, M, N	Male	7	None
T4D	F, K, M, N	Male	7	None
T4B	F, K, M, N	Male	6	None
T4E	F, K, M, N	Male	7	YES: 4bp deletion in exon 14
T6A	F,K,O,R	Male	3	None
T6B	F,K,O,R	Male	4	None
T7A	F,K	Male	3	None
T7E	F,K	Male	1	None
T7F	F,K	Male	5	YES: 3bp substitution in exon 9
T5A	F,K,O,R	Male	5	None
T7B	F,K	Male	3	None
T7C	F,K	Male	3	None
T7D	F,K	Female	5	YES: 10bp deletion exon 9, consistent with G0 genotype

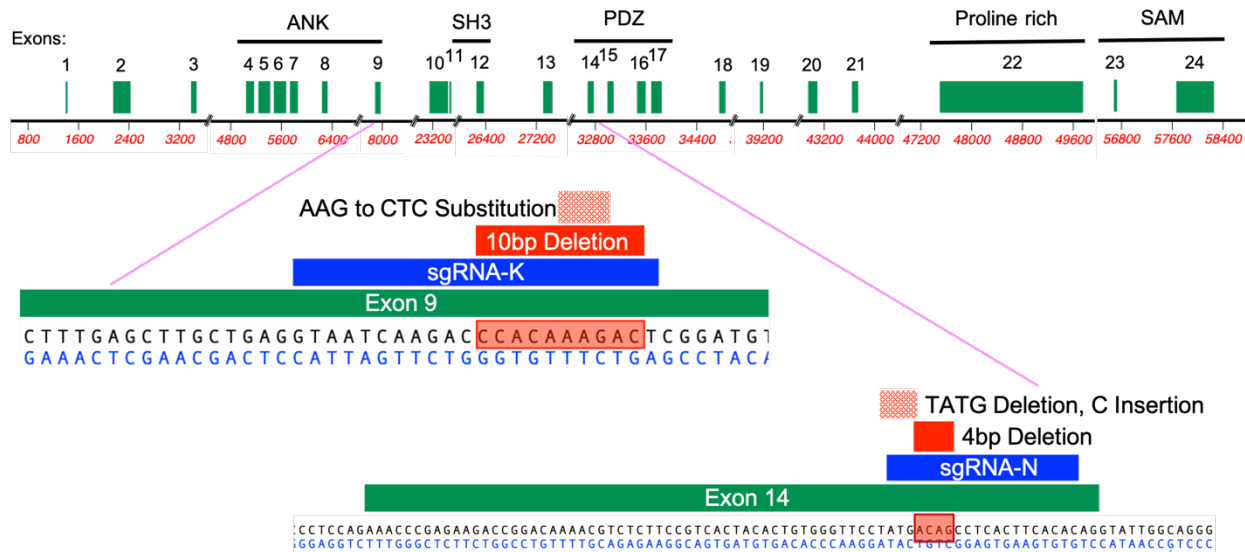


Figure 2.3 Four CRISPR-mediated mutation events in *Shank3*. The 10bp deletion by sgRNA-K in exon 9, and the 4bp deletion by sgRNA-N in exon 14 each depict unique frame shift mutations, indicative of a disruption or truncation in Shank3 functional protein. F1 voles with each of these 2 mutations were bred to form unique outcrossed prairie vole lines harboring each mutation.

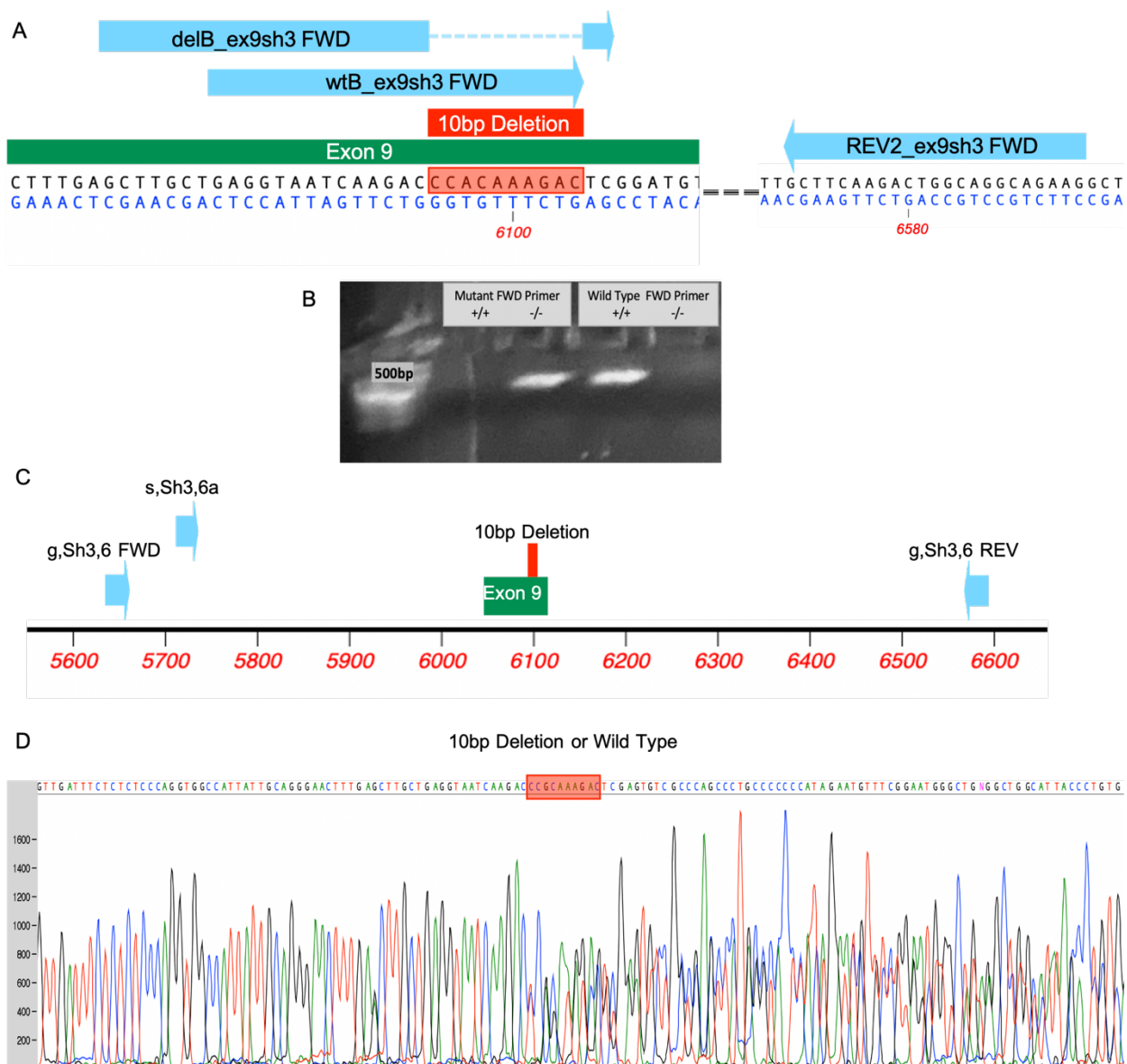


Figure 2.4 *Shank3* $\Delta E9$ mutation Detection. A) Genotyping Strategy for 10bp deletion. Map of primers for specifically identifying wild-type and mutant alleles around the 10bp deletion in *Shank3* exon 9. B) Representative gel of a heterozygote *Shank3* ^{$\Delta E9/+$} animal with genotyping protocol in A. C) PCR and sequencing primers to amplify and sequence $\Delta E9$ mutation and wild-type allele D) Doublet from Sanger sequencing of heterozygote *Shank3* ^{$\Delta E9/+$} animal.

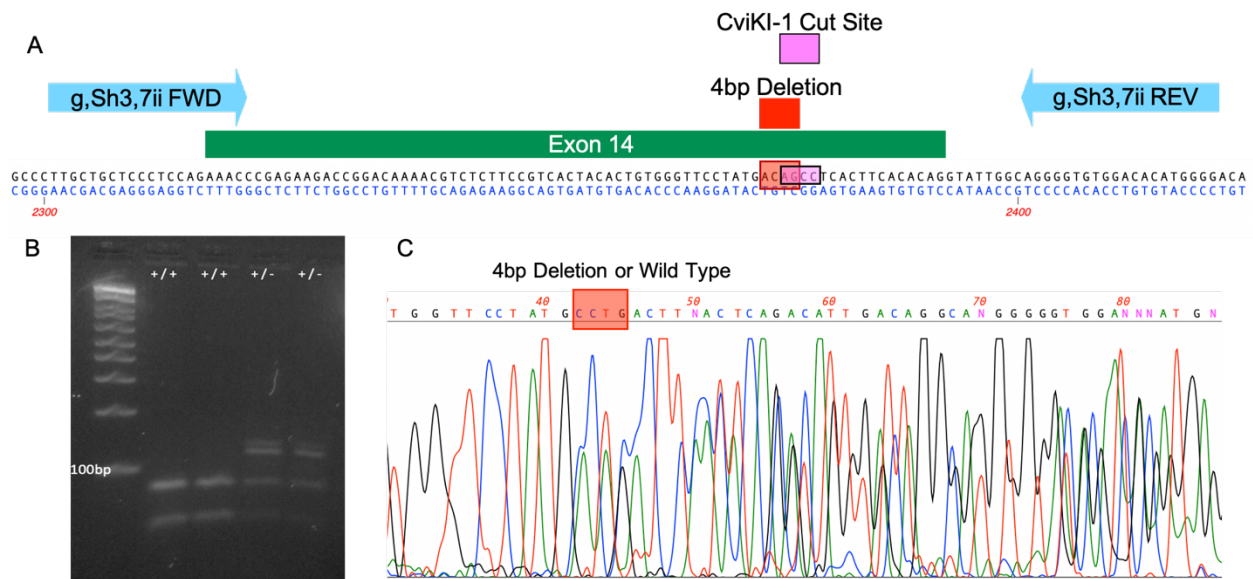


Figure 2.5 *Shank3* $\Delta E14$ mutation Detection. A) Genotyping Strategy for 4bp deletion. Map of primers for amplifying and sequencing 120bp band including all of exon 14. B) Representative gel of a wild-type and heterozygote *Shank3* ^{$\Delta E14/+$} animal following digestion with CVIKI-1. C) Doublet from Sanger sequencing of heterozygote *Shank3* ^{$\Delta E14/+$} animal.

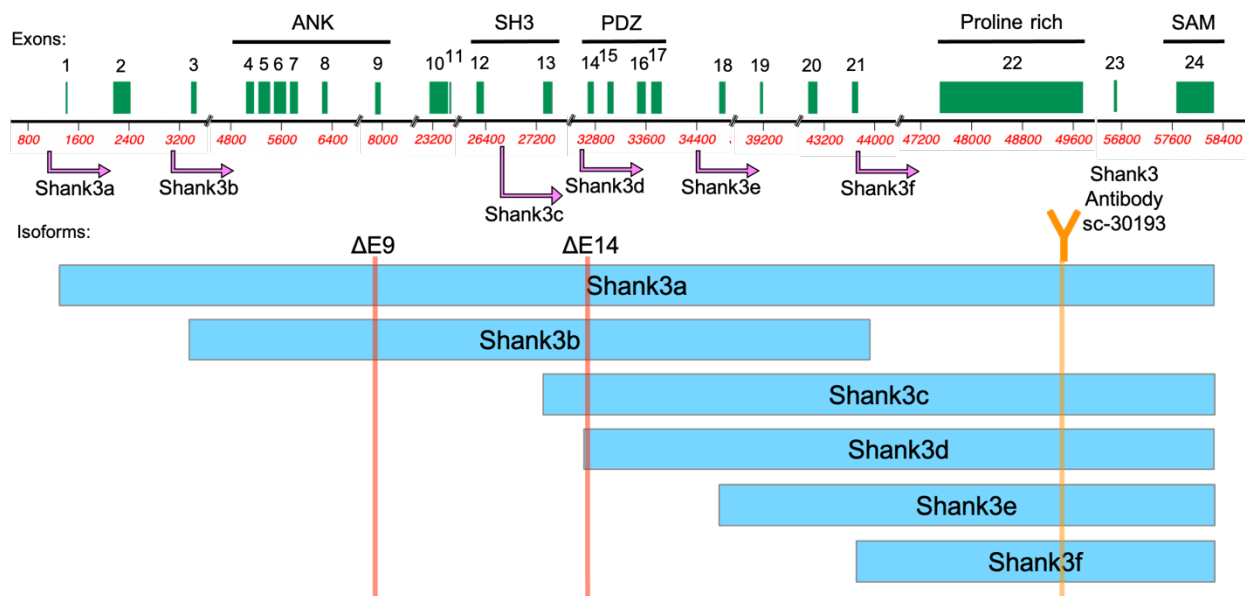


Figure 2.6 Schematic of Shank3 Isoforms in Prairie Vole. Map of intragenic promoter regions in vole based on alignment to promoter regions of mouse Shank3 (www.genome.ucsc.edu). In light blue we present the 5 most prevalent Shank3 isoforms based on homology to annotation of mouse Shank3. Purple arrows indicate promoter regions for respective isoforms. Orange line indicates epitope of Shank3 antibody used in Western Blot experiments. Vermillion lines indicate sites of frame shift in amino acid sequence for $\Delta E9$ and $\Delta E14$ mutations, respectively.

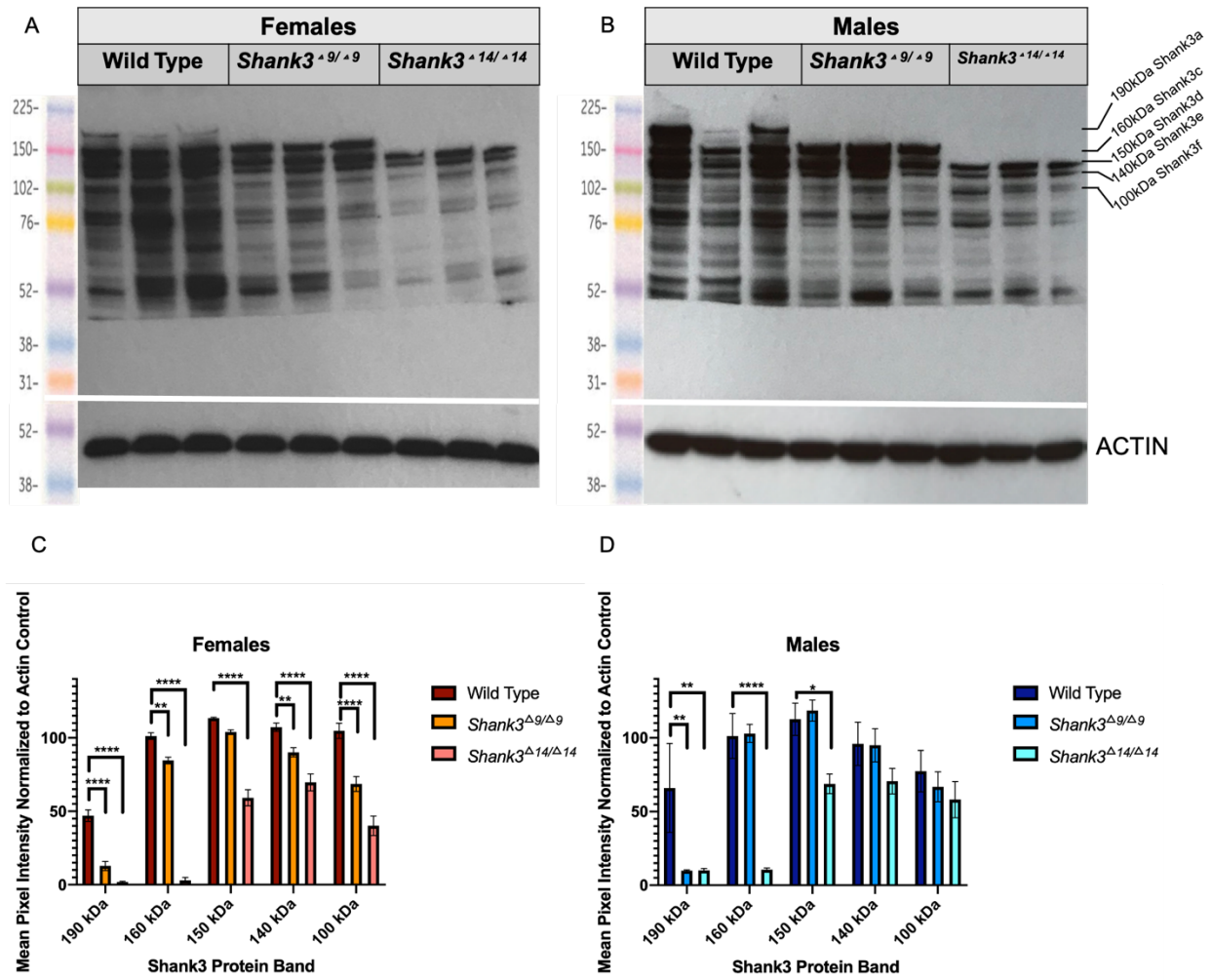


Figure 2.7 Western Blot of Shank3 Isoforms in wild type and *Shank3* mutant prairie voles. A,B: Gels from Shank3 Protein Western Blot: X-Ray images of Western Blot labeling Shank3 antibody (top) and control actin antibody (bottom) for n=3 samples of Wild Type, *Shank3*^{ΔE9/ΔE9}, and *Shank3*^{ΔE14/ΔE14} medial sagittal brain sections for female (A) and male (B) prairie voles. Ladder units are kDa, M_r x 10³ (Full Range Rainbow Recombinant Protein Molecular Weight Marker, Sigma Aldrich 16753093). C,D: Quantified Shank3 Protein Western Blot: Inverted mean intensity of each protein band labeled with Shank3 antibody with background subtraction and normalized to actin control across genotype for female (A) and male (B) wild type and *Shank3* mutant prairie voles. Data is plotted as the mean and SEM.

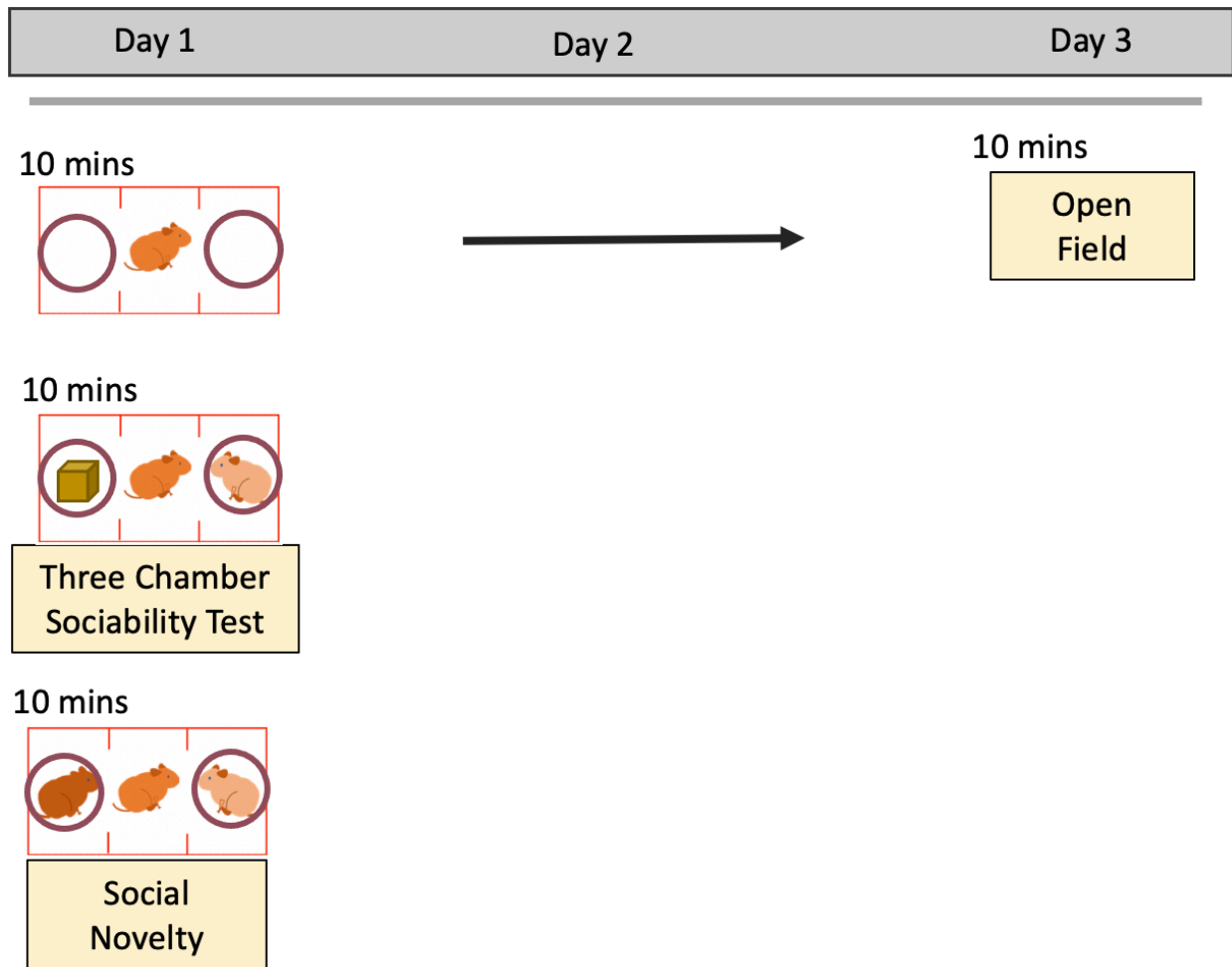


Figure 2.8 Control Behavior Paradigm. Male and female 8-10 week old prairie voles of either *Shank3*^{ΔE9/+} and *Shank3*^{ΔE14/+} genotypes, and their wild-type siblings, went through the above 3 day control behavior paradigm including Sociability, Social Novelty, and Open Field assays.

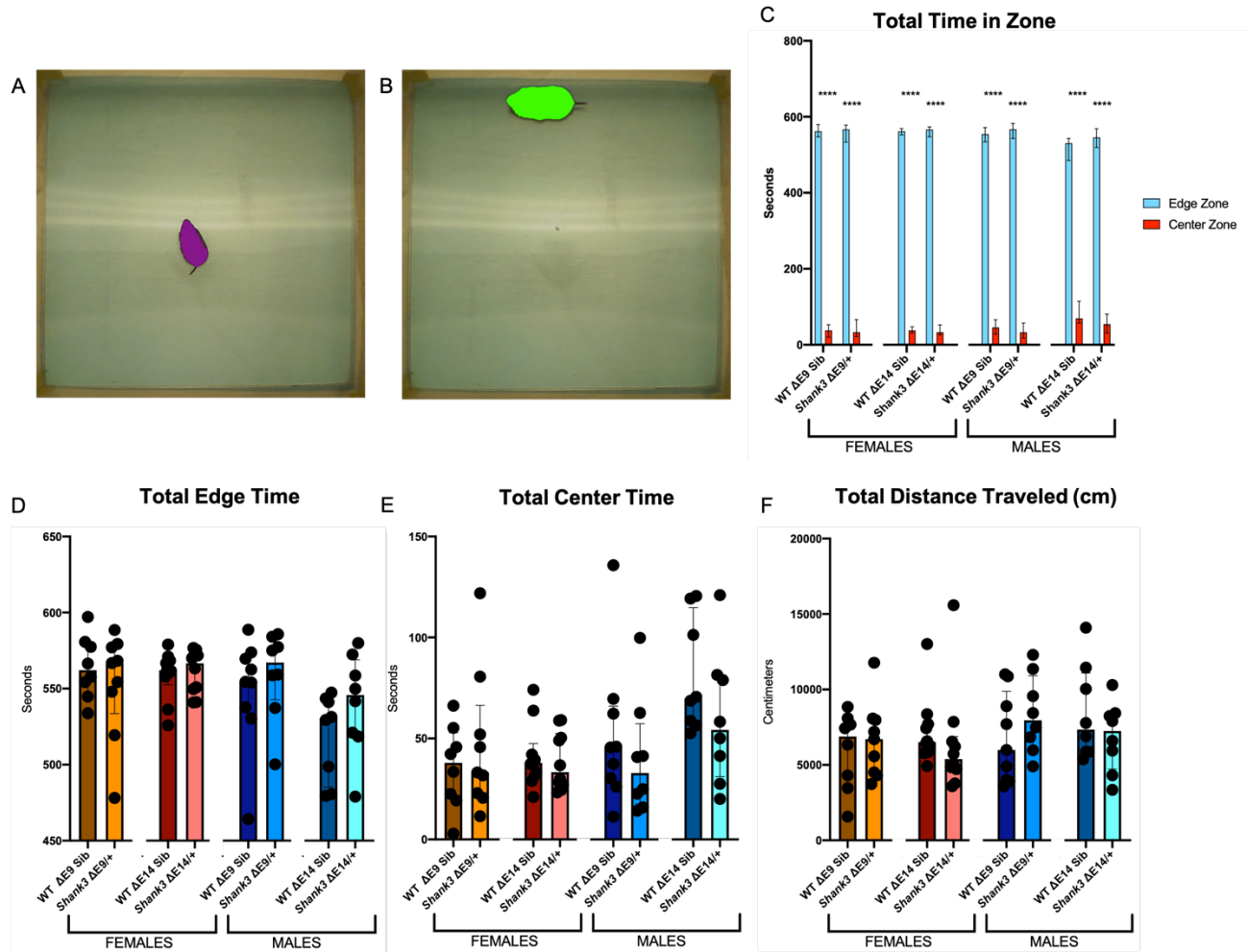


Figure 2.9 Open Field Test. Contour Tracing in Prairie Vole Open Field Test: Our contour tracing code defines the prairie vole's position by the centroid of its contour. The vole is traced in purple when it is in the center zone (A), and green when in the edge zone (B). The center is defined by a central box $\frac{1}{2}$ the area of the arena, and the edge is the surrounding perimeter. (C) Both females and males of all genotypes spend significantly more time in the edge zone than center zone ($p < 0.0001$ for all groups). *Shank3*^{ΔE9/+} and *Shank3*^{ΔE14/+} females and males show no significant difference in time spent in edge zone (A) and center zone (B), nor total distance traveled (F) when compared directly to their same-sex wild-type siblings. Data is plotted as the median and interquartile range.

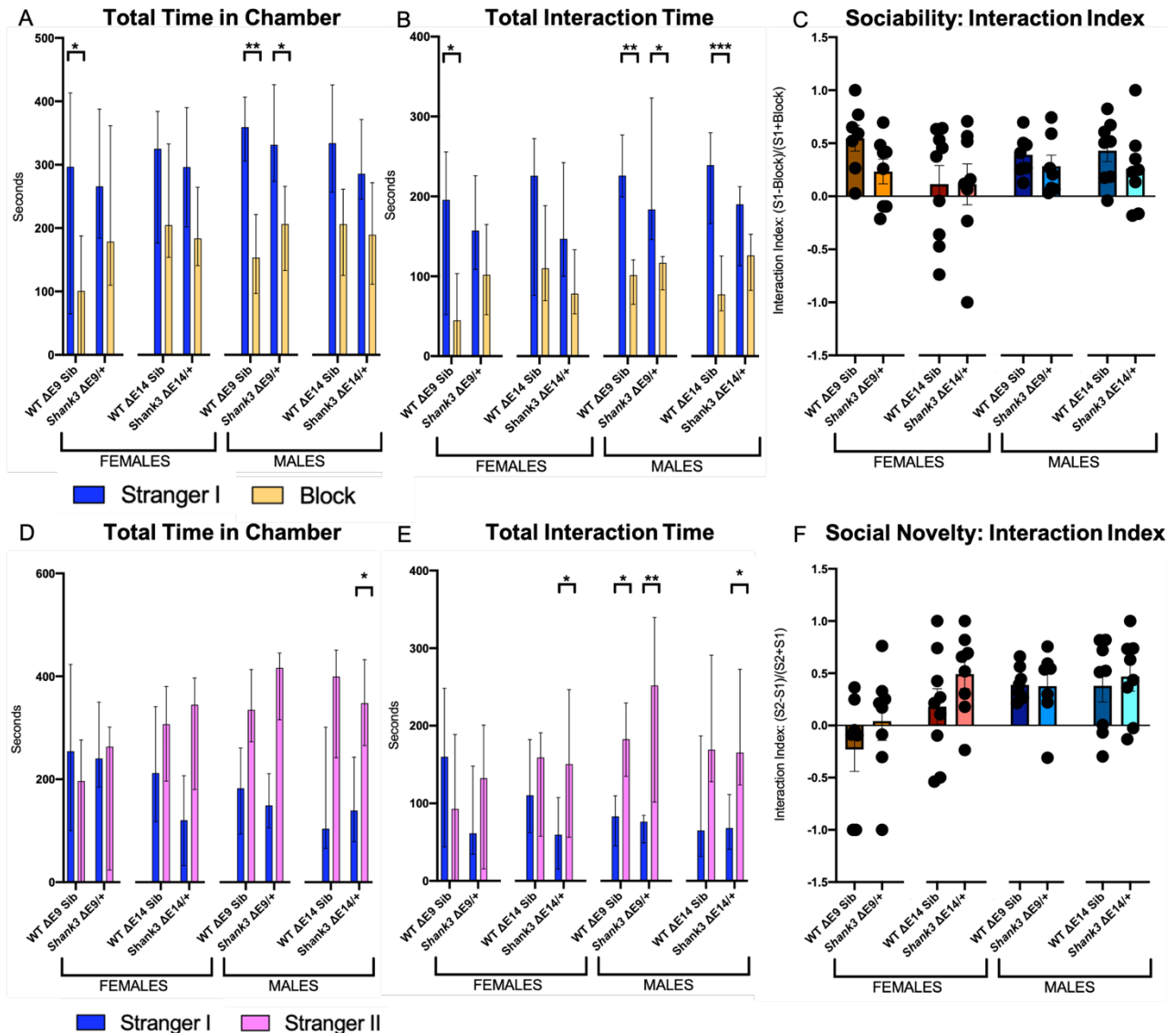


Figure 2.10 Sociability & Social Novelty. A-C: Three Chamber Sociability Test: Females and males of both *Shank3*^{ΔE9/+} and *Shank3*^{ΔE14/+} show no significant difference in preference for Stranger I as compared to their wild-type same-sex siblings. Significance in (A) and (B) indicates Bonferonni's multiple comparison test for Stranger I - Block between heterozygous animals and their wild-type same-sex siblings, separated by sex and by mutation, following two-way repeated-measures ANOVA. D-E: Social Novelty Test: Females and males of both *Shank3*^{ΔE9/+} and *Shank3*^{ΔE14/+} show no significant difference in preference for Stranger II as directly compared to their wild-type same-sex siblings. Significance in (D) and (E) indicates Bonferonni's multiple comparison test for Stranger II – Stranger I between heterozygous animals and their wild-type same-sex siblings, separated by sex and by mutation, following two-way repeated-measures ANOVA. Data A,B,D,E is plotted as the median and interquartile range; C,F is plotted as the mean and SEM. N=70.

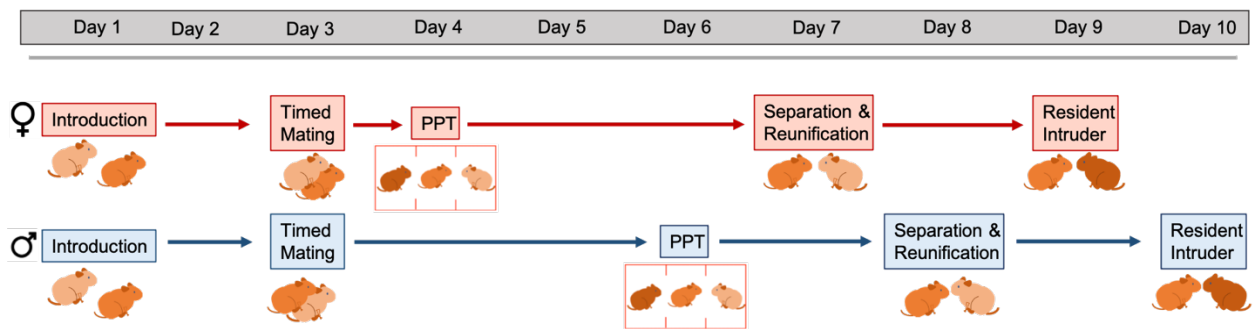
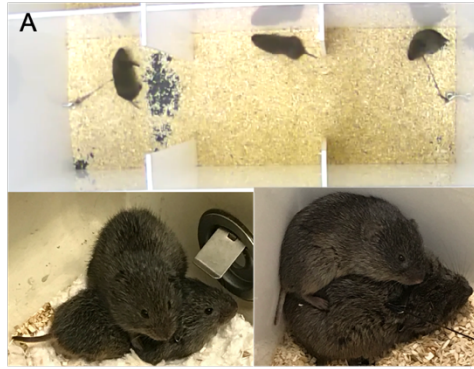
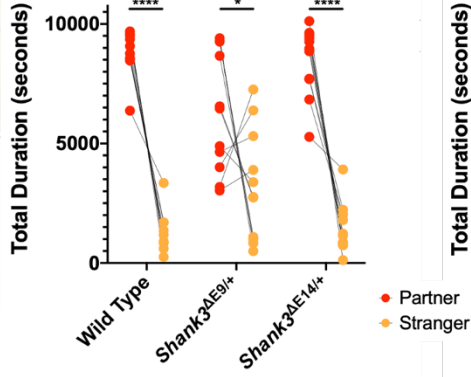


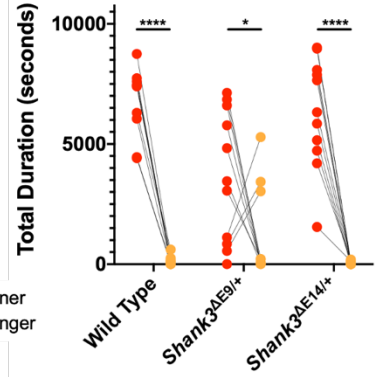
Figure 2.11 Behavior paradigm for social attachment behaviors across pair bonding.



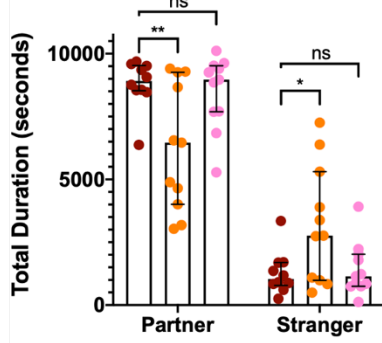
B Females: Duration in Chamber



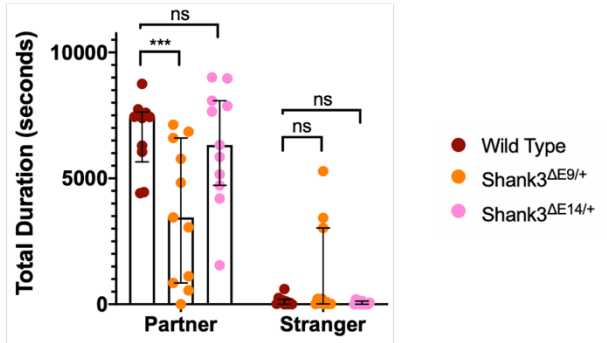
C Females: Huddle



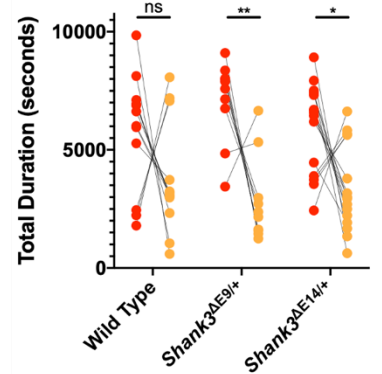
D Females: Duration in Chamber



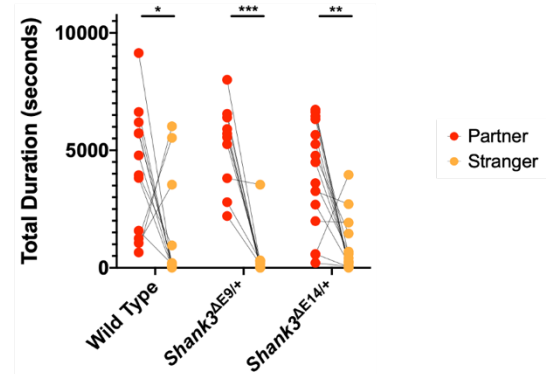
E Females: Huddle



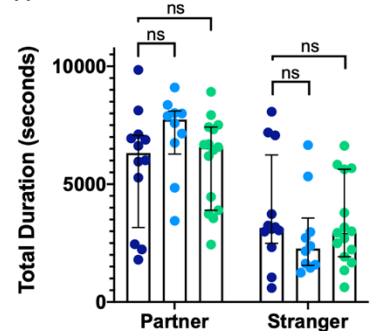
F Males: Duration in Chamber



G Males: Huddle



H Males: Duration in Chamber



I Males: Huddle

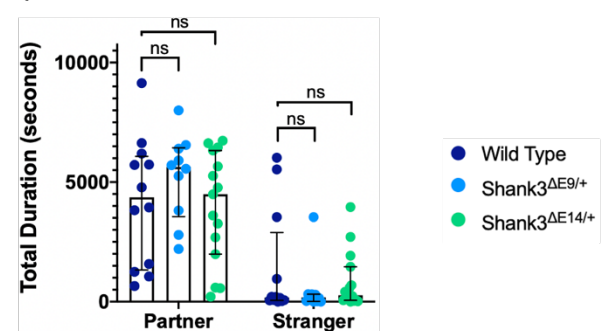


Figure 2.12 *Shank3*^{ΔE9/+} females show diminished preference for their partner. (A) PPT Apparatus (top) and huddle positions between vole pairs (bottom). Both females (B) and males (F) show preference for their partners by time spent in the partner's chamber over the stranger's chamber, across genotypes. Both females (C) and males (G) also show preference for huddling with their partner over a stranger, across genotypes. Female *Shank3*^{ΔE9/+} voles show a significant reduction in preference for their partner as compared to their wild-type siblings, both in chamber time (D) and huddle duration (E). *Shank3*^{ΔE14/+} do not show any diminished preferences (D,E). Bonded males of either mutant genotype do not show any difference in preference for their partner as compared to wild-type siblings (H,I). Assay duration is 10800s. Female Wild Type N=10, Female *Shank3*^{ΔE9/+} N=11, Female *Shank3*^{ΔE14/+} N=11, Male Wild Type N=12, Male *Shank3*^{ΔE9/+} N=10, Male *Shank3*^{ΔE14/+} N=15. Data is plotted as the median and interquartile range.

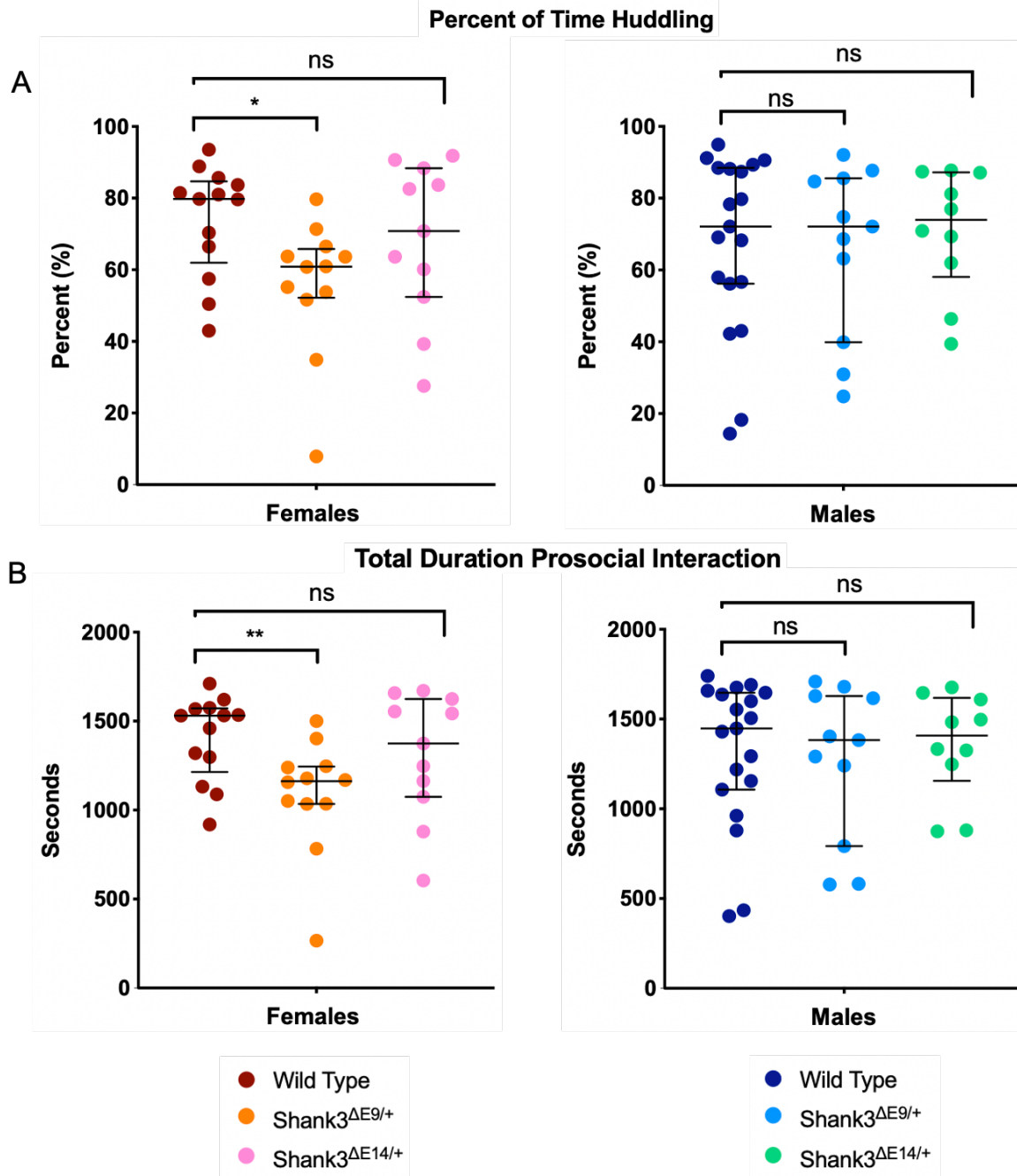


Figure 2.13 Bonded $Shank3^{\Delta E9/+}$ females show reduced attachment behaviors towards partners in reunification. $Shank3^{\Delta E9/+}$ females show significantly less time huddling with their partners (A) and engaging in prosocial behaviors with their partners (B) following acute separation, as compared to their wild-type siblings. Bonded $Shank3^{\Delta E14/+}$ females, as well as males of either mutant genotype, do not show any difference in huddling or prosocial behaviors as compared to their respective wild-type siblings. Assay duration is 1800s. Female Wild Type N=13, Female $Shank3^{\Delta E9/+}$ N=12, Female $Shank3^{\Delta E14/+}$ N=11, Male Wild Type N=19, Male $Shank3^{\Delta E9/+}$ N=11, Male $Shank3^{\Delta E14/+}$ N=10. Data is plotted as the median and interquartile range.

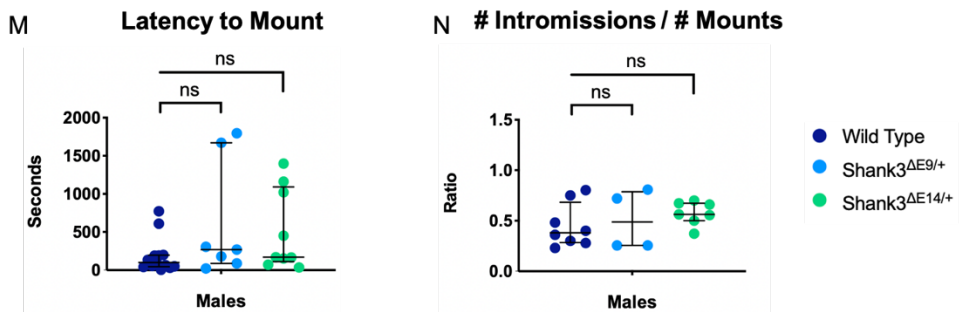
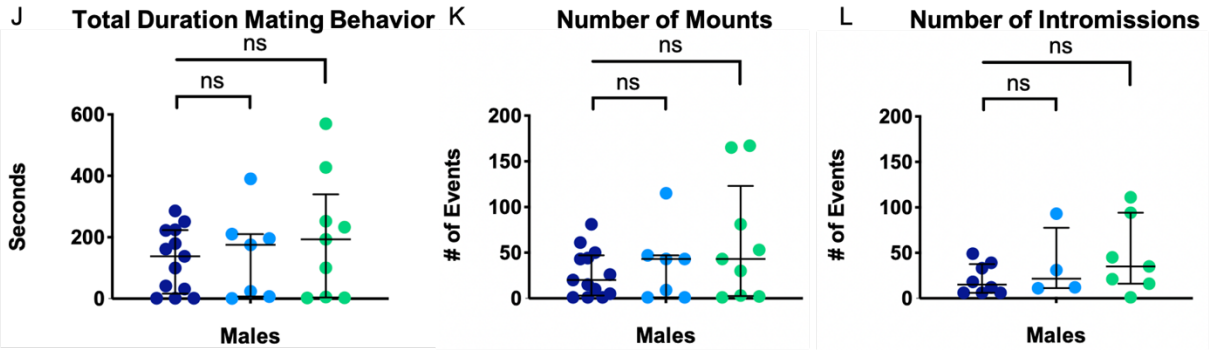
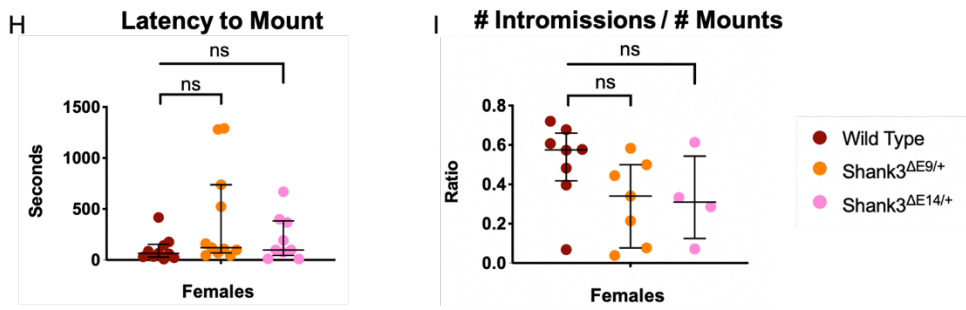
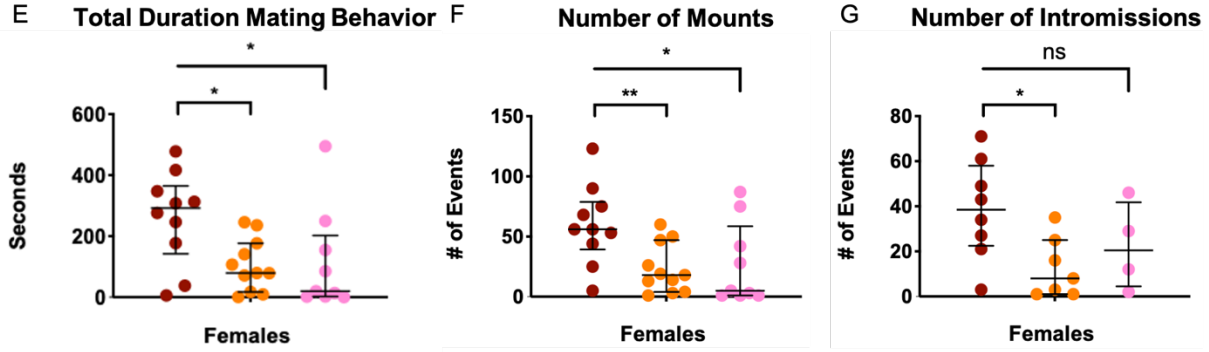
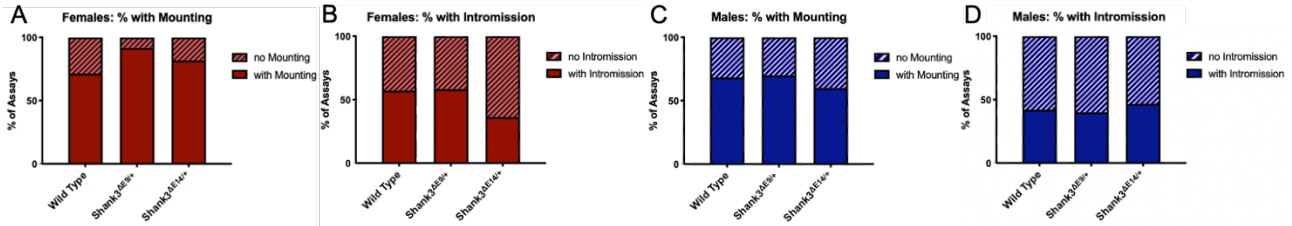


Figure 2.14 Bonded *Shank3*^{ΔE9/+} and *Shank3*^{ΔE14/+} females show reduced mating behaviors with male partners. There are no differences by genotype if a pair demonstrates mating behaviors during the timed mating assay (A,B,C,D). Of the pairs that performing mating behaviors, pairs including either a *Shank3*^{ΔE9/+} or *Shank3*^{ΔE14/+} female show decreased mating behaviors such as total duration of mounting and intromission (E), total number of mounts (F), and total number of intromission events (G). Male genotype did not affect any of these metrics of sexual activity in the timed mating assay (J,K,L,M,N). Assay duration is 1800s. Female Wild Type N=14, Female *Shank3*^{ΔE9/+} N=12, Female *Shank3*^{ΔE14/+} N=11, Male Wild Type N=19, Male *Shank3*^{ΔE9/+} N=10, Male *Shank3*^{ΔE14/+} N=15. Data is plotted as the median and interquartile range.

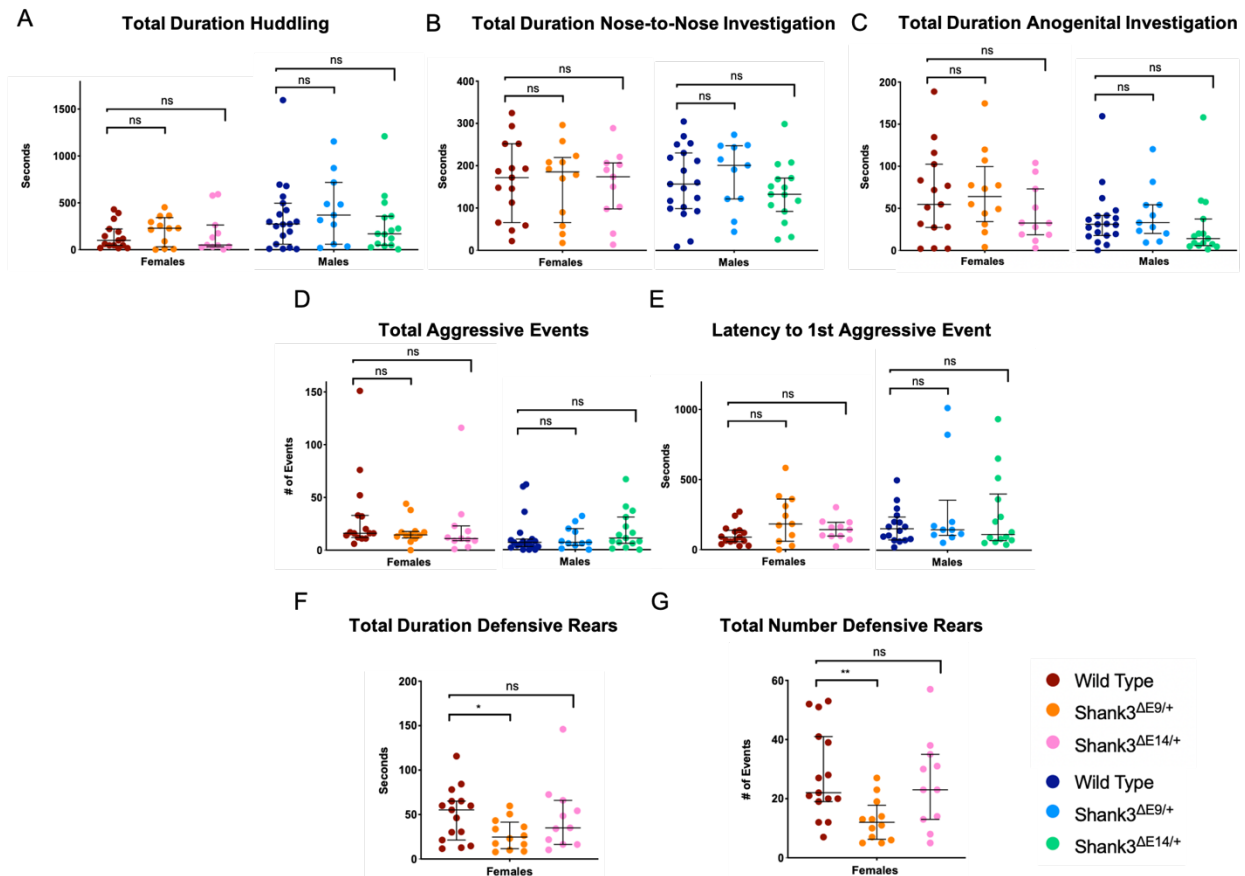


Figure 2.15 Sexually naïve *Shank3* mutant and wild-type voles show prosocial behaviors to a novel opposite sex vole. Both female and male *Shank3* mutants and wild type show huddling (A), nose-to-nose investigation (B), and anogenital investigation (C) at first introduction to their opposite sex partner. There is no genotype effect of aggressive behavior to a partner at first introduction in either sex (D,E). Sexually naïve $Shank3^{\Delta E9/+}$ females show a reduction in defensive rearing at introduction to a novel male as compared to their wild-type siblings (F,G), while sexually naïve $Shank3^{\Delta E14/+}$ females do not show a difference in defensive rearing (F,G). Assay duration is 1800s. Female Wild Type N=15, Female $Shank3^{\Delta E9/+}$ N=12, Female $Shank3^{\Delta E14/+}$ N=11, Male Wild Type N=19, Male $Shank3^{\Delta E9/+}$ N=11, Male $Shank3^{\Delta E14/+}$ N=15. Data is plotted as the median and interquartile range.

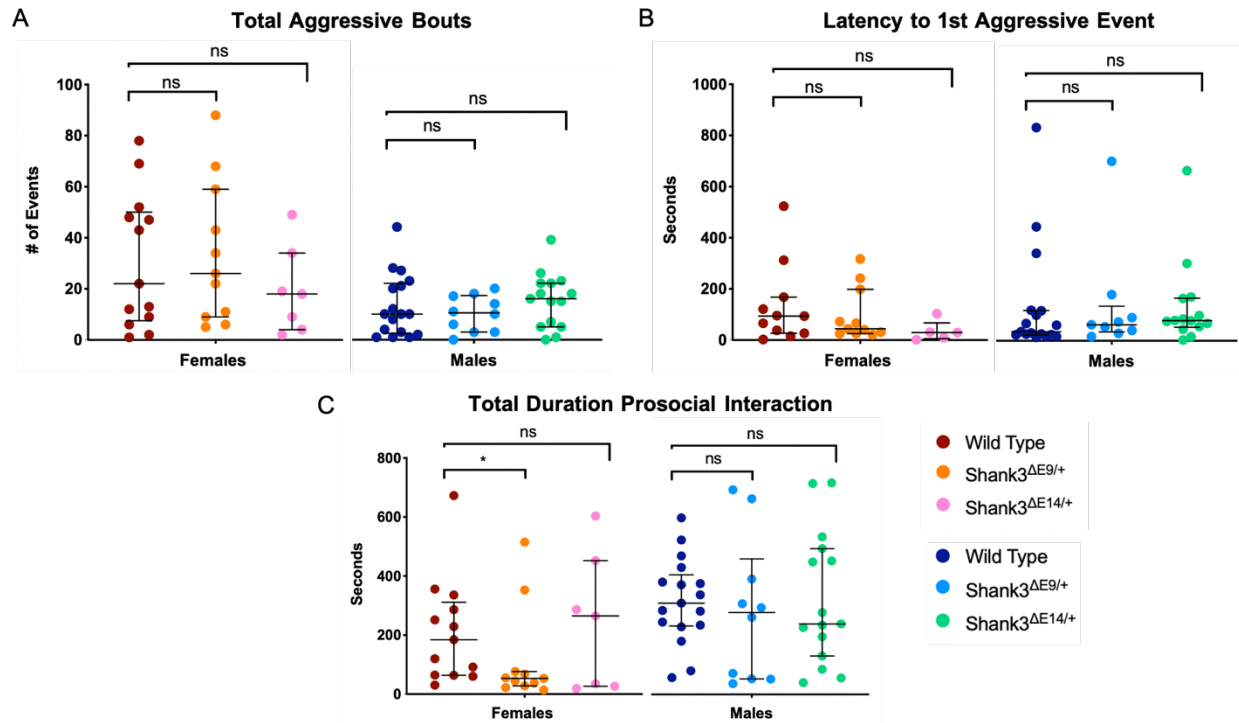


Figure 2.16 Bonded wild-type, *Shank3*^{ΔE9/+}, and *Shank3*^{ΔE14/+} voles show aggressive behaviors towards a novel stranger vole. Female and male *Shank3* mutants perform a total number of aggressive bouts (A) and show a latency to first aggressive bout (B) in accordance with their respective wild-type siblings. Bonded *Shank3*^{ΔE9/+} females show a reduction in prosocial interaction with a male stranger compared to their wild-type siblings (C), while sexually naïve *Shank3*^{ΔE14/+} females do not show a difference in time engaged in prosocial interaction (C). Assay duration is 1800s. Female Wild Type N=13, Female *Shank3*^{ΔE9/+} N=11, Female *Shank3*^{ΔE14/+} N=7, Male Wild Type N=17, Male *Shank3*^{ΔE9/+} N=10, Male *Shank3*^{ΔE14/+} N=15. Data is plotted as the median and interquartile range.

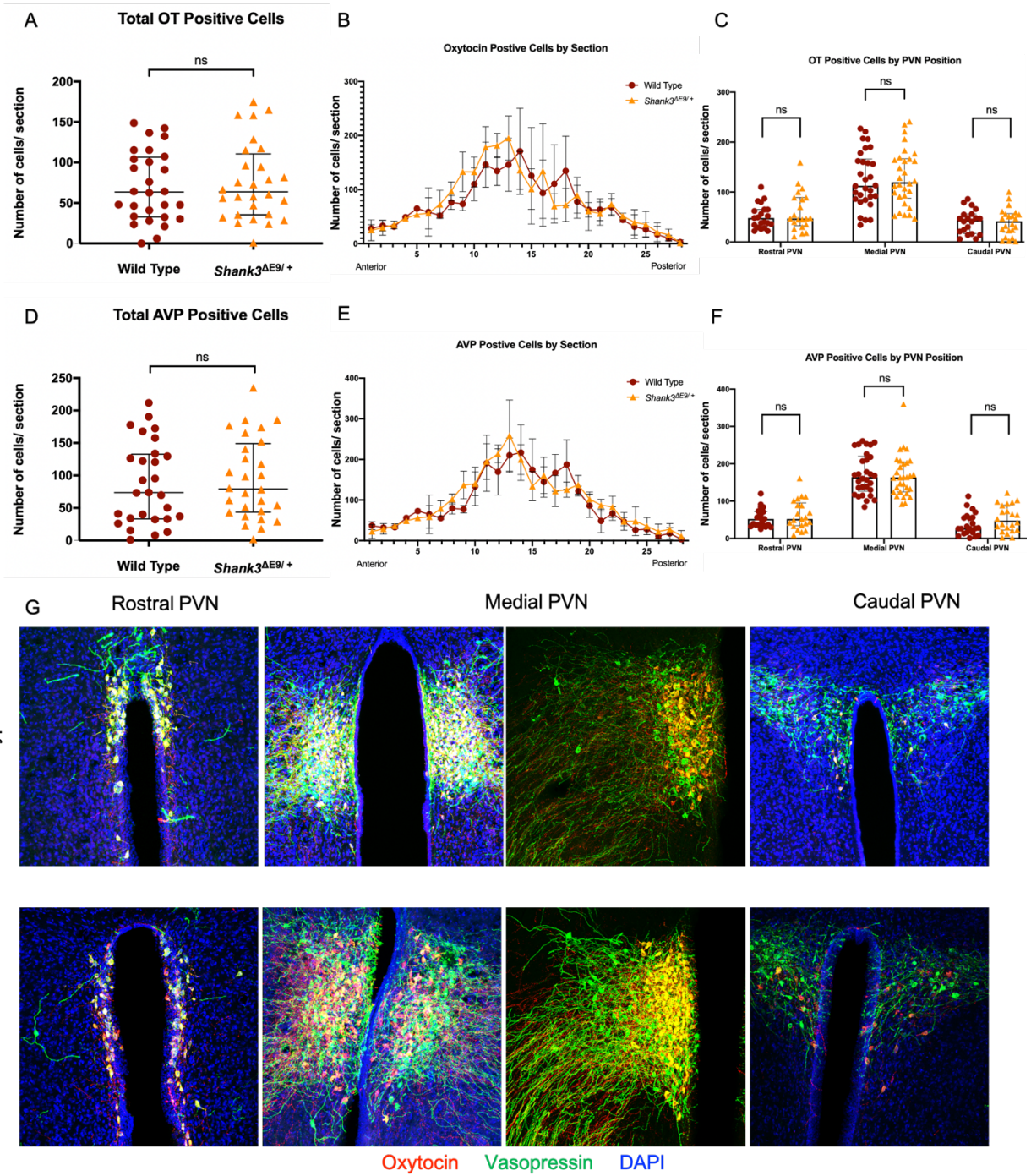


Figure 2.17 *Shank3*^{ΔE9/+} and wild-type females show comparable densities of OT and AVP positive cells across the PVN. *Shank3*^{ΔE9/+} females show no difference in total number of OT (A) or AVP (D) positive cells across the PVN compared to wild-type siblings. When comparing OT and AVP positive cell counts across anterior to posterior PVN section, the mutants show no difference in distribution from wild type (B,E). There are no regional differences in OT and AVP positive cell counts in rostral, medial, and caudal PVN between *Shank3*^{ΔE9/+} and wild-type females (C,F). Representative images of rostral, medial, and caudal PVN are depicted in G. The right panel of medial PVN shows only the left side of the third ventricle in medial PVN, in the absence of DAPI fluorescence, to highlight the OT and AVP positive fibers in this region. Female Wild Type N=3, Female *Shank3*^{ΔE9/+} N=3. A,C,D,F are plotted as the median and interquartile range, B,E are plotted as the mean and standard deviation.

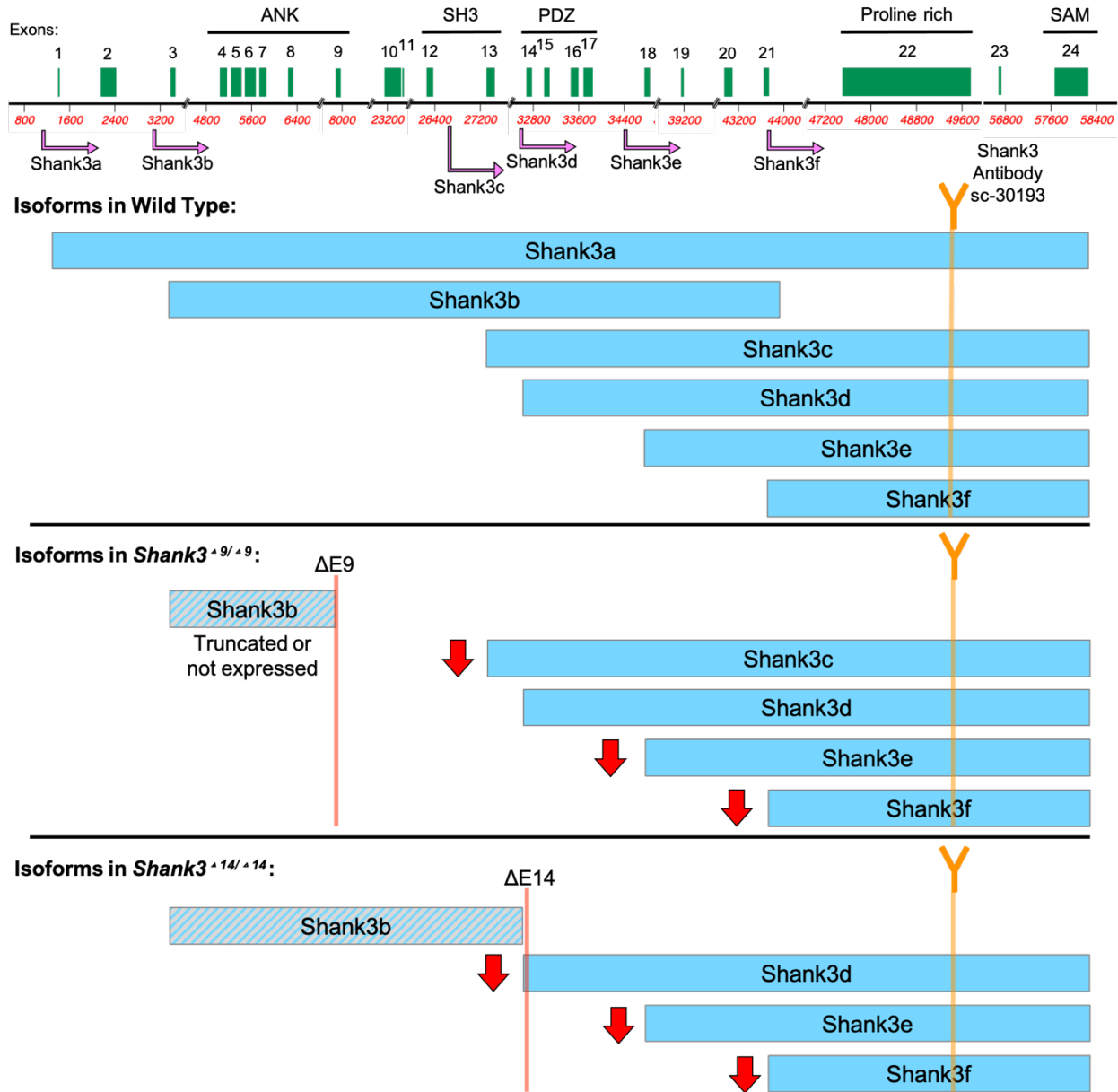


Figure 2.18 Predicted Shank3 isoforms in female mutants. Map of intragenic promoter regions and 5 most prevalent Shank3 isoforms in vole, from Figure 2.6, and schematics of predicted isoform expression for each *Shank3* mutation in females based on Western Blot Experiment (Figure 2.7). Both mutations yield full loss of Shank3a and decreased expression of both Shank3e and Shank3f. $\Delta E14$ also shows loss of Shank3c and decreased expression of Shank3d. $\Delta E9$ shows decreased expression of Shank3c, and we predict a full loss or truncated version of Shank3b, not detected by this epitope, including functional loss of ANK and/or SH3 domains. Purple arrows indicate promoter regions for respective isoforms. Orange line indicates epitope of Shank3 antibody used in Western Blot experiments. Vermillion lines indicate sites of frame shift in amino acid sequence for $\Delta E9$ and $\Delta E14$ mutations, respectively. Vermillion down arrows signal decreased expression.

METHODS

Animals. Subjects were laboratory-bred prairie voles (*Microtus ochrogaster*) of a colony founded by animals wild-caught near Champaign, Illinois. Voles were weaned at 24 ± 3 days and housed with same-sex age-matched voles of up to six per cage. All animals were maintained under a 14:10 h light-dark cycle and provided food and water *ad libitum*. Following 7 generations of outcrossing, *Shank3* mutant vole lines were maintained by breeder pairs of either one heterozygous animal and one wild-type outcrossed vole from our colony established for behavior experiments, or 2 heterozygous animals.

All experiments were performed and analyzed with the experimenter blinded to genotype. The protocol was approved by the Institutional Animal Care and Use Committee (IACUC) and directed by the Guide for the Care and Use of Laboratory Animals published by the National Research Council.

Genotyping. All DNA samples were tail clippings digested in lysis buffer (100mM Tris-HCl pH 8.5, 5mM EDTA, 0.2% SDS, 200nM NaCl) with 1:200 Proteinase K overnight at 55C. All tail DNA was used at 1:10 dilution for PCR template. The *Shank3* exon 9 mutant allele is amplified by primers FWD: GCTTGCTGAGGTAATCAAGACTC (delB_ex9sh3) and REV: CTTCTGCCTGCCAGTCTTGAAGC (REV2_ex9sh3) as a 521bp product. The *Shank3* exon 9 wild-type allele is amplified by primers FWD: GAGGTAATCAAGACCCACAAAGAC (wtB_ex9sh3) and REV: CTTCTGCCTGCCAGTCTTGAAGC (REV2_ex9sh3) a 513bp product. Both reactions are performed with Phusion polymerase, 63.5C annealing, 1 minute extension @ 72C. Each allele can alternatively be amplified with primers FWD:

GTTGAAGATTTGGGCACATCTGGA (g,Sh3,6 FWD) and REV: CCTTCTGCCTGCCAGTCTTGAAGC (g,Sh3,6 REV) and annealed at 62.5C for sequencing with primer AGAATGAGGGCTGAAAAGCTGT (s,Sh3,6a).

The *Shank3* exon 14 mutant versus wild-type allele can be identified by amplifying digested tail DNA with primers FWD: TTGCTGCTCCCTCCAGAAAC (g,Sh3,7ii FWD) and REV: CCCCATGTGTCCACACCCCT (g,Sh3,7ii FWD) with Phusion polymerase, 63.5C annealing, 1 minute extension @ 72C to yield a 120bp product. This product is then digested with CviKI-1 for 2 hours at 37C and the subsequent product is run on a 3% agarose gel. Wild-type exon 14 allele has a CviKI-1 recognition site while the mutant allele does not yielding a single 120bp band for homozygotes, 3 bands at 120bp, 77bp, and 43bp for heterozygotes, and 2 bands at 77bp and 43bp for wild types. The g,Sh3,7ii FWD primer can also be used to sequence the 120bp product.

Western Blot. Homozygous *Shank3*^{ΔE9/ ΔE9}, *Shank3*^{ΔE14/ ΔE14}, and wild-type male and female voles were euthanized with CO₂ and brains were immediately extracted. Brains were cut sagittally into 4 sections, flash frozen on dry ice, and then stored at -80C. One medial section of brain per animal was homogenized in RIPA buffer with a mortar and pestle on ice. We ran each sample through a BCA protein quantification assay (Thermo Fisher Scientific) and normalized protein concentration across samples.

Normalized samples were loaded into a NuPage 4 to 12%, Bis- Tris, 10-well gel and run through the NuPage electrophoresis system (Invitrogen) at 120V for 2.5 hours, and then transferred to membrane at 32V for 1 hour. Membranes were blocked for 1 hour in 5% powder milk in PBST. Membranes were then incubated on a rotator overnight at 4C in

primary antibody: 1:2,000 rabbit anti-Shank3 (Santa Cruz-30193). Next, membranes were washed 3 times in 1xPBST and then incubated for 1 hour in secondary antibody: 1:5,000 HRP anti-rabbit. Membranes were then washed 4 times with 1xPBST and applied reagents for chemiluminescent detection (Thermo Fisher Scientific) in a cassette for one minute. Imaging was done on X-Ray film in a dark room.

The membranes were then washed and went through secondary control straining with primary antibody 1:10,000 mouse anti-actin and secondary antibody 1:10,000 HRP anti-mouse and followed the same above protocol until imaging on X-Ray film.

Mean intensity of each actin band and the 5 largest Shank3 bands per lane were measured in Fiji as an 8-bit image. One region of interest was created per row of each gel, large enough to fit the bounds of the largest band in the row. The same region of interest was used to measure every band in one respective row and mean gray-scale intensity was measured. Background intensity was measured for Shank3 and actin sections of each gel, by selecting a region of interest spanning all 9 rows and measuring the mean intensity. All signal and background mean intensity measurements were inverted by $\text{Inverted} = 255 - x$, as maximum intensity on this 8-bit image measures 255, and correlates to white light. Next, all background measurements were subtracted from their respective signal measurements. Finally, we normalized Shank3 band signal to the actin control band. To do so, we averaged the actin signal across 3 samples per genotype and took a ratio of each sample's actin signal over this average. We then divided the intensity of each band in this sample by its respective actin ratio. We analyzed intensities of female and male blots separately, by two-way ANOVA with Dunnett's multiple comparisons test,

designating wild type as the control cell. All plots and statistics were generated in GraphPad Prism.

Social Behavior Testing. All animals used in behavior experiments were generated from heterozygous (*Shank3*^{ΔE9/+} or *Shank3*^{ΔE14/+}) to wild type crosses. All wild-type control subjects were age-matched siblings of mutant animals. Subjects were paired with an opposite-sex age-matched “partner” wild-type vole from separate families at 7-10 weeks of age at the start of testing. Subject animals’ cages were marked as “lab care only” during testing days, to ensure the animals were not disrupted by cage changes prior to testing. All “stranger” animals were wild-type opposite-sex age-matched controls from separate families, and housed in same-sex cages of 5 ± 1 animals. Each stranger was used no more than once per day, and a maximum of 3 days of testing total. Stranger animals were not used again after any Resident Intruder assay. All assays were recorded with FosCam IP cameras and as backup, Google Nest Cam cameras.

All experiments were conducted in light, between 13:00 and 20:00, in a room established for only behavior experiments. All animals are brought from the housing room to the behavior room on the day of testing and allowed at least 30 minutes acclimation before experiments begin. All animals are returned to the housing room upon completion of assays.

Introduction to Partner. A fresh cage with Sani Chips bedding was placed in an open top cooler with a FosCam anchored above for recording and a gooseneck light per cage to standardize lighting. The experimental animal was removed from its same-sex group

housing cage and placed in the fresh cage, which at this point is called the “home cage.” After a 2 minute acclimation, an opposite-sex age-matched wild-type “partner” animal is added to the cage and indicates the start of the 30 minute assay. At the end of the assay, nestlets, 2 red plastic tubes, and food and water are added to the cage and the pair is returned to the housing room.

Timed Mating. Approximately 24 hours after Introduction to Partner, the pair is divided within the cage by a laser cut ¼” thick piece of acrylic with ½” diameter holes. These holes allow nose-to-nose investigation but prevent complete physical contact, including mating. Each animal has one red tube, and access to food and water *ad libitum*. Another 24 hours after placement of the divider the cage is returned to the cooler under the FosCam, the divider is pulled out and the red tubes are removed. The last experimenter contact indicates the start of this 30 minute “Timed Mating” assay. The Manoli lab has established that prairie voles reliably mate under these conditions, given that the female has sustained sufficient contact to be induced into estrous by the male and thus has become sexually receptive. At the completion of the assay, the red tubes are replaced and the home cage is returned to the housing room.

Partner Preference Test. The Partner Preference Test (PPT) is a well-established three chamber choice test to assay the preference of an experimental animal between two stimulus animals (Williams et al., 1992). Our PPT apparatus is 10” x 32” white acrylic arena and divided into a left, central, and right chamber. Gooseneck lights are used to standardize lighting and FosCams, and backup Nest Cams, are anchored above for

recording. The floor of the assay is removable and covered with a thin layer of fresh Sani Chips bedding before each assay.

Experimental females are tested in the PPT 24 hours after the Timed Mating assay, and experimental males are tested in the PPT 72 hours after the Timed Mating assay. We empirically defined these times as close to the minimum amount of cohabitation post-mating for each sex to show a preference for their partner respectively, thus sensitizing the assay.

Prior to the start of the PPT, all experimental voles and respective strangers are brought into the behavior room to acclimate. At least 30 minutes prior to the start of the assay, we position tethers on all partner and stranger animals, consisting of a black zip tie collar attached to a 6" fishline connected by buckle locking carabiners on each side. The partner and stranger stimulus animals are returned to their respective home cages to adjust to the tethers before the start of assay. Following acclimation, the partner and a stranger vole are randomly tethered to either the left or right chamber of the PPT apparatus, by an eye screw hook drilled into opposite walls. This tethering allows the animals full range of movement and interaction with the experimental animal, while preventing them from leaving their designated chamber.

Prior to the start of assay, we also attach two black plastic dividers to either end of the center chamber with binder clips. The experimental vole is then tube transferred into this center chamber. We allow at least 5 minutes for all 3 animals to adjust to their chamber and conditions before the start of assay.

The PPT assay is initiated when the two black divider around the center chamber are removed, and the experimental vole has access to all 3 chambers and both stimulus

animals. The duration of the assay is 3 hours (10800s). Following the assay, all tethers are removed immediately and all animals are returned to their respective home cages.

Separation and Reunification. The Separation and Reunification assay is performed six days after pairing, for experimental females, and seven days after pairing, for experimental males. This timing maintains consistency between female and male behavior time points, while allowing male voles one rest day between their 72 hour post-mating PPT and the Separation and Reunification assay. In this assay, the experimental vole remains in the home cage, which is placed in the open top cooler with gooseneck lighting and FosCam recording, while the experimental vole's partner is transfer to a fresh cage and out of view. After a one hour duration of this separation, the partner animal is tube transferred into the home cage and thus the 30 minute Reunification assay is initiated and recorded. At the completion of the assay, the pair returns to the housing room in the home cage.

Resident Intruder. The Resident Intruder assay is performed eight days after pairing, for experimental females, and nine days after pairing, for experimental males. The timing was decided to allow all animals one rest day following Separation and Reunification. Again, the experimental vole is kept in the home cage which is placed in the behavior cooler for one hour, while the partner animal is transferred to a new cage. After one hour, an opposite-sex age-matched stranger stimulus vole, naïve to the Resident Intruder assay is tube transferred into the home cage. The addition of the stranger indicates the start of the assay, and the assay is recorded for a duration of 20 minutes. The

experimenter remains in the room for the duration of the assay to observe aggressive events. Any assay with 3 “tussle” events, an aggressive attack involving full body contact between the two voles, is immediately terminated.

Behavior Scoring. All assays were scored in The Observer XT by Noldus. All behaviors were coded to be mutually exclusive. For all home cage assays, the behavior code included state events: Sniffing (anogenital investigation), Investigation (non-anogenital investigation), Huddling, Mounting, Intromission, Tussle, Rear (defensive), and No Interaction; and point events: Offensive Aggression (this animal initiates aggression), Defensive Aggression (this animal was touched by the other animal prior to aggression), Receives Aggression, and Ejaculation. For the PPT, the behavior coded included state events: Left Chamber, Center Chamber, Right Chamber, Interact Left Stimulus Animal (in which “Interact” included any physical contact with less than 50% of bodies touching), Interact Right Stimulus Animal, Huddle Left Stimulus Animal (in which “Huddle” included any physical contact with at least 50% of bodies touching), and Huddle Right Stimulus Animal; and point events: Attack Left Stimulus Animal, Attack Right Stimulus Animal. In addition to genotype blinding across all assays, scorers were blinded to Partner vs Stranger identities in the PPT.

Statistical Analysis. We used Mann-Whitney Tests to compare mutants to their respective wild-type control for all behaviors except in the PPT. For the PPT, we used two way repeated measures ANOVA with Sidak’s multiple comparisons test. We used automated tests in GraphPad Prism to correct for P-values as needed. All scored

behavior data was plotted in GraphPad Prism. We plotted data as the median with interquartile range error bars and significance always represents in relation to the same sex wild-type control group unless otherwise stated. N is represented in Figure legends.

Control Behavior Testing. All animals used in control behavior experiments were generated from heterozygous (*Shank3*^{ΔE9/+} or *Shank3*^{ΔE14/+}) to wild type crosses, thus all wild-type control subjects were age-matched siblings of mutant animals. Control behavior animal subjects were 8 to 10 weeks at the start of testing and housed with 5 ± 1 same-sex cage mates. All stimulus animals were same-sex group-housed, and unrelated to the subject animal. Assays were performed in the same behavior room as the social behavior assays.

Open Field. The Open Field Test (OFT) apparatus was custom made and constructed at 22" x 22" with 15" high walls. The floor was made of 1/8" thick opaque ribbed acrylic, and the 5 other sides of the closed top box were made of 1/8" thick non-glare clear acrylic. This apparatus was designed to proportionally fit a prairie vole based on sizing for mouse and rat OFTs. The top was removable with a 1" hole cut in the center, through which a 720 pixel ELP USB camera was attached to record the entire field.

All subject animals were acclimated in the behavior room for 30 minutes before the start of testing, and then tube transferred into the apparatus to perform the OFT. The assay begins when the camera is refocused following addition of the subject vole, and the duration is 10 minutes. After the assay, the subject animal is immediately returned to its same-sex group housed home cage.

Sociability and Social Novelty. Two days after the open field test, the subject animals return to the behavior room with respective same-sex group-housed 5 to 7 week old stimulus animals from separate families, acclimate for 30 minutes, and undergo consecutive Sociability and Social Novelty assays. Both assays use the same PPT apparatus as described above, however we do not use bedding on the flooring and instead use a white floor to allow less background for automated scoring. In the center of the left chamber and the right chamber, we place 3" diameter x 4" high metal pen cups with the open side face down. Cups are held in place with a 1kg metal weight each, so that the cups do not move during the assay. We attach black plastic dividers to either side of the center chamber with binder clips, and tube transfer the subject animal into the center chamber. We remove the dividers and allow the animal to explore the apparatus with the two empty cups and weights for 10 minutes. We then bring the animal back to the center chamber, blocked by the black dividers, and randomly place a juvenile same-sex stranger animal under one cup, and a wooden block under the opposite cup. We then remove the dividers which initiates the 10 minute Sociability assay, which is recorded by Nest Cams anchored above the apparatus. At the completion of 10 minutes, we again restrict the subject animal to the center chamber with the black dividers, and replace the wooden block with a second, naïve same-sex juvenile stranger animal. We remove the dividers again which initiates the Social Novelty assay. We record this assay for 10 minutes and then return all animals to their respective home cages.

Automated Behavior Scoring. All OFTs were scored with contour tracing Python code developed in the Manoli lab which defines the contour of the vole as a dark object against a light background. Parameters of thresholding and acceptable contour size are defined as appropriate. The vole's position at any time point is defined by the centroid of the contour. In the OFT, the four corners of the arena are defined. The boundaries of the center zone are defined by subtracting $\frac{1}{4}$ of each length of the arena from the respective edge. The edge zone is the perimeter surrounding the center zone that makes up the rest of the arena.

The sociability and social novelty tests were both scored using the same contour tracing code, in which the bounds of the three chamber apparatus were defined as well as the boundary between left-center chamber and center-right chamber. We also defined contours for each assay of the left and right metal cups containing stimuli. "Interaction" time with stimuli was defined by touching of the vole contour to a cup contour. The Social Interaction Index = $(\text{Stranger I Interaction} - \text{Block Interaction}) / (\text{Stranger I Interaction} + \text{Block Interaction})$. The Novelty Interaction Index = $(\text{Stranger II Interaction} - \text{Stranger I Interaction}) / (\text{Stranger II Interaction} + \text{Stranger I Interaction})$. For both above indexes, any animal that had zero total interaction time was excluded from both plots and analyses. All data was aggregated through Jupyter Notebook.

Statistical Analysis. We used Mann-Whitney Tests to compare any single variable quantity of mutants to their respective wild-type control, such as total distance traveled in the OFT. We used two-way repeated measures ANOVA with Bonferroni's multiple comparison test to compare any choice task across 2 genotypes, such as time interacting

with Stranger I vs Stranger II in the social novelty task. We used automated tests in GraphPad Prism to correct for P-values as needed. All scored behavior data was plotted in GraphPad Prism. We plotted data as the median with interquartile range error bars and significance always represents in relation to the same sex wild-type control group unless otherwise stated.

Immunohistochemistry. *Shank3*^{ΔE9/+} and wild-type female voles, at 8 to 10 weeks old, were anaesthetized with Ketamine/Xylazine and perfused with 4% paraformaldehyde (PFA) in PBS. Brains were extracted, fixed with 4% PFA with 24 hours, then saturated with 30% sucrose, and embedded in OCT to be stored at -80C. Brains were sliced into 50 μm sections on a cryostat set at -20C, and collected as 6 serial sections. Free-floating sections were washed in 1x PBS and then rinsed twice with 1:500 MgCl₂ in PBS (Solution A) Sections were blocked for 1 hour at room temperature in 0.5% donkey serum and 0.1% Tritonx100 in Solution A (Solution ADT) and then incubated at 4C overnight with primary antibodies in ADT: 1:1,000 rabbit anti-oxytocin (Invitrogen) and 1:10,000 mouse anti-AVP (Millipore).

Sections were then washed 4x with ADT and incubated for two hours at room temperature in secondary antibody in ADT: 1:500 cy3 anti-rabbit (Jackson ImmunoResearch) and 1:500 488 anti-mouse (Thermo Fisher Scientific). Next sections were washed with 300nM DAPI in ADT, followed by 3x with ADT. Sections were then washed 2x with 1:1000 Tritonx100 in Solution A and fixed with 20 minutes with cold 4% PFA. Sections were then mounted with AquaMount.

Microscopy, Quantification, and Statistical Analysis. The PVN was imaged across 28 sections with a Zeiss LSM 700 confocal microscope using 20x magnification.

All images were processed and cells were counted in Fiji. We used Fiji's Cell Counter Plugin to scroll through the Z-stack of an image and count double positive (yellow) as Type 4 counter, red (oxytocin) as Type 1 counter, and green (vasopressin) as Type 2 counter. In Microsoft Excel we summed the double positive cell count per section with oxytocin cell count and vasopressin cell count, respectively, to generate total number of oxytocin and vasopressin cells per section. We designated the 9 most anterior sections as rostral PVN, the medial 10 sections as medial PVN, and the 9 most posterior sections as caudal PVN. Sample images are processed in Fiji as composites of all 3 color channels and Z-stacks of maximum intensity.

We used Mann-Whitney Tests to compare total OT and AVP cell counts between mutant and wild type. To compare across genotypes and region of PVN, we used a mixed-effects model (REML) with Sidak's multiple comparisons test. We used automated tests in GraphPad Prism to correct for P-values as needed. We plotted data in GraphPad Prism as the median with interquartile range error bars for total cell counts and cell counts displayed by PVN region. We plotted cell count by individual section as the mean and standard deviation. N is represented in Figure legends.

Chapter 3: The Role of Early Life Stress & Sensory Cues in Pair Bond Expression

INTRODUCTION

Early life stress has been attributed to increased adult vulnerability to psychiatric disease, with 80% of adults who report early life neglect or abuse being diagnosed with a psychiatric disorder (Lukkes et al., 2009a; Gutman et al., 2003; Fone et al., 2008). Early life social isolation, as a result of childhood rearing in deprived institutions, correlates with a wide range of changes in social and attachment behaviors. These changes range from an increase in disinhibited attachment, defined by lack of selectivity in social relationships, to the other end of the spectrum resulting in autistic-like features, such as impaired social relationships. Strikingly, these symptoms persist for at least 7 years after adoption into well-functioning families, suggesting that environmental factors may have influenced the brain during a developmentally sensitive period of attachment behaviors early in life (Rutter et al., 2007a; Rutter et al., 2007b).

Early life social isolation in rodents has been used to model early life adverse experience. Post-weaning social isolation in male rats, for 4-6 weeks, causes increases in anxiety, aggression, and reduced social contact in adults, even after re-socialization (Lukkes, et al., 2009b).

As a species with long term social bonds, prairie voles are acutely sensitive to social isolation. Prairie vole pups as young as postnatal day 4 (P4) respond to parental separation with ultrasonic vocalizations and 4-6 fold increases in plasma corticosterone levels, while pups from closely related, promiscuous montane voles do not (Shapiro and Insel, 1990). Male prairie voles isolated post-weaning show increased anxiety behaviors

and a diminished preference for an empty cage over a novel male in a two chamber affiliation test, as compared to group housed voles, suggesting disinhibited attachment resulting from such stress (Pan et al., 2009). A single prolonged stress by consecutive restraint, forced swimming, and ether anesthesia, followed by a seven day recovery period, impairs pair-bonding in sexually naïve male prairie voles. Voles which have been exposed to such stress indiscriminately huddle with either partner or novel stranger, and preferentially spend time in a novel female's chamber instead of a partner female's chamber (Arai et al., 2016).

We wished to investigate the effect of early life stress, in the form of early life social isolation, on adult attachment behaviors in male and female prairie voles. Here we report that 4 weeks of juvenile isolation in female prairie voles is sufficient to disrupt typical attachment behaviors, as measured through preference for their male partner in a choice task.

The Partner Preference Test (PPT) used in this experiment differs from the apparatus described in Chapter 2, in that stimulus voles are confined behind a barrier and experimental voles do not have full free moving access to them (Figure 3.1A). We found an unexpected sexual dimorphism in how prairie voles display preference for a partner between the two PPT assays used. Female prairie voles displayed partner preference when the apparatus allowed for full chemosensory investigation (as provided when tethering the stimulus animals to a side in an open arena), as well as when the stimulus animals were placed behind a clear divider that prevents physical contact. In contrast, males only showed preference for the partner when allowed full chemosensory investigation, and not when the stimulus animals were placed behind clear dividers. This

finding has motivated an investigation into the sex differences in sensory cues which drive pair bond expression, as displayed by partner preference.

Previous studies report that prairie voles rely on both non-volatile odorant cues and volatile pheromones, as well as auditory cues, to communicate and to engage in typical adult attachment behaviors such as mating and mating-induced pair bond expression (Carter et al., 1980; Curtis and Wang, 2001; Kirkpatrick et al., 1994; Ma et al., 2014). Kirkpatrick et al., 1994 showed that odorant recognition by the main olfactory bulb is necessary for prairie vole social behaviors, as males with bilateral olfactory bulbectomies show decreased social behaviors including mating behavior, parental behavior, and sociability towards a same-sex sibling. Curtis and Wang, 2001, reported that sensory processing of pheromones by the vomeronasal organ (VNO) is necessary for vole attachment behaviors, as female prairie voles with VNO lesions do not display male-induced estrous nor preference for a partner in the PPT. Ma et al., 2014 demonstrate that male prairie voles emit increased ultrasonic vocalizations when presented a novel social stimulus or an estrous female, leading to a hypothesis that female voles may respond to such auditory cues.

We hypothesized that male prairie voles require non-volatile chemosensory cues to recognize their partner or display behavioral preference. We developed a paradigm of bedding assays in which we provide males a 2 chamber choice between bedding soiled by a partner female versus a stranger female. Preliminary results suggest that the olfactory cues in bedding are sufficient to elicit preference for a partner in male prairie voles.

RESULTS

Female prairie voles show a deficit in adult preference for a partner following early life social isolation

We established a paradigm for early life social isolation in which juvenile prairie voles were randomly assigned to either an isolation or group-housed condition at weaning age (P21) for four weeks through adolescence, until sexual maturity. After four weeks, the subject voles were paired in a new cage with an unrelated, opposite sex, age-matched sexually naïve prairie vole (“partner”) from a group-housing condition. Following two weeks of cohabitation, we assayed the partner preference of the subject vole in our original barrier apparatus for 30 minutes (Figure 3.1A). In this paradigm, the subject vole is placed in a center chamber with a metal grated bottom and allowed to freely explore the center, left, and right chambers. The partner vole and an opposite sex, age-matched, sexually naïve stranger vole were randomly assigned to either the left or right chamber and restricted to one half of the respective chamber by a divider of laser cut acrylic with ½” slits. This PPT apparatus restricts physical contact between subject and stimulus animal to only nose-to-nose investigation and therefore, significantly limits direct contact such as anogenital investigation and huddling, while permitting visual, auditory, and volatile olfactory cues to be detected, as well as some lachrymal cues exchanged during limited nose-to-nose contacts.

Group-housed female prairie voles showed significant preference for their partner in this PPT apparatus, as measured by percent of time spent in the partner versus stranger chamber (Figure 3.1B; Mann-Whitney Test: Group Housed Females, Partner vs Stranger $p < 0.0001$). This preference for the partner was notably abolished in females that

were in the isolation condition through adolescence (Figure 3.1B; Mann-Whitney Test: Isolated Females, Partner vs Stranger $p=0.2099$).

Interestingly, group-housed male prairie voles do not show preference for their partner in this PPT apparatus, suggesting a sexual dimorphism in the sensory cues prairie voles use to recognize or show preference for their partners (Figure 3.1C; Mann-Whitney Test: Group Housed Males, Partner vs Stranger $p=0.3107$).

Bonded male prairie voles prefer their bonded female partner's bedding-associated chemosensory cues over cues from a sexually naïve stranger female

Male prairie voles were paired at 7 weeks with an age-matched sexually naïve female prairie vole and the pair cohabitated for one week. The pair was cohoused for 2 additional days, with a divider between animals to control for markings in bedding between individuals. Bedding was collected and matched for moistness by mixing with fresh, clean bedding. Males were then transferred to a new cage which had one half coated in bedding collected from their partner female, and the other half coated in bedding collected from a single sexually naïve female. Males were tube transferred to the center of the cage and recorded for 10 minutes. Bonded males spent significantly more time on the side of the cage with bedding of their bonded female than the sexually naïve females (Figure 3.2A,B; Wilcoxon Matched-Pairs Signed Rank Test: $p=0.0182$).

Next we investigated if female prairie voles will also display preference for a partner based on chemosensory cues left in bedding. The same assay was repeated for bonded females and no significant difference was found between time spent in bedding

of their partner male and a sexually naïve stranger male (Figure 3.2C,D; Wilcoxon Matched-Pairs Signed Rank Test: $p=0.9219$).

These findings suggest that male, but not female, prairie voles display a preference for bedding-associated cues, likely contact-mediated pheromonal cues from urine, from their partner (Figure 3.2E).

Neither males nor females discriminate between bedding collected from their partner versus another opposite bonded vole

Next we wanted to investigate if the male preference for their bonded female's bedding could be explained by chemosensory signatures of a bonded, or likely pregnant, female prairie vole. Therefore, we repeated the two-choice bedding discrimination assay with bedding collected from the male's female partner versus bedding collected from the bonded female partner of a different pair. In a choice between bedding from two bonded females, male prairie voles showed no preference (Figure 3.3A; Wilcoxon Matched-Pairs Signed Rank Test: $p=0.6406$).

Female prairie voles also showed no preference between bedding of their bonded male partner versus bedding collected from a bonded male of a different pair (Figure 3.3B; Wilcoxon Matched-Pairs Signed Rank Test: $p=0.2324$).

Therefore, neither sex shows preference for their partner when choosing between chemosensory cues collected in their partner's bedding versus bedding collected from another bonded opposite sex vole (Figure 3.3C). This finding may indicate that male prairie voles prefer the chemosensory cues generated from the markings of a bonded,

and likely either pregnant or sexually receptive, female prairie vole, more so than the recognition of a specific partner vole.

DISCUSSION

Our finding that early life social isolation disrupts adult attachment, as measured by preference for a partner in the barrier PPT apparatus, in female but not male prairie voles raises multiple directions of investigation. Firstly, this finding suggests that early life social isolation may have sex-specific impacts on prairie vole social circuitry. Early work on prairie vole adult attachment has identified that the sexes may be differently sensitive to different types of stressors. The stress of swimming or exogenous injections of corticosterone has been shown to heighten preference for a female partner in male prairie voles, yet disrupt display of preference towards a male partner in female prairie voles (DeVries et al., 1996).

However, an important and intriguing difference in our observations is that group-housed males do not show a preference for their partner in this 30 minute barrier PPT apparatus assay, while they show a significant preference for their partner in the three hour PPT apparatus with stimulus animals tethered, as described in Chapter 2. To determine if early life stress differentially affects female and male prairie voles' adult attachment behavior, we suggest repeating the early life isolation paradigm and testing subject voles in the more common PPT apparatus with tethered stimulus voles. This apparatus can be used to observe significant preference for a partner by male prairie voles. It also allows for observation of stronger partner preference in female prairie voles as described in Chapter 2, as compared to the barrier PPT apparatus. Based on previous

literature, we expect that early life stress may diminish preference for a partner in female prairie voles, and enhance preference for a partner in male prairie voles under these conditions.

Future work will investigate if female prairie voles that were isolated in early life show different patterns of neuronal activation in brain regions related to pair bonding, as compared to their group-housed counterparts. We will pair bond female prairie voles that were assigned either an isolation or group-housing condition for 4 weeks post weaning, and after 2 weeks of cohabitation with their partner, we will move the females to one half of a new cage, maintained by acrylic dividers analogous to those in the barrier PPT. After acclimation, we will present the female with either their partner or a novel male stranger in the other half of a cage, restricting any contact beyond nose-to-nose investigation, as in the barrier PPT. We will allow the female to explore the stimulus animal through the divider for 2.5 hours, perfuse her, and subsequently use immunohistochemistry to identify patterns of molecular markers of neural activity, in particular c-fos or phosphorylation of the ribosome S6 subunit (pS6) (Knight et al., 2012). By confocal microscopy, we will image and quantify the number of c-fos or pS6 positive cells in key brain regions involved in pair bonding, including the lateral septum, the paraventricular nucleus of the hypothalamus, the medial and basolateral amygdala, and bed nucleus of the stria terminalis. We will report differences in c-fos or pS6 positive cell counts between four conditions: group-housed females presented a partner, group-housed females presented a stranger, isolated females presented a partner, and isolated females presented a stranger. Ultimately, further research will employ an immunoprecipitation of pS6 or single-cell RNA-sequencing approaches to describe the transcriptional profiles of active neurons

in brain regions with quantifiable differences between isolated and group-housed female responses to stimulus animal presentations. This work will aim to identify the molecular signature of social isolation and which components regulate the ensuing deficits in attachment related behaviors.

A second direction of investigation identified in these findings is how male and female prairie voles may differently use sensory cues to either form or maintain a pair bond to a partner, or possibly recognize the identity of a partner. Because of the robust pair bond displayed by both prairie vole sexes, it was unexpected that females but not males would show a preference for their partner in this barrier PPT apparatus. We find that females display a preference for their partner in the absence of full physical contact, while males require cues received through direct contact other than nose-to-nose investigation, for example during anogenital investigation, to display a partner preference. This observation has led us to begin to examine if females use acoustic cues in pair bond formation and maintenance, or partner recognition, while males do not. Similarly, we are investigating if non-volatile chemosensory cues are sufficient and or necessary for males to display partner preference.

Our findings indicate that male prairie voles use non-volatile chemosensory cues, such as the markings found in bedding of a home cage, to either recognize or show preference for their bonded female partner in a partner versus stranger choice task. This finding is consistent with male prairie vole's lack of preference for their partner in the barrier PPT apparatus, in which males do not have access to the non-volatile chemosensory cues in urine or through anogenital investigation of their female partner.

However, we also found that male prairie voles do not discriminate between bedding of a bonded female partner and a bonded female stranger. This finding indicates that males may have an inherent preference for chemosensory cues of females that are bonded, more than the identity or recognition of their unique female partner, and therefore rely on additional sensory and behavioral cues to identify their specific partner. This inherent preference may be instructed by biological pressures to create or care for progeny, as bonded females are likely induced into estrous following one week of cohabitation with a male, which may be recognizable by chemosensory signatures in their urine identifiable by the males. It is also likely that the bonded females have already become pregnant during cohabitation, which also may be recognizable by males through chemosensory cues in their urine. The finding that bonded male prairie voles show preference for the bonded status of a female prairie vole, over the unique identity of a female prairie vole, indicates the importance of knowing pregnancy status of partner and stranger female prairie voles used as stimulus animals in all subsequent male behavioral experiments.

FIGURES

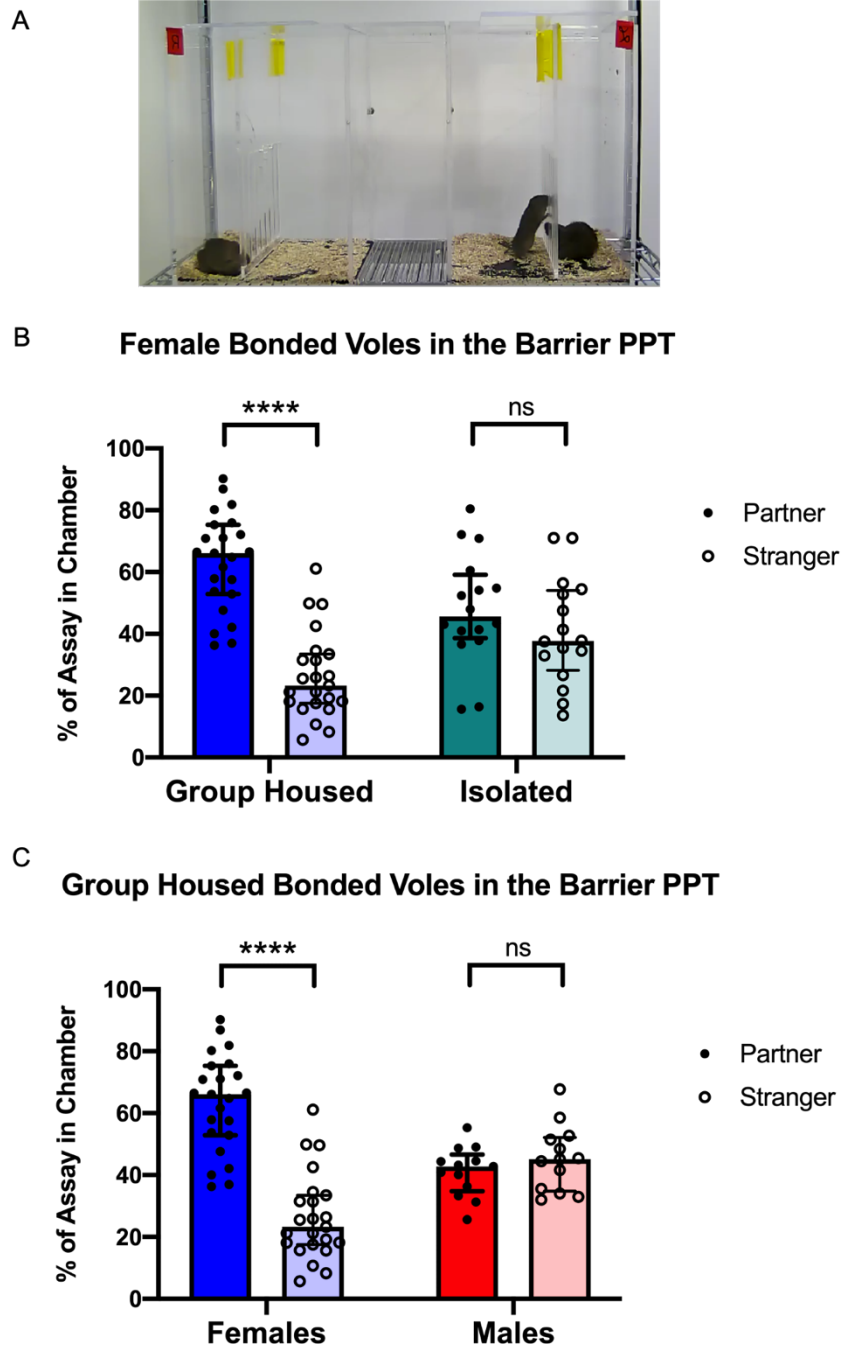


Figure 3.1 Female prairie voles do not display partner preference following early life social isolation. Female prairie voles tested in the barrier PPT apparatus (A), demonstrate preference for a partner when raised in group housing (B). Females that were isolated for 4 weeks as juveniles do not express partner preference (B). Group housed males do not demonstrate partner preference in this barrier PPT apparatus (C). Data is plotted as the median and interquartile range. Group Housed Females N=23, Isolated Females N=16, Group Housed Males N=13.

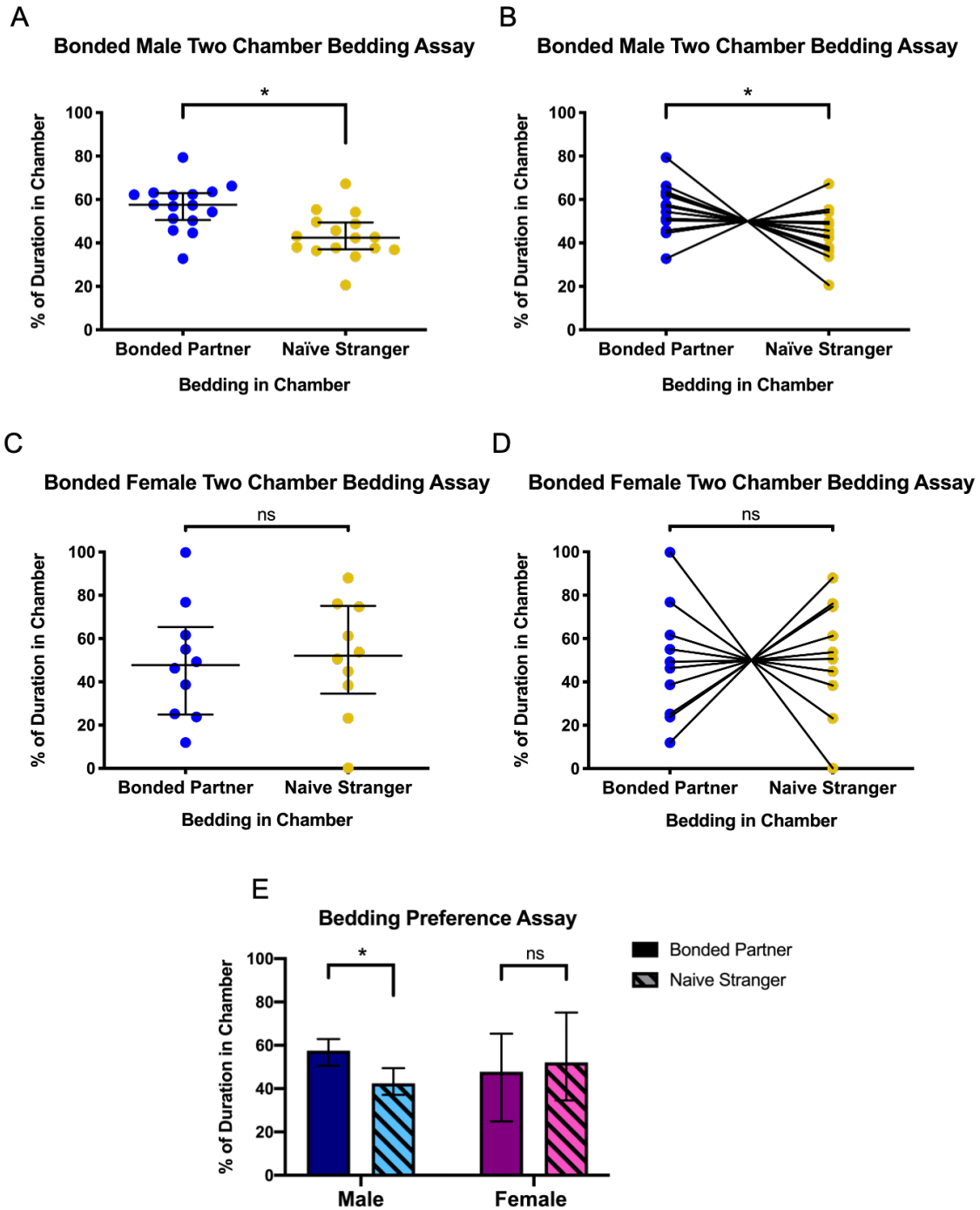


Figure 3.2 Bedding preference assay between bonded partner and naïve stranger. Bonded males prefer bedding collected from a bonded partner over bedding collected from a naïve stranger (A,B,E). Bonded females do not show a preference between bonded partner and naïve stranger bedding (C,D,E). Data is plotted as the median and interquartile range. Males N=16; Females N=10.

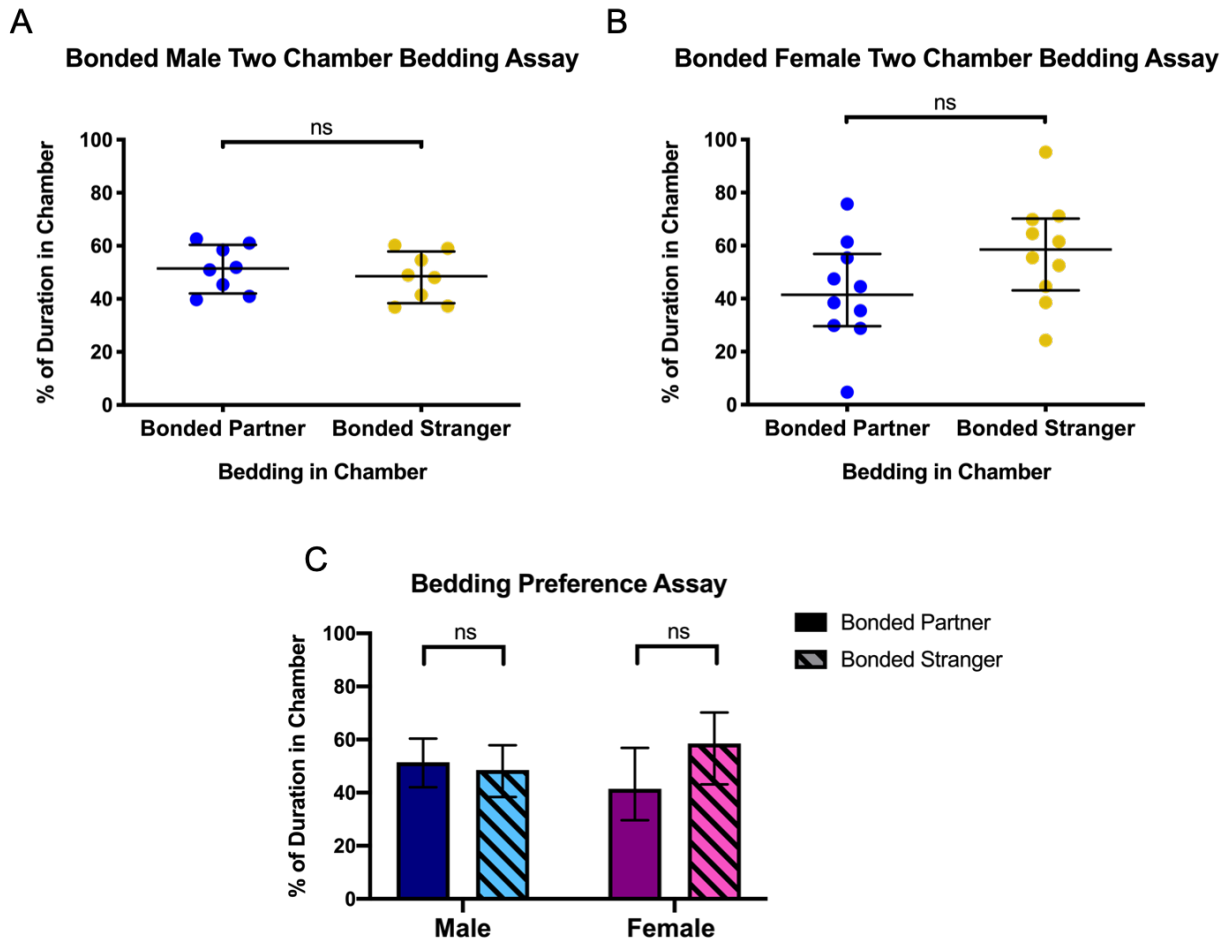


Figure 3.3 Bedding preference assay between bonded partner and bonded stranger. Neither males (A,C) nor females (B,C) show preference between bedding collected from a bonded partner and bedding collected from a bonded stranger. Data is plotted as the median and interquartile range. Males N=8; Females N=10.

METHODS

Animals. All prairie voles were bred from the behavior colony maintained by the Manoli lab as described in Chapter 2 Methods. The protocol was approved by the Institutional Animal Care and Use Committee (IACUC) and directed by the Guide for the Care and Use of Laboratory Animals published by the National Research Council.

Voles in the isolation condition were weaned into solitary housing, with nestlets and enrichment tubes. They were checked daily by experimenters and handling was minimized. Voles in the group-housed condition were weaned into cages of 5 same-sex voles either from the same litter or from one other litter weaned the same day.

Stranger animals were sexually naïve, age matched, and group-housed from day of weaning. Stranger animals were not reused for PPT nor presentation assays.

Partner Preference Test. The original, “barrier” PPT apparatus measured 27”L x 8.5” W x 13.75” H. Five minutes before the start of the assay the two stimulus animals were tube transferred into half of their assigned chamber, behind the plastic barriers. The subject vole was placed in the center chamber and restricted here by 2 black dividers for 5 minutes as well. When the 2 black center chamber dividers are removed, the assay is initiated and runs for 30 minutes. The assay was recorded with FosCam and scored by a blind experimenter in Noldus’ Observer.

Bedding Collection. Sexually naïve grouped-housed prairie voles were paired with opposite sex animals at 7 weeks old and cohoused for one week before start of testing. At one week, pairs were divided in cages with plastic dividers that allowed for physical

contact limited to nose pokes. Pairs remained divided for two subsequent nights and bedding was changed each day. The next day, bedding from the bonded female side was collected and the bonded male was tested. Following the assay, the male was returned to the divided half of its home cage, with a fresh bedding change again on both sides of the divider. On the following day, bedding from the bonded male was collected and bonded females were tested.

Sexually naïve stranger voles were cohoused in same sex pairs of 2 voles. Three days before an assay, these pairs were divided within the cage, and bedding was changed every day for 2 nights. On the third day, bedding was collected from the divided side holding an individual animal for assays to be used that same day.

Collected bedding was matched for moistness by mixing with fresh, clean bedding. All bedding was Sani Chips bedding.

Bedding Assay Behavioral Scoring. All assays were filmed for a 10 minute duration with a FosCam anchored above the apparatus. Videos were scored for left or right side by a blinded experimenter in Noldus' Observer.

Statistical Analysis. We used Mann-Whitney Tests to compare partner vs stranger preference in the PPT. We used Wilcoxon Matched-Pairs Signed Rank Test to compare preference in the bedding assays. We used GraphPad Prism to run automated tests and plot data. We plotted data as the median with interquartile range error bars. N is represented in Figure legends.

REFERENCES

- Acevedo, B. P., Aron, A., Fisher, H. E., & Brown, L. L. (2012). Neural correlates of long-term intense romantic love. *Social cognitive and affective neuroscience*, 7(2), 145–159. <https://doi.org/10.1093/scan/nsq092>
- Albers H. E. (2015). Species, sex and individual differences in the vasotocin/vasopressin system: relationship to neurochemical signaling in the social behavior neural network. *Frontiers in neuroendocrinology*, 36, 49–71. <https://doi.org/10.1016/j.yfrne.2014.07.001>
- Amadei, E. A., Johnson, Z. V., Jun Kwon, Y., Shpiner, A. C., Saravanan, V., Mays, W. D., Ryan, S. J., Walum, H., Rainnie, D. G., Young, L. J., & Liu, R. C. (2017). Dynamic corticostriatal activity biases social bonding in monogamous female prairie voles. *Nature*, 546(7657), 297–301. <https://doi.org/10.1038/nature22381>
- American Psychiatric Association. (2013). *Diagnostic and statistical manual of mental disorders* (5th ed.). <https://doi.org/10.1176/appi.books.9780890425596>
- Arai, A., Hirota, Y., Miyase, N., Miyata, S., Young, L. J., Osako, Y., Yuri, K., & Mitsui, S. (2016). A single prolonged stress paradigm produces enduring impairments in social bonding in monogamous prairie voles. *Behavioural brain research*, 315, 83–93. <https://doi.org/10.1016/j.bbr.2016.08.022>
- Autism Genome Project Consortium, Szatmari, P., Paterson, A. D., Zwaigenbaum, L., Roberts, W., Brian, J., Liu, X. Q., Vincent, J. B., Skaug, J. L., Thompson, A. P., Senman, L., Feuk, L., Qian, C., Bryson, S. E., Jones, M. B., Marshall, C. R., Scherer, S. W., Vieland, V. J., Bartlett, C., Mangin, L. V., ... Meyer, K. J. (2007).

Mapping autism risk loci using genetic linkage and chromosomal rearrangements. *Nature genetics*, 39(3), 319–328.

<https://doi.org/10.1038/ng1985>

Auyeung, B., Lombardo, M. V., Heinrichs, M., Chakrabarti, B., Sule, A., Deakin, J. B., Bethlehem, R. A., Dickens, L., Mooney, N., Sipple, J. A., Thiemann, P., & Baron-Cohen, S. (2015). Oxytocin increases eye contact during a real-time, naturalistic social interaction in males with and without autism. *Translational psychiatry*, 5(2), e507. <https://doi.org/10.1038/tp.2014.146>

Baird, G., Cass, H. and Slonims, V. (2003). Diagnosis of Autism. *British Medical Journal*, 237, 488-493. <http://doi.org/10.1097/00005072-199807000-00001>.

Bales, K. L., Mason, W. A., Catana, C., Cherry, S. R., and Mendoza, S. P. (2007). Neural correlates of pair-bonding in a monogamous primate. *Brain Res.* 1184, 245–253. doi: 10.1016/j.brainres.2007.09.087

Batson, C. D., Dyck, J. L., Brandt, J. R., Batson, J. G., Powell, A. L., McMaster, M. R., & Griffitt, C. (1988). Five studies testing two new egoistic alternatives to the empathy-altruism hypothesis. *Journal of Personality and Social Psychology*, 55(1), 52–77. <https://doi.org/10.1037/0022-3514.55.1.52>

Beery AK, Christensen JD, Lee NS and Blandino KL (2018) Specificity in Sociality: Mice and Prairie Voles Exhibit Different Patterns of Peer Affiliation. *Front. Behav. Neurosci.* 12:50. doi: 10.3389/fnbeh.2018.00050

Berkel, S., Eltokhi, A., Fröhlich, H., Porrás-González, D., Rafiullah, R., Sprengel, R., & Rappold, G. A. (2018). Sex Hormones Regulate *SHANK* Expression. *Frontiers in molecular neuroscience*, 11, 337. <https://doi.org/10.3389/fnmol.2018.00337>

- Boccuto, L., Lauri, M., Sarasua, S. M., Skinner, C. D., Buccella, D., Dwivedi, A., Orteschi, D., Collins, J. S., Zollino, M., Visconti, P., Dupont, B., Tiziano, D., Schroer, R. J., Neri, G., Stevenson, R. E., Gurrieri, F., & Schwartz, C. E. (2013). Prevalence of SHANK3 variants in patients with different subtypes of autism spectrum disorders. *European journal of human genetics : EJHG*, *21*(3), 310–316. <https://doi.org/10.1038/ejhg.2012.175>
- Bozdagi, O., Sakurai, T., Papapetrou, D., Wang, X., Dickstein, D. L., Takahashi, N., Kajiwara, Y., Yang, M., Katz, A. M., Scattoni, M. L., Harris, M. J., Saxena, R., Silverman, J. L., Crawley, J. N., Zhou, Q., Hof, P. R., & Buxbaum, J. D. (2010). Haploinsufficiency of the autism-associated Shank3 gene leads to deficits in synaptic function, social interaction, and social communication. *Molecular autism*, *1*(1), 15. <https://doi.org/10.1186/2040-2392-1-15>
- Brownstein, M.J., Russell, J.T., Gainer, H. (1980) Synthesis, transport, and release of posterior pituitary hormones. *Science* *207*:373–378.
- Brunnlieb, C., Nave, G., Camerer, C. F., Schosser, S., Vogt, B., Münte, T. F., & Heldmann, M. (2016). Vasopressin increases human risky cooperative behavior. *Proceedings of the National Academy of Sciences of the United States of America*, *113*(8), 2051–2056. <https://doi.org/10.1073/pnas.1518825113>
- Camacho Londoño, J., & Philipp, S. E. (2016). A reliable method for quantification of splice variants using RT-qPCR. *BMC molecular biology*, *17*, 8. <https://doi.org/10.1186/s12867-016-0060-1>
- Cantor, R. M., Kono, N., Duvall, J. A., Alvarez-Retuerto, A., Stone, J. L., Alarcón, M., Nelson, S. F., & Geschwind, D. H. (2005). Replication of autism linkage: fine-

- mapping peak at 17q21. *American journal of human genetics*, 76(6), 1050–1056.
<https://doi.org/10.1086/430278>
- Carter, C. S., & Getz, L. L. (1993). Monogamy and the prairie vole. *Scientific American*, 268(6), 100–106. <https://doi.org/10.1038/scientificamerican0693-100>
- Carter, C. S., DeVries, A. C., & Getz, L. L. (1995). Physiological substrates of mammalian monogamy: the prairie vole model. *Neuroscience and biobehavioral reviews*, 19(2), 303–314. [https://doi.org/10.1016/0149-7634\(94\)00070-h](https://doi.org/10.1016/0149-7634(94)00070-h)
- Carter, C. S., Getz, L. L., Gavish, L., McDermott, J. L., & Arnold, P. (1980). Male-related pheromones and the activation of female reproduction in the prairie vole (*Microtus ochrogaster*). *Biology of reproduction*, 23(5), 1038–1045.
<https://doi.org/10.1095/biolreprod23.5.1038>
- Carter, C. S., Grippo, A. J., Pournajafi-Nazarloo, H., Ruscio, M. G., & Porges, S. W. (2008). Oxytocin, vasopressin and sociality. *Progress in brain research*, 170, 331–336. [https://doi.org/10.1016/S0079-6123\(08\)00427-5](https://doi.org/10.1016/S0079-6123(08)00427-5)
- Carter, C. S., Witt, D. M., Schneider, J., Harris, Z. L., & Volkening, D. (1987). Male stimuli are necessary for female sexual behavior and uterine growth in prairie voles (*Microtus ochrogaster*). *Hormones and behavior*, 21(1), 74–82.
[https://doi.org/10.1016/0018-506x\(87\)90032-8](https://doi.org/10.1016/0018-506x(87)90032-8)
- Castelbaum, L., Sylvester, C. M., Zhang, Y., Yu, Q., & Constantino, J. N. (2020). On the Nature of Monozygotic Twin Concordance and Discordance for Autistic Trait Severity: A Quantitative Analysis. *Behavior genetics*, 50(4), 263–272.
<https://doi.org/10.1007/s10519-019-09987-2>

- Chaste, P., and Leboyer, M. (2012). Autism risk factors: genes, environment, and gene-environment interactions. *Dialogues Clin. Neurosci.* 14, 281–292.
- Cho, M. M., DeVries, A. C., Williams, J. R., & Carter, C. S. (1999). The effects of oxytocin and vasopressin on partner preferences in male and female prairie voles (*Microtus ochrogaster*). *Behavioral neuroscience*, 113(5), 1071–1079. <https://doi.org/10.1037//0735-7044.113.5.1071>
- Constantino, J. N., & Gruber, C. P. (2012). *Social responsiveness scale: SRS-2*. Torrance, CA: Western Psychological Services.
- Costales, J. L., & Kolevzon, A. (2015). Phelan-McDermid Syndrome and SHANK3: Implications for Treatment. *Neurotherapeutics : the journal of the American Society for Experimental NeuroTherapeutics*, 12(3), 620–630. <https://doi.org/10.1007/s13311-015-0352-z>
- Curtis, J. T., Liu, Y., & Wang, Z. (2001). Lesions of the vomeronasal organ disrupt mating-induced pair bonding in female prairie voles (*Microtus ochrogaster*). *Brain research*, 901(1-2), 167–174. [https://doi.org/10.1016/s0006-8993\(01\)02343-5](https://doi.org/10.1016/s0006-8993(01)02343-5)
- De Rubeis, S., Siper, P. M., Durkin, A., Weissman, J., Muratet, F., Halpern, D., Trelles, M., Frank, Y., Lozano, R., Wang, A. T., Holder, J. L., Jr, Betancur, C., Buxbaum, J. D., & Kolevzon, A. (2018). Delineation of the genetic and clinical spectrum of Phelan-McDermid syndrome caused by *SHANK3* point mutations. *Molecular autism*, 9, 31. <https://doi.org/10.1186/s13229-018-0205-9>
- DeVries, A. C., DeVries, M. B., Taymans, S. E., & Carter, C. S. (1996). The effects of stress on social preferences are sexually dimorphic in prairie voles. *Proceedings*

of the National Academy of Sciences of the United States of America, 93(21), 11980–11984. <https://doi.org/10.1073/pnas.93.21.11980>

DeVries, G. J., & Buijs, R. M. (1983). The origin of the vasopressinergic and oxytocinergic innervation of the rat brain with special reference to the lateral septum. *Brain research*, 273(2), 307–317. [https://doi.org/10.1016/0006-8993\(83\)90855-7](https://doi.org/10.1016/0006-8993(83)90855-7)

Durand, C. M., Betancur, C., Boeckers, T. M., Bockmann, J., Chaste, P., Fauchereau, F., Nygren, G., Rastam, M., Gillberg, I. C., Anckarsäter, H., Sponheim, E., Goubran-Botros, H., Delorme, R., Chabane, N., Mouren-Simeoni, M. C., de Mas, P., Bieth, E., Rogé, B., Héron, D., Burglen, L., ... Bourgeron, T. (2007). Mutations in the gene encoding the synaptic scaffolding protein SHANK3 are associated with autism spectrum disorders. *Nature genetics*, 39(1), 25–27. <https://doi.org/10.1038/ng1933>

Ebert, D. H., & Greenberg, M. E. (2013). Activity-dependent neuronal signaling and autism spectrum disorder. *Nature*, 493(7432), 327–337. <https://doi.org/10.1038/nature11860>

Ebstein, R. P., Israel, S., Chew, S. H., Zhong, S., & Knafo, A. (2010). Genetics of human social behavior. *Neuron*, 65(6), 831–844. <https://doi.org/10.1016/j.neuron.2010.02.020>

Elder, J. H., Kreider, C. M., Brasher, S. N., & Ansell, M. (2017). Clinical impact of early diagnosis of autism on the prognosis and parent-child relationships. *Psychology research and behavior management*, 10, 283–292. <https://doi.org/10.2147/PRBM.S117499>

- Fisher, H. E., Xu, X., Aron, A., & Brown, L. L. (2016). Intense, Passionate, Romantic Love: A Natural Addiction? How the Fields That Investigate Romance and Substance Abuse Can Inform Each Other. *Frontiers in psychology, 7*, 687. <https://doi.org/10.3389/fpsyg.2016.00687>
- Fone, K. C., & Porkess, M. V. (2008). Behavioural and neurochemical effects of post-weaning social isolation in rodents—relevance to developmental neuropsychiatric disorders. *Neuroscience & Biobehavioral Reviews, 32*(6), 1087-1102.
- Fuld, S. (2018) Autism Spectrum Disorder: The Impact of Stressful and Traumatic Life Events and Implications for Clinical Practice. *Clinical Social Work Journal, 46*:210–219.
- Gauthier, J., Spiegelman, D., Piton, A., Lafrenière, R. G., Laurent, S., St-Onge, J., Lapointe, L., Hamdan FF, Cossette P, Mottron L, Fombonne E, Joober R, Marineau C, Drapeau P, Rouleau, G. A. (2009). Novel *de novo* SHANK3 mutation in autistic patients. *American Journal of Medical Genetics Part B: Neuropsychiatric Genetics, 150B*(3), 421–424. doi:10.1002/ajmg.b.30822
- Geschwind, D. H., & State, M. W. (2015). Gene hunting in autism spectrum disorder: on the path to precision medicine. *The Lancet. Neurology, 14*(11), 1109–1120. [https://doi.org/10.1016/S1474-4422\(15\)00044-7](https://doi.org/10.1016/S1474-4422(15)00044-7)
- Getz, L.L., Carter, C.S, Gavish, L. (1981). The mating system of the prairie vole, *Microtus ochrogaster*: field and laboratory evidence for pair-bonding. *Behavioral Ecology and Sociobiology. 8*(3), 189-194.

- Getz, L.L., McGuire, B., Hofmann, J., Pizzuto, T., Frase, B. (1994). Natal dispersal and philopatry in the prairie vole (*Microtus ochrogaster*): Settlement, survival, and potential reproductive success. *Ethology Ecology & Evolution*, 6, 267–284.
- Goin-Kochel, R. P., Abbacchi, A., Constantino, J. N., & Autism Genetic Resource Exchange Consortium (2007). Lack of evidence for increased genetic loading for autism among families of affected females: a replication from family history data in two large samples. *Autism : the international journal of research and practice*, 11(3), 279–286. <https://doi.org/10.1177/1362361307076857>
- Gong, X., Jiang, Y. W., Zhang, X., An, Y., Zhang, J., Wu, Y., Wang, J., Sun, Y., Liu, Y., Gao, X., Shen, Y., Wu, X., Qiu, Z., Jin, L., Wu, B. L., & Wang, H. (2012). High proportion of 22q13 deletions and SHANK3 mutations in Chinese patients with intellectual disability. *PloS one*, 7(4), e34739. <https://doi.org/10.1371/journal.pone.0034739>
- Grove, J., Ripke, S., Als, T. D., Mattheisen, M., Walters, R. K., Won, H., Pallesen, J., Agerbo, E., Andreassen, O. A., Anney, R., Awashti, S., Belliveau, R., Bettella, F., Buxbaum, J. D., Bybjerg-Grauholm, J., Bækvad-Hansen, M., Cerrato, F., Chambert, K., Christensen, J. H., Churchhouse, C., ... Børglum, A. D. (2019). Identification of common genetic risk variants for autism spectrum disorder. *Nature genetics*, 51(3), 431–444. <https://doi.org/10.1038/s41588-019-0344-8>
- Gutman, D. A., & Nemeroff, C. B. (2003). Persistent central nervous system effects of an adverse early environment: clinical and preclinical studies. *Physiology & behavior*, 79(3), 471-478.

- Halladay, A. K., Bishop, S., Constantino, J. N., Daniels, A. M., Koenig, K., Palmer, K., Messinger, D., Pelphrey, K., Sanders, S. J., Singer, A. T., Taylor, J. L., & Szatmari, P. (2015). Sex and gender differences in autism spectrum disorder: summarizing evidence gaps and identifying emerging areas of priority. *Molecular autism*, 6, 36. <https://doi.org/10.1186/s13229-015-0019-y>
- Hallmayer, J., Cleveland, S., Torres, A., Phillips, J., Cohen, B., Torigoe, T., Miller, J., Fedele, A., Collins, J., Smith, K., Lotspeich, L., Croen, L. A., Ozonoff, S., Lajonchere, C., Grether, J. K., & Risch, N. (2011). Genetic heritability and shared environmental factors among twin pairs with autism. *Archives of general psychiatry*, 68(11), 1095–1102. <https://doi.org/10.1001/archgenpsychiatry.2011.76>
- Hammock, E. A., & Young, L. J. (2004). Functional microsatellite polymorphism associated with divergent social structure in vole species. *Molecular biology and evolution*, 21(6), 1057–1063. <https://doi.org/10.1093/molbev/msh104>
- Hammock, E. A., & Young, L. J. (2005). Microsatellite instability generates diversity in brain and sociobehavioral traits. *Science*, 308(5728), 1630-1634.
- Horie, K., Inoue, K., Suzuki, S., Adachi, S., Yada, S., Hirayama, T., Hidema, S., Young, L. J., & Nishimori, K. (2019). Oxytocin receptor knockout prairie voles generated by CRISPR/Cas9 editing show reduced preference for social novelty and exaggerated repetitive behaviors. *Hormones and behavior*, 111, 60–69. <https://doi.org/10.1016/j.yhbeh.2018.10.011>
- Idring, S., Lundberg, M., Sturm, H., Dalman, C., Gumpert, C., Rai, D., Lee, B. K., & Magnusson, C. (2015). Changes in prevalence of autism spectrum disorders in

- 2001-2011: findings from the Stockholm youth cohort. *Journal of autism and developmental disorders*, 45(6), 1766–1773. <https://doi.org/10.1007/s10803-014-2336-y>
- Insel T. R. (2010). The challenge of translation in social neuroscience: a review of oxytocin, vasopressin, and affiliative behavior. *Neuron*, 65(6), 768–779. <https://doi.org/10.1016/j.neuron.2010.03.005>
- Insel, T. R., & Hulihan, T. J. (1995). A gender-specific mechanism for pair bonding: oxytocin and partner preference formation in monogamous voles. *Behavioral neuroscience*, 109(4), 782–789. <https://doi.org/10.1037//0735-7044.109.4.782>
- Insel, T. R., & Shapiro, L. E. (1992). Oxytocin receptor distribution reflects social organization in monogamous and polygamous voles. *Proceedings of the National Academy of Sciences of the United States of America*, 89(13), 5981–5985. <https://doi.org/10.1073/pnas.89.13.5981>
- Insel, T. R., Wang, Z. X., & Ferris, C. F. (1994). Patterns of brain vasopressin receptor distribution associated with social organization in microtine rodents. *The Journal of neuroscience : the official journal of the Society for Neuroscience*, 14(9), 5381–5392. <https://doi.org/10.1523/JNEUROSCI.14-09-05381.1994>
- Insel, T. R., Winslow, J. T., Wang, Z., & Young, L. J. (1998). Oxytocin, vasopressin, and the neuroendocrine basis of pair bond formation. *Advances in experimental medicine and biology*, 449, 215–224. https://doi.org/10.1007/978-1-4615-4871-3_28
- Iossifov, I., O’Roak, B. J., Sanders, S. J., Ronemus, M., Krumm, N., Levy, D., Stessman, H. A., Witherspoon, K. T., Vives, L., Patterson, K. E., Smith, J. D.,

- Paeper, B., Nickerson, D. A., Dea, J., Dong, S., Gonzalez, L. E., Mandell, J. D., Mane, S. M., Murtha, M. T., Sullivan, C. A., ... Wigler, M. (2014). The contribution of de novo coding mutations to autism spectrum disorder. *Nature*, *515*(7526), 216–221. <https://doi.org/10.1038/nature13908>
- Kenkel, W. M., Perkeybile, A. M., & Carter, C. S. (2017). The neurobiological causes and effects of alloparenting. *Developmental neurobiology*, *77*(2), 214–232. <https://doi.org/10.1002/dneu.22465>
- Kiecolt-Glaser, J. K., & Newton, T. L. (2001). Marriage and health: his and hers. *Psychological bulletin*, *127*(4), 472–503. <https://doi.org/10.1037/0033-2909.127.4.472>
- Kim, E., & Sheng, M. (2004). PDZ domain proteins of synapses. *Nature reviews. Neuroscience*, *5*(10), 771–781. <https://doi.org/10.1038/nrn1517>
- Kim, Y. S., Leventhal, B. L., Koh, Y. J., Fombonne, E., Laska, E., Lim, E. C., Cheon, K. A., Kim, S. J., Kim, Y. K., Lee, H., Song, D. H., & Grinker, R. R. (2011). Prevalence of autism spectrum disorders in a total population sample. *The American journal of psychiatry*, *168*(9), 904–912. <https://doi.org/10.1176/appi.ajp.2011.10101532>
- King, L. B., Walum, H., Inoue, K., Eyrich, N. W., & Young, L. J. (2016). Variation in the Oxytocin Receptor Gene Predicts Brain Region-Specific Expression and Social Attachment. *Biological psychiatry*, *80*(2), 160–169. <https://doi.org/10.1016/j.biopsych.2015.12.008>
- Kirkpatrick, B., Carter, C. S., Newman, S. W., & Insel, T. R. (1994). Axon-sparing lesions of the medial nucleus of the amygdala decrease affiliative behaviors in

the prairie vole (*Microtus ochrogaster*): behavioral and anatomical specificity. *Behavioral neuroscience*, 108(3), 501–513.

<https://doi.org/10.1037//0735-7044.108.3.501>

Kirkpatrick, B., Williams, J. R., Slotnick, B. M., & Carter, C. S. (1994). Olfactory bulbectomy decreases social behavior in male prairie voles (*M. ochrogaster*). *Physiology & behavior*, 55(5), 885–889.

[https://doi.org/10.1016/0031-9384\(94\)90075-2](https://doi.org/10.1016/0031-9384(94)90075-2)

Kirmayer, L.J., & Gold, I. (2011) Re-Socializing Psychiatry: Critical Neuroscience and the Limits of Reductionism. In S. Choudhury & J. Slaby (Eds.), *Critical Neuroscience* (pp. 305-330). Wiley-Blackwell.

<http://doi.org/10.1002/9781444343359.ch15>

Knight, Z. A., Tan, K., Birsoy, K., Schmidt, S., Garrison, J. L., Wysocki, R. W., Emiliano, A., Ekstrand, M. I., & Friedman, J. M. (2012). Molecular profiling of activated neurons by phosphorylated ribosome capture. *Cell*, 151(5), 1126–1137.

<https://doi.org/10.1016/j.cell.2012.10.039>

Kouser, M., Speed, H. E., Dewey, C. M., Reimers, J. M., Widman, A. J., Gupta, N., Liu, S., Jaramillo, T. C., Bangash, M., Xiao, B., Worley, P. F., & Powell, C. M. (2013). Loss of predominant Shank3 isoforms results in hippocampus-dependent impairments in behavior and synaptic transmission. *The Journal of neuroscience : the official journal of the Society for Neuroscience*, 33(47), 18448–18468.

<https://doi.org/10.1523/JNEUROSCI.3017-13.2013>

- Lammel, S., Lim, B. K., & Malenka, R. C. (2014). Reward and aversion in a heterogeneous midbrain dopamine system. *Neuropharmacology*, *76 Pt B(0 0)*, 351–359. <https://doi.org/10.1016/j.neuropharm.2013.03.019>
- Leblond, C. S., Nava, C., Polge, A., Gauthier, J., Huguet, G., Lumbroso, S., Giuliano, F., Stordeur, C., Depienne, C., Mouzat, K., Pinto, D., Howe, J., Lemièrre, N., Durand, C. M., Guibert, J., Ey, E., Toro, R., Peyre, H., Mathieu, A., Amsellem, F., ... Bourgeron, T. (2014). Meta-analysis of SHANK Mutations in Autism Spectrum Disorders: a gradient of severity in cognitive impairments. *PLoS genetics*, *10(9)*, e1004580. <https://doi.org/10.1371/journal.pgen.1004580>
- Levy, D., Ronemus, M., Yamrom, B., Lee, Y. H., Leotta, A., Kendall, J., Marks, S., Lakshmi, B., Pai, D., Ye, K., Buja, A., Krieger, A., Yoon, S., Troge, J., Rodgers, L., Iossifov, I., & Wigler, M. (2011). Rare de novo and transmitted copy-number variation in autistic spectrum disorders. *Neuron*, *70(5)*, 886–897. <https://doi.org/10.1016/j.neuron.2011.05.015>
- Lim, M. M., Bielsky, I. F., & Young, L. J. (2005). Neuropeptides and the social brain: potential rodent models of autism. *International journal of developmental neuroscience : the official journal of the International Society for Developmental Neuroscience*, *23(2-3)*, 235–243. <https://doi.org/10.1016/j.ijdevneu.2004.05.006>
- Lim, S., Sala, C., Yoon, J., Park, S., Kuroda, S., Sheng, M., & Kim, E. (2001). Sharpin, a novel postsynaptic density protein that directly interacts with the shank family of proteins. *Molecular and cellular neurosciences*, *17(2)*, 385–397. <https://doi.org/10.1006/mcne.2000.0940>

- López-Gutiérrez, M. F., Gracia-Tabuenca, Z., Ortiz, J. J., Camacho, F. J., Young, L. J., Paredes, R. G., Díaz, N. F., Portillo, W., & Alcauter, S. (2021). Brain functional networks associated with social bonding in monogamous voles. *eLife*, *10*, e55081. <https://doi.org/10.7554/eLife.55081>
- Lord, C., Risi, S., Lambrecht, L., Cook, E. H., Jr, Leventhal, B. L., DiLavore, P. C., Pickles, A., & Rutter, M. (2000). The autism diagnostic observation schedule-generic: a standard measure of social and communication deficits associated with the spectrum of autism. *Journal of autism and developmental disorders*, *30*(3), 205–223.
- Lukkes, J. L., Mokin, M. V., Scholl, J. L., & Forster, G. L. (2009). Adult rats exposed to early-life social isolation exhibit increased anxiety and conditioned fear behavior, and altered hormonal stress responses. *Hormones and behavior*, *55*(1), 248–256. <https://doi.org/10.1016/j.yhbeh.2008.10.014>
- Lukkes, J. L., Watt, M. J., Lowry, C. A., & Forster, G. L. (2009). Consequences of post-weaning social isolation on anxiety behavior and related neural circuits in rodents. *Frontiers in behavioral neuroscience*, *3*, 18. <https://doi.org/10.3389/neuro.08.018.2009>
- Ma, S. T., Resendez, S. L., & Aragona, B. J. (2014). Sex differences in the influence of social context, salient social stimulation and amphetamine on ultrasonic vocalizations in prairie voles. *Integrative zoology*, *9*(3), 280–293. <https://doi.org/10.1111/1749-4877.12071>
- Mandell, D. S., Wiggins, L. D., Carpenter, L. A., Daniels, J., DiGuseppi, C., Durkin, M. S., Giarelli, E., Morrier, M. J., Nicholas, J. S., Pinto-Martin, J. A., Shattuck, P. T.,

- Thomas, K. C., Yeargin-Allsopp, M., & Kirby, R. S. (2009). Racial/ethnic disparities in the identification of children with autism spectrum disorders. *American journal of public health, 99*(3), 493–498.
<https://doi.org/10.2105/AJPH.2007.131243>
- McGraw, L. A., & Young, L. J. (2010). The prairie vole: an emerging model organism for understanding the social brain. *Trends in neurosciences, 33*(2), 103–109.
<https://doi.org/10.1016/j.tins.2009.11.006>
- Meyer-Lindenberg, A., Domes, G., Kirsch, P., & Heinrichs, M. (2011). Oxytocin and vasopressin in the human brain: social neuropeptides for translational medicine. *Nature reviews. Neuroscience, 12*(9), 524–538.
<https://doi.org/10.1038/nrn3044>
- Moessner, R., Marshall, C. R., Sutcliffe, J. S., Skaug, J., Pinto, D., Vincent, J., Zwaigenbaum, L., Fernandez, B., Roberts, W., Szatmari, P., & Scherer, S. W. (2007). Contribution of SHANK3 mutations to autism spectrum disorder. *American journal of human genetics, 81*(6), 1289–1297.
<https://doi.org/10.1086/522590>
- Naisbitt, S., Kim, E., Tu, J. C., Xiao, B., Sala, C., Valtschanoff, J., ... & Sheng, M. (1999). Shank, a novel family of postsynaptic density proteins that binds to the NMDA receptor/PSD-95/GKAP complex and cortactin. *Neuron, 23*(3), 569–582.
- Ophir, A. G., Campbell, P., Hanna, K., & Phelps, S. M. (2008). Field tests of cis-regulatory variation at the prairie vole *avpr1a* locus: association with V1aR abundance but not sexual or social fidelity. *Hormones and behavior, 54*(5), 694–702. <https://doi.org/10.1016/j.yhbeh.2008.07.009>

- Ophir, A. G., Wolff, J. O., & Phelps, S. M. (2008). Variation in neural V1aR predicts sexual fidelity and space use among male prairie voles in semi-natural settings. *Proceedings of the National Academy of Sciences*, *105*(4), 1249-1254.
- Ozonoff, S., Young, G. S., Carter, A., Messinger, D., Yirmiya, N., Zwaigenbaum, L., Bryson, S., Carver, L. J., Constantino, J. N., Dobkins, K., Hutman, T., Iverson, J. M., Landa, R., Rogers, S. J., Sigman, M., & Stone, W. L. (2011). Recurrence risk for autism spectrum disorders: a Baby Siblings Research Consortium study. *Pediatrics*, *128*(3), e488–e495. <https://doi.org/10.1542/peds.2010-2825>
- Pan, Y., Liu, Y., Young, K. A., Zhang, Z., & Wang, Z. (2009). Post-weaning social isolation alters anxiety-related behavior and neurochemical gene expression in the brain of male prairie voles. *Neuroscience letters*, *454*(1), 67–71. <https://doi.org/10.1016/j.neulet.2009.02.064>
- Peça, J., Feliciano, C., Ting, J. T., Wang, W., Wells, M. F., Venkatraman, T. N., Lascola, C. D., Fu, Z., & Feng, G. (2011). Shank3 mutant mice display autistic-like behaviours and striatal dysfunction. *Nature*, *472*(7344), 437–442. <https://doi.org/10.1038/nature09965>
- Pfaus, J. G., & Heeb, M. M. (1997). Implications of immediate-early gene induction in the brain following sexual stimulation of female and male rodents. *Brain research bulletin*, *44*(4), 397–407. [https://doi.org/10.1016/s0361-9230\(97\)00219-0](https://doi.org/10.1016/s0361-9230(97)00219-0)
- Phelan, K., & McDermid, H. E. (2012). The 22q13.3 Deletion Syndrome (Phelan-McDermid Syndrome). *Molecular syndromology*, *2*(3-5), 186–201. <https://doi.org/10.1159/000334260>

- Pitkow, L. J., Sharer, C. A., Ren, X., Insel, T. R., Terwilliger, E. F., & Young, L. J. (2001). Facilitation of affiliation and pair-bond formation by vasopressin receptor gene transfer into the ventral forebrain of a monogamous vole. *The Journal of neuroscience : the official journal of the Society for Neuroscience*, 21(18), 7392–7396. <https://doi.org/10.1523/JNEUROSCI.21-18-07392.2001>
- Potretzke, S., & Ryabinin, A. E. (2019). The Prairie Vole Model of Pair-Bonding and Its Sensitivity to Addictive Substances. *Frontiers in psychology*, 10, 2477. <https://doi.org/10.3389/fpsyg.2019.02477>
- Ramaswami, G and Geschwind, DH. (2018). Genetics of autism spectrum disorder. Chapter 21. Handbook of Clinical Neurology, Vol. 147 (3rd series) Neurogenetics, Part I
D.H. Geschwind, H.L. Paulson, and C. Klein, Editors
<https://doi.org/10.1016/B978-0-444-63233-3.00021-X>
- Reich, R., Cloninger, C. R., & Guze, S. B. (1975). The multifactorial model of disease transmission: I. Description of the model and its use in psychiatry. *The British journal of psychiatry : the journal of mental science*, 127, 1–10. <https://doi.org/10.1192/bjp.127.1.1>
- Rein, B., Ma, K., & Yan, Z. (2020). A standardized social preference protocol for measuring social deficits in mouse models of autism. *Nature protocols*, 15(10), 3464–3477. <https://doi.org/10.1038/s41596-020-0382-9>
- Resendez, S. L., Namboodiri, V., Otis, J. M., Eckman, L., Rodriguez-Romaguera, J., Ung, R. L., Basiri, M. L., Kosyk, O., Rossi, M. A., Dichter, G. S., & Stuber, G. D. (2020). Social Stimuli Induce Activation of Oxytocin Neurons Within the

- Paraventricular Nucleus of the Hypothalamus to Promote Social Behavior in Male Mice. *The Journal of neuroscience : the official journal of the Society for Neuroscience*, 40(11), 2282–2295. <https://doi.org/10.1523/JNEUROSCI.1515-18.2020>
- Ronemus, M., Iossifov, I., Levy, D., & Wigler, M. (2014). The role of de novo mutations in the genetics of autism spectrum disorders. *Nature reviews. Genetics*, 15(2), 133–141. <https://doi.org/10.1038/nrg3585>
- Ross, H. E., Freeman, S. M., Spiegel, L. L., Ren, X., Terwilliger, E. F., & Young, L. J. (2009). Variation in oxytocin receptor density in the nucleus accumbens has differential effects on affiliative behaviors in monogamous and polygamous voles. *The Journal of neuroscience : the official journal of the Society for Neuroscience*, 29(5), 1312–1318. <https://doi.org/10.1523/JNEUROSCI.5039-08.2009>
- Rutter, M., Colvert, E., Kreppner, J., Beckett, C., Castle, J., Groothues, C., Hawkins, A., O'Connor, T. G., Stevens, S. E., & Sonuga-Barke, E. J. (2007). Early adolescent outcomes for institutionally-deprived and non-deprived adoptees. I: disinhibited attachment. *Journal of child psychology and psychiatry, and allied disciplines*, 48(1), 17–30. <https://doi.org/10.1111/j.1469-7610.2006.01688.x>
- Rutter, M., Kreppner, J., Croft, C., Murin, M., Colvert, E., Beckett, C., Castle, J., & Sonuga-Barke, E. (2007). Early adolescent outcomes of institutionally deprived and non-deprived adoptees. III. Quasi-autism. *Journal of child psychology and psychiatry, and allied disciplines*, 48(12), 1200–1207. <https://doi.org/10.1111/j.1469-7610.2007.01792.x>

- Rylaarsdam L and Guemez-Gamboa A (2019) Genetic Causes and Modifiers of Autism Spectrum Disorder. *Front. Cell. Neurosci.* 13:385. doi: 10.3389/fncel.2019.00385
- Sailer, L., Duclot, F., Wang, Z., & Kabbaj, M. (2019). Consequences of prenatal exposure to valproic acid in the socially monogamous prairie voles. *Scientific reports*, 9(1), 2453. <https://doi.org/10.1038/s41598-019-39014-7>
- Sanders, S. J., Ercan-Sencicek, A. G., Hus, V., Luo, R., Murtha, M. T., Moreno-De-Luca, D., Chu, S. H., Moreau, M. P., Gupta, A. R., Thomson, S. A., Mason, C. E., Bilguvar, K., Celestino-Soper, P. B., Choi, M., Crawford, E. L., Davis, L., Wright, N. R., Dhodapkar, R. M., DiCola, M., DiLullo, N. M., ... State, M. W. (2011). Multiple recurrent de novo CNVs, including duplications of the 7q11.23 Williams syndrome region, are strongly associated with autism. *Neuron*, 70(5), 863–885. <https://doi.org/10.1016/j.neuron.2011.05.002>
- Sanders, S. J., He, X., Willsey, A. J., Ercan-Sencicek, A. G., Samocha, K. E., Cicek, A. E., Murtha, M. T., Bal, V. H., Bishop, S. L., Dong, S., Goldberg, A. P., Jinlu, C., Keaney, J. F., 3rd, Klei, L., Mandell, J. D., Moreno-De-Luca, D., Poultney, C. S., Robinson, E. B., Smith, L., Solli-Nowlan, T., ... State, M. W. (2015). Insights into Autism Spectrum Disorder Genomic Architecture and Biology from 71 Risk Loci. *Neuron*, 87(6), 1215–1233. <https://doi.org/10.1016/j.neuron.2015.09.016>
- Sandin, S., Lichtenstein, P., Kuja-Halkola, R., Larsson, H., Hultman, C. M., & Reichenberg, A. (2014). The familial risk of autism. *JAMA*, 311(17), 1770–1777. <https://doi.org/10.1001/jama.2014.4144>
- Sato, D., Lionel, A. C., Leblond, C. S., Prasad, A., Pinto, D., Walker, S., O'Connor, I., Russell, C., Drmic, I. E., Hamdan, F. F., Michaud, J. L., Endris, V., Roeth, R.,

- Delorme, R., Huguet, G., Leboyer, M., Rastam, M., Gillberg, C., Lathrop, M., Stavropoulos, D. J., ... Scherer, S. W. (2012). SHANK1 Deletions in Males with Autism Spectrum Disorder. *American journal of human genetics*, *90*(5), 879–887. <https://doi.org/10.1016/j.ajhg.2012.03.017>
- Schneiderman, I., Zagoory-Sharon, O., Leckman, J. F., and Feldman, R. (2012). Oxytocin during the initial stages of romantic attachment: relations to couples' interactive reciprocity. *Psychoneuroendocrinology* *37*, 1277–1285. doi: 10.1016/j.psyneuen.2011.12.021
- Shapiro, L. E., & Insel, T. R. (1990). Infant's response to social separation reflects adult differences in affiliative behavior: a comparative developmental study in prairie and montane voles. *Developmental psychobiology*, *23*(5), 375–393. <https://doi.org/10.1002/dev.420230502>
- Sheng, M., & Kim, E. (2011). The postsynaptic organization of synapses. *Cold Spring Harbor perspectives in biology*, *3*(12), a005678.
- Shin, S. M., Zhang, N., Hansen, J., Gerges, N. Z., Pak, D. T., Sheng, M., & Lee, S. H. (2012). GKAP orchestrates activity-dependent postsynaptic protein remodeling and homeostatic scaling. *Nature neuroscience*, *15*(12), 1655–1666. <https://doi.org/10.1038/nn.3259>
- Smeltzer, M. D., Curtis, J. T., Aragona, B. J., and Wang, Z. (2006). Dopamine, oxytocin, and vasopressin receptor binding in the medial prefrontal cortex of monogamous and promiscuous voles. *Neurosci. Lett.* *394*, 146–151. doi: 10.1016/j.neulet.2005.10.019

- Stone, J. L., Merriman, B., Cantor, R. M., Yonan, A. L., Gilliam, T. C., Geschwind, D. H., & Nelson, S. F. (2004). Evidence for sex-specific risk alleles in autism spectrum disorder. *American journal of human genetics*, *75*(6), 1117–1123.
<https://doi.org/10.1086/426034>
- Tabak, B. A., Meyer, M. L., Castle, E., Dutcher, J. M., Irwin, M. R., Han, J. H., et al. (2015). Vasopressin, but not oxytocin, increases empathic concern among individuals who received higher levels of paternal warmth: a randomized controlled trial. *Psychoneuroendocrinology* *51*, 253–261. doi: 10.1016/j.psyneuen.2014.10.006
- Tabbaa, M., Paedae, B., Liu, Y., & Wang, Z. (2016). Neuropeptide Regulation of Social Attachment: The Prairie Vole Model. *Comprehensive Physiology*, *7*(1), 81–104.
<https://doi.org/10.1002/cphy.c150055>
- Turner, T. N., Hormozdiari, F., Duyzend, M. H., McClymont, S. A., Hook, P. W., Lossifov, I., Raja, A., Baker, C., Hoekzema, K., Stessman, H. A., Zody, M. C., Nelson, B. J., Huddleston, J., Sandstrom, R., Smith, J. D., Hanna, D., Swanson, J. M., Faustman, E. M., Bamshad, M. J., Stamatoyannopoulos, J., ... Eichler, E. E. (2016). Genome Sequencing of Autism-Affected Families Reveals Disruption of Putative Noncoding Regulatory DNA. *American journal of human genetics*, *98*(1), 58–74. <https://doi.org/10.1016/j.ajhg.2015.11.023>
- Vaags, A. K., Lionel, A. C., Sato, D., Goodenberger, M., Stein, Q. P., Curran, S., Ogilvie, C., Ahn, J. W., Drmic, I., Senman, L., Chrysler, C., Thompson, A., Russell, C., Prasad, A., Walker, S., Pinto, D., Marshall, C. R., Stavropoulos, D. J., Zwaigenbaum, L., Fernandez, B. A., ... Scherer, S. W. (2012). Rare deletions

- at the neurexin 3 locus in autism spectrum disorder. *American journal of human genetics*, 90(1), 133–141. <https://doi.org/10.1016/j.ajhg.2011.11.025>
- Waga, C., Okamoto, N., Ondo, Y., Fukumura-Kato, R., Goto, Y. I., Kohsaka, S., & Uchino, S. (2011). Novel variants of the SHANK3 gene in Japanese autistic patients with severe delayed speech development. *Psychiatric genetics*, 21(4), 208-211.
- Walsh, R. N., & Cummins, R. A. (1976). The open-field test: A critical review. *Psychological Bulletin*, 83(3), 482–504.
- Walum, H., & Young, L. J. (2018). The neural mechanisms and circuitry of the pair bond. *Nature reviews. Neuroscience*, 19(11), 643–654. <https://doi.org/10.1038/s41583-018-0072-6>
- Wang, X., McCoy, P. A., Rodriguiz, R. M., Pan, Y., Je, H. S., Roberts, A. C., Kim, C. J., Berrios, J., Colvin, J. S., Bousquet-Moore, D., Lorenzo, I., Wu, G., Weinberg, R. J., Ehlers, M. D., Philpot, B. D., Beaudet, A. L., Wetsel, W. C., & Jiang, Y. H. (2011). Synaptic dysfunction and abnormal behaviors in mice lacking major isoforms of Shank3. *Human molecular genetics*, 20(15), 3093–3108. <https://doi.org/10.1093/hmg/ddr212>
- Wang, X., Xu, Q., Bey, A. L., Lee, Y., & Jiang, Y. H. (2014). Transcriptional and functional complexity of Shank3 provides a molecular framework to understand the phenotypic heterogeneity of SHANK3 causing autism and Shank3 mutant mice. *Molecular autism*, 5, 30. <https://doi.org/10.1186/2040-2392-5-30>.
- Werling, D. M., & Geschwind, D. H. (2013). Understanding sex bias in autism spectrum disorder. *Proceedings of the National Academy of Sciences*, 110(13), 4868-4869.

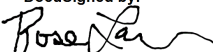
- Williams, J. R., Catania, K. C., & Carter, C. S. (1992). Development of partner preferences in female prairie voles (*Microtus ochrogaster*): the role of social and sexual experience. *Hormones and behavior*, 26(3), 339–349. [https://doi.org/10.1016/0018-506x\(92\)90004-f](https://doi.org/10.1016/0018-506x(92)90004-f)
- Williams, J. R., Insel, T. R., Harbaugh, C. R., & Carter, C. S. (1994). Oxytocin administered centrally facilitates formation of a partner preference in female prairie voles (*Microtus ochrogaster*). *Journal of neuroendocrinology*, 6(3), 247–250. <https://doi.org/10.1111/j.1365-2826.1994.tb00579.x>
- Wilson, S.C. (1982). Parent-young contact in prairie and meadow voles. *Journal of Mammalogy*, 63(2), 300-305.
- Winslow, J. T., Hastings, N., Carter, C. S., Harbaugh, C. R., & Insel, T. R. (1993). A role for central vasopressin in pair bonding in monogamous prairie voles. *Nature*, 365(6446), 545–548. <https://doi.org/10.1038/365545a0>
- Woolley, J. D., Chuang, B., Lam, O., Lai, W., O'Donovan, A., Rankin, K. P., Mathalon, D. H., & Vinogradov, S. (2014). Oxytocin administration enhances controlled social cognition in patients with schizophrenia. *Psychoneuroendocrinology*, 47, 116–125. <https://doi.org/10.1016/j.psyneuen.2014.04.024>
- Young, K. A., Gobrogge, K. L., Liu, Y., & Wang, Z. (2011). The neurobiology of pair bonding: insights from a socially monogamous rodent. *Frontiers in neuroendocrinology*, 32(1), 53–69. <https://doi.org/10.1016/j.yfrne.2010.07.006>
- Young, L. J., & Wang, Z. (2004). The neurobiology of pair bonding. *Nature neuroscience*, 7(10), 1048–1054. <https://doi.org/10.1038/nn1327>

- Zhang, Yi & Li, Na & Li, Chao & Zhang, Ze & Teng, Huajing & Wang, Yan & Zhao, Tingting & Shi, Leisheng & Zhang, Kun & Xia, Kun & Li, Jinchun & Sun, Zhongsheng. (2020). Genetic evidence of gender difference in autism spectrum disorder supports the female-protective effect. *Translational Psychiatry*. 10. 4. 10.1038/s41398-020-0699-8.
- Zhou, Y., Kaiser, T., Monteiro, P., Zhang, X., Van der Goes, M. S., Wang, D., Barak, B., Zeng, M., Li, C., Lu, C., Wells, M., Amaya, A., Nguyen, S., Lewis, M., Sanjana, N., Zhou, Y., Zhang, M., Zhang, F., Fu, Z., & Feng, G. (2016). Mice with Shank3 Mutations Associated with ASD and Schizophrenia Display Both Shared and Distinct Defects. *Neuron*, 89(1), 147–162.
<https://doi.org/10.1016/j.neuron.2015.11.023>
- Zhou, Y., Sharma, J., Ke, Q., Landman, R., Yuan, J., Chen, H., Hayden, D. S., Fisher, J. W., 3rd, Jiang, M., Menegas, W., Aida, T., Yan, T., Zou, Y., Xu, D., Parmar, S., Hyman, J. B., Fanucci-Kiss, A., Meisner, O., Wang, D., Huang, Y., ... Yang, S. (2019). Atypical behaviour and connectivity in SHANK3-mutant macaques. *Nature*, 570(7761), 326–331. <https://doi.org/10.1038/s41586-019-1278-0>

Publishing Agreement

It is the policy of the University to encourage open access and broad distribution of all theses, dissertations, and manuscripts. The Graduate Division will facilitate the distribution of UCSF theses, dissertations, and manuscripts to the UCSF Library for open access and distribution. UCSF will make such theses, dissertations, and manuscripts accessible to the public and will take reasonable steps to preserve these works in perpetuity.

I hereby grant the non-exclusive, perpetual right to The Regents of the University of California to reproduce, publicly display, distribute, preserve, and publish copies of my thesis, dissertation, or manuscript in any form or media, now existing or later derived, including access online for teaching, research, and public service purposes.

DocuSigned by:

55F84B6183884E7... Author Signature

8/30/2021
Date